THE EFFECTS OF AIR POLLUTION PARTICLES ON CLEARANCE MECHANISMS WITHIN THE LUNG

PETER GEORGE BARLOW

A Thesis Submitted In Partial Fulfilment Of The Requirements Of Napier University For The Degree of Doctor of Philosophy

November 2004

A Project Funded By Napier University, Edinburgh

DECLARATION

I certify that all of the work contained in this manuscript was carried out by myself unless otherwise stated.

P. Barlow.

PETER BARLOW

ACKNOWLEDGEMENTS

I would like to start by offering my gratitude to my supervisor, Dr. Vicki Stone, for her help, guidance, tolerance, humour and most of all, her enthusiasm. Vicki has fully supported me from the outset of her supervision and I cannot hope to offer enough thanks for her excellent help. But I would just like to say now... thanks Vick!

I would also like to give thanks to my second supervisor Dr. Janis MacCallum for always helping me with my studies and for making Monday morning physiology labs a lot of fun. I would like to thank Professor Ken Donaldson for his advice and for his ingenious ideas which helped in the production of this thesis. I would also like to thank my first-year supervisor Dr. Anna Clouter-Baker for guiding me through my first year.

Thanks all the people in the Biomedicine Research Group especially Drs' David Brown and Martin Wilson for their technical help and for always answering questions with a smile. Thanks to Dr. Keith Guy for his help with the flow cytometry and for all of his advice (in the lab and on the golf course). Thanks must also go to Dr. Lorna Proudfoot for her assistance and to the others in BRG and the School of Life Sciences.

I would like to note my thanks to a talented young scientist and a good friend, Gary Hutchison, for all of his support and for making the last three years a lot of fun. Thanks also, to Laura Hutchison, for her help and her great sense of humour

Finally, I would like to offer the biggest thank you to my family, especially to my parents, for always supporting and encouraging me and for always helping me believe that anything can be done. I would like to thank my wonderful wife Kelly, because she is, quite simply, always there when I need her the most.

Dalla sua pace la mia dipende,
quel che a lei piace vita ma rende,
quel che le increscе morte mi dà.
S'ella sospira, sospiro anch'io,
è mia quell'ira, quel pianto è mio
e non ho bene s'ella non l'ha

My peace depends upon hers:
what pleases her gives me life,
that which pains her gives me death.
If she sighs, I will sigh as well,
her anger and her sorrows are mine
and I have no joy unless she shares it.

Mozart, *Don Giovanni*
Taken from *Acqua Alta* by Donna Leon

PUBLICATIONS

The following publications were a direct result of the work contained in this thesis:

Barlow, P.G., Donaldson, K., MacCallum, J., Clouter, A. and Stone, V. (2005). Serum exposed to nanoparticle carbon black displays increased potential to induce macrophage migration. *Toxicol. Lett.* **155**(3): 397-401.

SUMMARY

The effects of inhaled air pollution particles on lung clearance mechanisms is an important factor in understanding how the mammalian lung deals with such pollutants and, as such, how exposure to these pollutants can be regulated. The nanoparticle (diameter $\leq$ 100nm) and transition metal components of PM_{10} (particulate matter with a diameter less than 10μm) have been implicated as playing major roles in the impairment of alveolar macrophage function and the subsequent retention of particles in the respiratory system. The aim of this study was to investigate the effects of components of PM_{10} on macrophage functions both directly, by examining macrophage phagocytosis and migration, and indirectly, by studying peripheral factors affecting macrophage function such as recruitment by type II cells and complement based mechanisms.

We hypothesised that the alveolar epithelial type II cell line would release leukocyte chemoattractants in response to particle exposure and that this could be measured by use of a macrophage migration assay. A sub-toxic dose (125μg/ml) of surrogate air pollution particles (fine and nanoparticle carbon black and titanium dioxide) was established by measuring LDH release from a murine alveolar macrophage cell line (J774.2) and an alveolar epithelial type II cell line (L-2) in response to particle exposure. Optimisation of a chemotaxis assay and measurement of macrophage migration towards conditioned medium obtained from the particle-exposed type II cells was conducted and it was determined that carbon black nanoparticles induced type II cells to secrete a chemoattractant that resulted in significant increases in macrophage migration compared

to the negative control. This was in contrast to other particle types tested in this study which did not induce any increases in macrophage migration.

It was also hypothesised that complement proteins could be involved in macrophage recruitment to sites of particle deposition and, as such, the migration of macrophages towards particle exposed blood serum was examined *in vitro*. Foetal bovine serum (FBS) was exposed to fine and nanoparticle carbon black and titanium dioxide (1-5mg/ml) for 2 hours. It was found, in accord with the previous study involving type II cells, that carbon black nanoparticles could activate the generation of chemotactic factors in serum that could subsequently induce significant increases ($p<0.001$) in macrophage migration when serum was diluted to 10% using serum-free RPMI 1640 culture medium. This effect could be ameliorated by co-incubating the particle-treated serum in the presence of the antioxidant Trolox suggesting that oxidative stress played a role in the generation of the chemoattractant molecules. However, incubation of the serum with a pure oxidant at a range of doses did not result in the generation of chemotactic molecules suggesting that another factor could be involved in the chemoattractant generation. Further investigation to determine the exact molecular mechanism behind the chemoattractant generation is warranted.

In contrast to the previous studies, we have also found evidence that components of PM_{10} can cause decreased efficacy of macrophage clearance mechanisms *in vivo* and *in vitro*. It was hypothesised that PM_{10} instillation would result in a decrease in macrophage phagocytic potential and an increase in chemotactic potential *ex vivo*. Rats were instilled

with 125 and 250μg of PM_{10} collected from North Kensington, London or sterile saline (negative control). Post-instillation (18 hours), significantly elevated concentrations of TNFα were detected in the BAL fluid together with a significant increase in the number of BAL neutrophils. Phagocytosis and chemotaxis assays conducted with BAL macrophages *ex vivo* showed that macrophage migration towards a positive chemoattractant, Zymosan Activated Serum (ZAS), was significantly lower than the macrophages obtained from the negative control rats. Macrophage phagocytosis of latex beads *ex vivo* was also found to be significantly decreased when PM_{10} was visible inside the cell. An *in vitro* study where a macrophage cell line (J774.A1) was exposed to a low dose of nanoparticle carbon black (31.25μg) together with varying concentrations (100μM – 100nM) of zinc chloride ($ZnCl_2$) was also conducted Exposure of macrophages to nanoparticle carbon black and zinc chloride alone induced a decrease in macrophage phagocytosis. It was found that when macrophages were co-exposed to nanoparticle carbon black and $ZnCl_2$, there was an additive decrease in macrophage phagocytic potential.

The results contained within this manuscript demonstrate that the components of PM_{10} can induce adverse effects on specific aspects of macrophage clearance mechanisms, but that nanoparticles can also stimulate the production of chemoattractants to aid in the recruitment of phagocytes and subsequent particle clearance. Although a contrary relationship appears to exist between these findings, the recruitment of leukocytes in response to particulate exposure is a mechanism that supports particle clearance. However, the retardation of phagocytic and chemotactic mechanisms in particle exposed

macrophages may help to explain the increased toxicity, inflammation and retention time observed with nanoparticle inhalation.

CONTENTS

LIST OF FIGURES AND TABLES

Figure 5.4.1 Flow cytometry scatter plots of J774.A1 cells. The plots represent (1) Untreated cells (negative control), (2) Cells treated with bioparticles (positive control), (3) Cells treated with 31.25μg nanoparticle carbon black (NCB) only (4) Cells treated with $ZnCl_2$ (100μM) and bioparticles, (5) Cells treated with $ZnCl_2$ (1μM) and bioparticles, (6) Cells treated with $ZnCl_2$ (100nM) and bioparticles, (7) Cells treated with $ZnCl_2$ (100μM), NCB and bioparticles, (8) Cells treated with $ZnCl_2$ (1μM), NCB and bioparticles, (9) Cells treated with $ZnCl_2$ (100nM), NCB and bioparticles.

Figure 5.4.2 A histogram plot of treated and untreated J774.A1 cells analysed by flow cytometry. Untreated J774.A1 cells are represented by the purple area of the graph. J774.A1 cells treated with bioparticles are represented by the red area of the graph.

Figure 5.4.3 A histogram plot of treated J774.A1 cells analysed by flow cytometry. J774.A1 cells treated with bioparticles only are represented by the red outline area of the graph. J774.A1 cells treated with 31.25μg nanoparticle carbon black and bioparticles are represented by the purple area of the graph.

Figure 5.4.4 A histogram plot of J774.A1 cells analysed by flow cytometry. J774.A1 cells treated with 100μM $ZnCl_2$ and bioparticles are represented by the red outline area of the graph. J774.A1 cells co-treated with 100μM $ZnCl_2$ / 31.25μg nanoparticle carbon black and then bioparticles are represented by the purple area of the graph.

Figure 5.4.5 A histogram plot of J774.A1 cells analysed by flow cytometry. J774.A1 cells treated with 1μM $ZnCl_2$ and bioparticles are represented by the red outline area of the graph. J774.A1 cells co-treated with 1μM $ZnCl_2$ / 31.25μg nanoparticle carbon black and then bioparticles are represented by the purple area of the graph.

ABBREVIATIONS

ANOVA	Analysis of variance
APS	Ammonium persulphate
ARDS	Acute respiratory distress syndrome
BAL	Bronchoalveolar lavage
BSA	Bovine serum albumin
C2	Complement protein C2
C3	Complement protein C3
C3a	Complement protein C3a
C3b	Complement protein C3b
C5	Complement protein C5
C5a	Complement protein C5a
CB	Carbon black
CM	Conditioned medium
CO_2	Carbon dioxide
COPD	Chronic obstructive pulmonary disease
DEFRA	Department for environment, food and rural affairs
DMSO	Dimethyl sulphoxide
DNA	Deoxyribonucleic acid
DTT	Dithiothreitol
ECACC	European collection of cell cultures
E.Coli	*Escherichia coli*
ELF	Epithelial lining fluid
ELISA	Enzyme linked immunosorbent assay
FBS	Foetal bovine serum
$FeCl_3$	Iron chloride
FITC	Fluoroscein isothiocyanate
G-CSF	Granulocyte colony stimulating factor
GM-CSF	Granulocyte monocyte – colony stimulating factor
GSH	Glutathione

H_2O_2	Hydrogen peroxide
HBSS	Hanks balanced salt solution
HCl	Hydrochloric acid
HIS	Heat inactivated foetal bovine serum
IARC	International agency for research on cancer
IFNα	Interferon alpha
IFNγ	Interferon gamma
IL-1α	Interleukin-1 alpha
IL-1β	Interleukin-1 beta
Il-4	Interleukin-4
IL-6	Interleukin-6
IL-8	Interleukin-8
IL-9	Interleukin-9
IL-14	Interleukin-14
IPF	Idiopathic pulmonary fibrosis
LDH	Lactate dehydrogenase
LPS	Lipopolysaccharide
MCE	Mucociliary escalator
MCP-1	Monocyte chemoattractant protein 1
M-CSF	Monocyte colony stimulating factor
MIF	Macrophage migration inhibitory factor
MIP-1	Macrophage inflammatory protein 1
MIP-2	Macrophage inflammatory protein 2
NADH	Nicotinamide adenine dinucleotide (reduced)
NADPH	Nicotinamide adenine dinucleotide phosphate (reduced)
NCB	Nanoparticle carbon black
NF-κB	Nuclear factor kappa B
PBS	Phosphate buffered saline
pH	Pondus hydrogenii
PM	Particulate matter
PM_{10}	Particulate air pollution with a diameter of 10μm or less

PMN	Polymorphonuclear neutrophils
ROS	Reactive oxygen species
RPMI 1640	Roswell park memorial institute medium 1640
S-HRP	Streptavidin-horse radish peroxidase
SEM	Standard error of the mean
SDS-PAGE	Sodium dodecyl sulphate – polyacrylamide gel electrophoresis
tBHP	tert-butyl hydroperoxide
TEOM	Tapered element oscillating microbalance
TGFβ	Transforming growth factor beta
TiO_2	Titanium dioxide
TMB	Tetramethylbenzidine
TNFα	Tumour necrosis factor alpha
UK	United Kingdom
US	United States of America
VOC	Volatile organic compound
ZAS	Zymosan activated serum
$ZnCl_2$	Zinc chloride

CHAPTER 1

GENERAL INTRODUCTION

1.1 GROSS ANATOMY OF THE MAMMALIAN LUNG

The lung has evolved to act as the respiratory centre for mammals and, as such, is the area where gaseous exchange between the organism and the environment takes place. The body's blood supply is supplied to the lungs via the pulmonary artery and in the lungs the blood is oxygenated and carbon dioxide is removed. The oxygenated blood then flows out of the lungs via the pulmonary vein which returns the blood to the left atrium of the heart, ready for transport around the rest of the body. Since the body's blood supply passes through the lungs, they are therefore exposed to any systemic toxins or inflammatory substances contained within the blood that perfuses the lung tissue. In addition, the respiratory tissues will also be exposed to any potentially toxic substances present in inhaled air.

Structurally the lung can be separated into two distinct areas; the conducting zone and the respiratory zone. The conducting zone leads from the pharynx down the trachea to the bronchi and terminal bronchioles and is concerned with the transport of air into the respiratory section of the lung. The respiratory zone is where gas exchange takes place and is a honeycombed area of respiratory bronchioles, alveolar sacs and alveoli (Tortora & Grabowski, 1992). Humans possess up to 23 branching airway generations from the proximal bronchi to the distal alveoli (Malpel & Cardroso, 2001).

There are many types of cells which make up the various areas of the lung and these differ from region to region depending on the structural and functional requirements of a particular area. The varying cell types are exposed to differing concentrations and

compositions of inhaled material and as such, can respond in a different manner to a given material as is shown in subsequent chapters.

1.2 CELLS OF THE LUNG

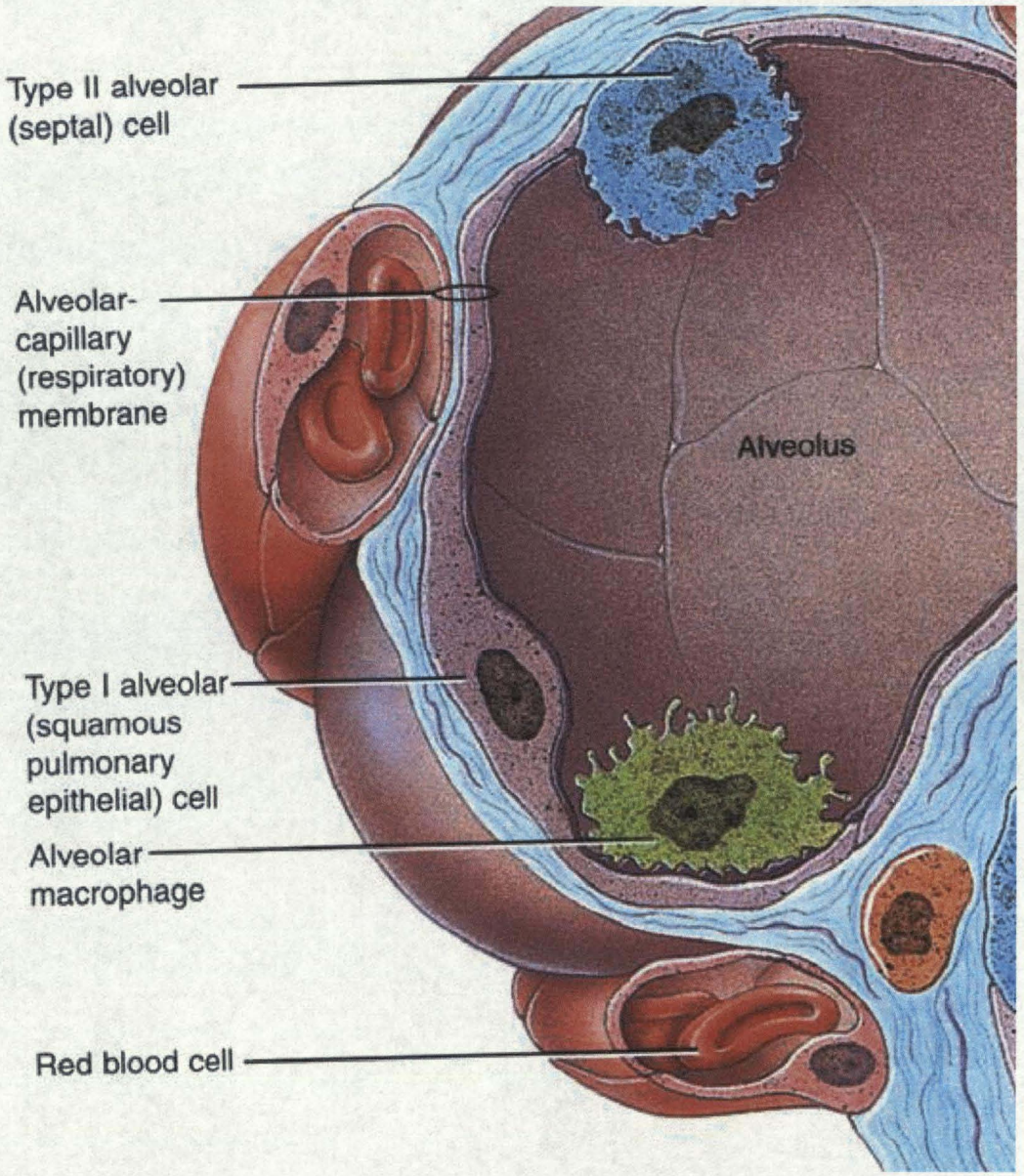

Figure 1.1 – Illustration of cells in the alveolar region of a mammalian lung (Picture taken from Principals of Anatomy and Physiology, 5th Ed., Tortora & Grabowski)

1.2.1 Type II Epithelial Cells

The type II epithelial cells make up around 15% of the total number of lung cells but only covers around 5-7% of the alveolar surface (Dobbs, 1990). Type II cells have several important functions including maintaining the alveolar structure, as well as participating in the physiological and biochemical processes that occur in the lung (Simon & Paine III, 1995). The type II cells are cuboidal in shape but the size depends upon the state of lung growth and repair (Dobbs, 1990). A study of human lung cells by Crapo *et al.*, (1982) found that the mean diameter of the cell nuclei was around 7.5μm but this can vary in other mammals (Dobbs, 1990). The cells have a microvillous apical surface and can be identified by the presence of lamella bodies within the cytoplasm (Fehrenbach, 2001).

The type II cell has several roles in maintaining the structural and biochemical homeostasis of the lung. Arguably, the most important function of type II cells is the production and secretion of lung surfactant, a complex mixture of lipids, including several types of phospholipids, and several proteins such as Apoprotein A (utilised in surfactant homeostasis). The surfactant generates a low surface tension and, as a result, prevents alveolar collapse and ensures equal gaseous exchange over the surface of the alveoli (Dormans & van Bree, 1995). Although surfactant components can be generated by other types of cells such as Clara cells, the type II cell is the only cell that is capable of producing all of the substances required for the surfactant. The type II cells also take-up, metabolise and re-secrete up to 85% of the surfactant in order to maintain a novel and steady supply of surfactant (Fehrenbach, 2001).

Another important function of the type II cells is their almost unlimited capacity to proliferate and differentiate into type I cells in response to injury. This is important in maintaining the structural integrity of the lung following cell death (Fehrenbach, 2001 and Adamson & Bowden, 1974). The cell death/proliferation cycle is carefully maintained in order to create a balance in the number of cells. Although type II cells are relatively resistant to injury due to high intracellular levels of antioxidants and xenobiotic metabolising enzymes, damage can occur to the cells (Cross, 1974). However, it is still not understood if all type II cells can act as stem cells, as opposed to just a small sub-population possessing this capacity (Uhal, 1997). Fehrenbach (2001) also reviewed the capacity of the alveolar type II cells to phagocytose apoptotic type II cells, further aiding the balance in cell death and renewal. However, the proliferative ability of the type II cells must be controlled as abnormal proliferation may result in the development of lung tumours such as adenocarcinomas (Tsutahara *et al.*, 1993).

The final and equally important major function of the type II cells is the ability to communicate with other cells, including adjacent epithelial pneumocytes, but, more importantly, the mobile cells such as neutrophils and alveolar macrophages (Fehrenbach, 2001). This interaction with leukocytes enables the type II cells to signal to the macrophages that are already present in the alveolar space, as well as recruiting circulating macrophages to local sites of pulmonary inflammation such as that induced by respirable particulate deposition. It has been shown that type II cells can secrete many chemoattractants including interkeukin-8 (IL-8), macrophage inflammatory proteins 1 and 2 (MIP-1 & MIP-2), RANTES, granulocyte monocyte – colony stimulating factor

(GM-CSF) and tumour necrosis factor alpha (TNFα) (O'Brien *et al.*, 1998, Driscoll *et al.*, 1996b, Donaldson *et al.*, 2000a, Rosseau *et al.*, 2000). Type II cells have also been shown to be capable of secreting proteins of both the alternative and classical complement pathways (Strunk *et al.*, 1988). Pre-existing inflammation such as that caused by oxidative stress has also been shown to prime type II cells to release excessive amounts of inflammatory mediators. This may result in a higher level of cellular injury than would otherwise normally be induced by an inflammogenic material (Stringer & Kobzik, 1998).

1.2.2 Type I Epithelial Cells

Alveolar type I cells cover up to 93% of the alveolar surface (Crapo *et al.*, 1982). The primary function of the type I cell is to act as a surface for gaseous exchange to take place. The type I and type II epithelial cell membranes can overlap and can join together by tight junctions which create a relatively solid barrier against the unwanted diffusion of electrolytes and hydrophilic solutes. Type I cells contain numerous vesicles and membrane buds which are expected to assist in the internalisation of proteins but it is unknown which type of transport processes are employed by type I cells compared to type II cells (Kim & Malik, 2003). The fluid transport that takes place between the alveolar region and the vasculature of the lung is carefully controlled to ensure adequate hydration of the alveolar space and swift resolution to any pulmonary oedema, resulting from diseases such as congestive heart failure or acute lung injury (Verkman *et al.*, 2000). Any damage to the epithelial cells can result in increased vascular permeability and the sloughing of cells into the air spaces which could result in decreased gas

exchange and an increase in pulmonary oedema (Newman *et al.*, 2000). However, any loss of type I cells can be remedied by the differentiation of type II cells to ensure the structural stability of the airspaces (Adamson & Bowden, 1974).

1.2.3 Neutrophils

Polymorphonuclear neutrophils (PMN) are white blood cells that typically comprise up to 70% of circulating leukocytes in the peripheral blood of individuals in a normal immunological state. In the lung, the primary function of neutrophils is the phagocytosis of inhaled pathogens or particulates. Neutrophils possess a large array of proteolytic enzymes and the potential to produce reactive oxygen species to aid in the destruction of ingested items. As with macrophages, neutrophils migrate towards a site of localised inflammation or opsonised pathogens via the process of chemotaxis and, as such, possess a wide range of chemotaxin receptors on their surface. The granules that are contained within the neutrophil cytoplasm can contain proteases, acid hydrolases and metalloproteinases as well as lysozyme (Faurschou & Borregaard, 2003). The degranulation of neutrophils in response to an inflammatory response is carefully controlled as excessive production of these toxic substances can result in conditions such as septic shock, disseminated intravascular coagulation and, in the lung, acute respiratory distress syndrome (ARDS) (Neumann *et al.*, 1999).

Neutrophil sequestration into the pulmonary vasculature and alveolar space as well as the factors involved in recruitment has been investigated in a wide range of disease states. Several studies have demonstrated increased neutrophil influx into the lung as a result of

an inflammatory response to inhaled particles and, indeed, neutrophils are now commonly used as a marker of particle induced pulmonary inflammation (Brown *et al.*, 1995, Li *et al.*, 1996). Studies have demonstrated increased levels of neutrophil chemoattractants in the lungs of individuals with diseases such as idiopathic pulmonary fibrosis (IPF) and asthma (Hunninghake *et al.*, 1981 and Teran *et al.*, 1997). In an investigation by Drost & MacNee (2002) which examined neutrophil deformability and chemotaxis induced by cytokines such as TNFα and IL-8, it was illustrated that both cytokines could enhance the neutrophil migratory response as well as increasing the response to stimulated cell deformability, a process which is pertinent in neutrophil sequestration through the pulmonary vasculature. Increased neutrophil presence in the lungs of pollution exposed animals could be correlated with the increased levels of both TNFα and MIP-2 that have been shown to occur in the bronchoalveolar lavage (BAL) fluid of particle exposed rats (Schins *et al.*, 2004, Becher *et al.*, 2001, Driscoll *et al.*, 2000).

1.2.4 Alveolar Macrophages

Alveolar macrophages are a distinct population of cells that act as the primary defence against inhaled particulates and bacteria in the alveolar space. The cells reside in the alveolar space in the film of pulmonary surfactant as free cells and are one of four pulmonary macrophage populations. Other forms include the pulmonary interstitial macrophage, the pulmonary intravascular macrophage and a dendritic "macrophage-like" cell which displays some phagocytic ability (Sibelle & Reynolds 1990 and Dorger & Krombach, 2000). Macrophages have also been identified in the upper airways which

may be alveolar macrophages transported up by the mucociliary escalator (MCE). However Brain *et al.*, (1984) describes the adherence of these macrophages to epithelial cells which suggests that they play a role in the removal of deposited elements from the airways.

The alveolar macrophage is the only macrophage population in the body that is exposed to environmental air and, as such, this exposure may have some influence upon its behaviour (Lohmann-Matthes *et al.*, 1994 and Sibille & Reynolds, 1990). It is thought that the majority of lung macrophages are sourced from the bone marrow and are derived from peripheral blood monocytes (Blusse van Oud Ablas *et al.*, 1979 and Fels & Cohn 1986). Some studies have also shown that alveolar macrophages may be capable of local replication under certain conditions (Shellito *et al.*, 1987; Tarling & Coggle, 1982 and Tarling *et al.*, 1987). Bitterman *et al.*, (1984) reported that, under chronic inflammation conditions in the lung, alveolar macrophages undergoing mitotic division were present, supporting the localised macrophage replication hypothesis.

The studied functions of the alveolar macrophage have expanded over the past five decades to encompass many antimicrobial activities involving phagocytosis of foreign bodies, recruitment of other inflammatory cells such as PMNs, and antigen presentation (Sibille & Reynolds, 1990 and Fels & Cohn, 1986). Macrophages are capable of secreting more than 100 different products which include cytokines, complement proteins, fibroblastic growth factors, enzymes and reactive oxygen species. A more comprehensive list is detailed in table 1.2. The production of these substances is essential

to the macrophages primary function i.e. the phagocytosis and removal of foreign particulates from the alveolar space in an attempt to maintain a sterile environment. The potential for the macrophage to produce an armoury of proteolytic enzymes and reactive oxygen species only serves to achieve this goal. The activation and recruitment of macrophages to sites of inflammation is described in detail in sections 1.3.3. and 1.3.4.

1.2.5 Clara Cells

Clara cells are non-ciliated epithelial cells that are cuboidal in shape and are functionally similar to type II epithelial cells in that they are capable of secreting surfactant components, especially in the distal airways (McCormack, 2001 and Mills *et al.*, 1999). They also contain high levels of cytochrome P450 for xenobiotic metabolism (Widdicombe & Pack, 1982). The Clara cells are located in the terminal and respiratory bronchioles and are thought to under go differentiation when acting as stem cells to repair ciliated cells of the bronchial epithelium following damage (Bishop, 2004 and Otto, 2002). They possess a dome-shaped apical projection which protrudes into the lumen and contains high numbers of mitochondria and electron dense secretory granules (Mercer *et al.*, 1994). A limited number of studies have investigated interactions between air pollution particles and Clara cells. An important investigation by Murphy *et al.*, (1998) observed that Clara cells exposed to both diesel exhaust and carbon black particles showed particle internalisation and decreased biotransformation capability. Finkelstein *et al.*, (1997) also showed increased mRNA expression for the cytokines IL-1, IL-6 and TNFα in Clara cells in response to particulate exposure.

1.3 LUNG DEFENCE

1.3.1 Non-Specific Lung Defence Mechanisms

Complementing the cellular defence mechanisms in the lung such as macrophages and neutrophils are physiological adaptations which help to prevent particles and organisms from being retained within the lung. The first method of defence includes the hairs lining the nose and upper airways. The hairs trap particles and prevent them from entering the delicate airways and bronchioles. This prevents some particulates from ever entering an area of the airways where an inflammatory response could be initiated. The second stage of defence, the mucociliary escalator (MCE), is situated primarily in the proximal airways and involves a mucus coating of the airways that generally traps particles that are greater than 5μm in diameter, as well as other respirable matter. The mucus is secreted by goblet cells that are part of the lining of the primary airways. Once particles have been trapped in the mucus, ciliated cells propel the mucus up towards the oesophagus where it can either be expelled or swallowed. Thompson *et al.*, (1995) has also demonstrated that mucus has an antioxidant capacity which would help protect the pneumocytes from damaging free radicals.

1.3.2 Lung Surfactant

Lung surfactant is primarily produced by type II epithelial cells and is released into the epithelial lining fluid (ELF) in the gaseous exchange regions of the lung. Surfactant is a complex mixture of lipids, including several types of phospholipids such as phosphatidylcholine and phosphatidylglycerol, and several proteins, such as Apoprotein A (utilised in surfactant homeostasis). The surfactant generates a low surface tension and

as a result, prevents alveolar collapse and ensures equalised gaseous exchange over the surface of the alveoli (Dormans & Van Bree, 1995). Surfactant has also been reported to play an important role in lung defence against oxidants as it is also known to have a high antioxidant activity (Matalon *et al.*, 1990 and Lang *et al.*, 2002). Roveri *et al.*, (1989) demonstrated that epithelial lining fluid contains antioxidant enzymes such as glutathione, glutathione peroxidase, superoxide dismutase and catalase which are all involved in the reduction of oxygen. A clever defence mechanism is also in place to ensure that the production of surfactant by epithelial cells is not compromised by oxidant damage. Brown (1994) illustrated how glutathione protects the signal transduction pathways of the type II cells against oxidants to make sure that more surfactant is released.

Surfactant also has an important role concerning phagocytosis and removal of foreign particles from the lung. It has been shown that surfactant improves the chemotactic responses of pulmonary macrophages, as well as enhancing the phagocytic function of the macrophages (LaForce *et al.*, 1973 and Hoffman *et al.*, 1987). Clark *et al.*, (2002) also suggested that surfactant proteins promote the rapid removal of apoptotic and necrotic macrophages from the lung.

1.3.3 Macrophages in Pulmonary Homeostasis and Inflammation

The movement of macrophages towards foreign particles or bacteria that are to be phagocytosed is controlled by the process of chemotaxis. Chemotaxis is defined by Wilkinson, (1998) as the directed movement of leukocytes towards a chemotactic

substance. For macrophages, this can be stimulated by several different signalling molecules such as complement proteins, immunoglobulins and members of the cytokine family known as chemokines (Fels & Cohn, 1986 and Lohmann-Matthes *et al.*, 1994). However, there can be differences between species as to which signalling pathway proves to be the most effective. For example, it has been shown that rat alveolar macrophage movement is greatest towards complement-based stimuli, but on the other hand, hamster macrophage migration is based on a non-complement mechanism (Dorger & Krombach, 2000). The movement of the macrophage also depends upon the state of activation of the macrophage, since activated macrophages show an increased chemotactic response compared to resting macrophages (Schneider and Dy, 1985).

1.3.4 Macrophage Activation

The concept of 'activated' macrophages has been used to describe the enhanced macrophage state during an immune response to pathogenic organisms and has been studied since Metchnikoff introduced the idea of leukocyte phagocytosis (Schenider & Dy, 1985 and Metchnikoff, 1905). An activated macrophage can be characterised by increased response to chemotactic stimuli, morphological changes, including an increase in size and spreading as well as a change in surface receptor and secretory product patterns (Schneider & Dy, 1985 and Driscoll *et al.*, 1990). The change in surface receptors aids the macrophage in recognising many of the complement proteins and immunoglobulins which are involved in the opsonisation of inhaled organisms (Aderem and Underhill, 1999).

A macrophage can be activated by the binding of substances to the cell membrane. These substances can either be modulated by the organisms own immune system during the antigen presentation process or they could be sourced from a pathogenic origin such as bacterial products and surface proteins (Adams & Hamilton, 1984). The macrophage has a small number of ligands present on the surface but can bind to immunoglobulins via Fc receptors which exponentially increases the macrophages antigen recognition capability (Fels & Cohn, 1986). Other immunological mediators include complement proteins and cytokines such as interferon gamma (IFNγ) which is considered to be a potent effector of macrophage activation. IFNγ induces increased production of cytokines by macrophages and can result in the expression of increased numbers of immunological receptors on the macrophage surface (Heasman *et al.*, 2004 and Schneider & Dy (1985). It is thought that traditional or 'type I' activation of macrophages occurs in response to pathogen infection but recently the concept of alternative or type II activation by IL-4 and IL-13 has also been discussed, particularly during parasitic infection (Gordon, 2003, Namangala *et al.*, 2001 and Goerdt *et al.*, 1999)

1.3.5 Phagocytosis

The phagocytosis of an opsonised particle or bacterium begins with location and recognition by the macrophage of the subject, aided by the binding of an opsonin such as C3b or immunoglobulin to the phagocytic subject (Donaldson & Tran, 2002). The item to be phagocytosed is normally larger than 0.5μm, although Kruth *et al.*, (1999) have described a process of macrophage endocytosis, that they have termed 'patocytosis' which describes macrophage uptake of polystyrene microspheres with a diameter of less

than 0.5μm. Once a macrophage has located the item to be phagocytosed, the subject is engulfed by the macrophage by extending its plasma membrane around the item and enclosing it inside a phagosome. Following uptake the phagosome fuses with lysosomes to become a phagolysosome. This may take anywhere in the region of 30 minutes to several hours (Aderem & Underhill, 1999). The lysosome contains powerful enzymes such as lysozyme, proteases, lipases, deoxyribonucleases, phosphatases and lipoproteinases which can break down the biologic components of the phagocytosed substances. The macrophage also has the potential to produce reactive oxygen species (ROS) such as hydrogen peroxide, superoxide and hydroxyl radicals (Fels & Cohn, 1986). Free radicals and ROS have been shown to be damaging to living cells, capable of inducing lipid peroxidation, membrane damage, DNA scission and protein denaturation (Freeman & Crapo, 1982). If destruction of the phagocytosed material in the phagolysosome is unsuccessful, such is commonly the case with inorganic particles and fibres; the macrophage will normally migrate towards the mucociliary escalator and be carried out of the lung along with its particle burden. Alternatively, if the normal pathways of clearance fail, the particles will either transfer into the lymph nodes or remain in the interstitium

1.3.6 The Macrophage Phagocytic Burst

Macrophage phagocytosis is associated with an increase in the production of reactive oxygen and reactive nitrogen species, which are involved in the destruction of phagocytosed material (Bogdan, 2001). The primary pathway of oxidative metabolism is via the activation of the transmembrane enzyme NADPH oxidase which results in the

generation of extracellular superoxide which can subsequently be converted to hydrogen peroxide by superoxide dismutase or to hydroxyl radicals via the Haber-Weiss reaction (Bogdan *et al.*, 2000, Adams & Hamilton, 1984 and Fels & Cohn, 1986). Extracellular nitric oxide species can be generated by the conversion of l-arginine and molecular oxygen by nitric oxide synthases, a pathway which also requires NADPH (Bogdan *et al.*, 2000).

1.3.7 Macrophage Products

Macrophages have also been shown to release powerful inflammatory mediators which can influence the pathogenesis of a particle induced disease and may cause harm in some situations (Sibille & Reynolds, 1990). The capacity of the macrophage to induce recruitment of inflammatory cells, such as neutrophils, eosinophils and more macrophages, to a location of particle deposition may initially seem like an appropriate response. However, several studies have shown that low doses of toxic particles such as quartz, or large particulate doses of low toxicity particles, for example, titanium dioxide (TiO_2) can cause macrophages to release excessive amounts of pro-inflammatory substances such as cytokines, enzymes and ROS which, in addition to the damage caused by particulates, can also cause further injury to the lung tissue (Becher *et al.*, 2001, Driscoll *et al.*, 1990, 1997a, 1997b and Rehn *et al.*, 2003).

As mentioned previously in section 1.2.4 and as shown in table 1.2, macrophages can secrete a wide range of immunomodulatory mediators. Many of the secretory products are only produced during the inflammatory response but other secreted substances such

as apolipoprotein are utilised in normal lung homeostasis. It should be noted however, that although the macrophage secretes a wide range of substances, many, such as IL-1, TNFα and IL-6 share a common target or function. Other products that do not appear to have a particularly potent effect when studied singularly, may interact with other macrophage secretions in a synergistic or antagonistic manner, although this depends on the physiological state of the microenvironment into which the secretions are released (Keshav *et al.*, 1990). For example, pre-existing inflammation, such as that displayed in COPD patients, could cause increased cytokine release. Gilmour *et al.*, (2001) demonstrated that lung epithelial cells that had been transfected with the adenoviral gene E1A showed increased IL-8 release in response to LPS stimulation.

1.3.8 Macrophage Products in Pulmonary Inflammatory Modulation

Several of the products of macrophages are involved in the modulation of inflammatory response. The family of cytokines secreted by the macrophage has received much attention in attempting to elucidate the targets and functions of each cytokine. IL-1 is released by many other cells types as well as macrophages and is similar in function to TNFα. It is involved in the acute phase response and in the development of fibrosis, fever, shock and inflammation (Laskin & Laskin, 1996). It has been reported that elevated levels of IL-1 are found in the lung as a result of acute inflammatory lung injury (Brieland *et al.*, 1995). Driscoll *et al.*, (1990) reported increases in IL-1 secretion by macrophages from rats treated with silica. Other studies found increased IL-1 as a result of ozone exposure (Pendino *et al.*, 1994) and asbestos exposure (Perkins *et al.*, 1993).

TNFα is secreted by many different pneumocytes but activated macrophages are thought to be a major source. TNFα is known to modulate several pro-inflammatory reactions and has been implicated in inducing the release of other pro-inflammatory mediators including IL-1, IL-6, TGFβ, colony stimulating factors and reactive oxygen species from phagocytic cells. It has also been reported to be involved with cell apoptosis, neutrophil and lymphocyte recruitment, cytotoxicity and tissue necrosis. It has also been shown to induce epithelial cells to release chemotactic factors for leukocyte recruitment. Numerous studies have shown increases in TNFα production in animal and cell models following exposure to particulates and fibres. For example, Driscoll *et al.*, (1990) reported elevated TNFα levels in rats following pulmonary exposure to silica or TiO_2. Becher *et al.*, (2001) reported increased concentrations of TNFα released from macrophages exposed to quartz particles *in vitro*. Many studies have also reported increased TNFα concentrations from cells as a result of air pollution particle exposure (Becker *et al.*, 1996; Li *et al.*, 1999; Jimenez *et al.*, 2002 and Schins *et al.*, 2004). Thus TNFα has been implicated as a major factor in the pathogenesis of particle induced lung disease.

MAJOR SECRETORY PRODUCTS OF MACROPHAGES

COMPLEMENT PROTEINS
C1
C2
C3
C3b Inactivator
C4
C5

ENZYMES
Lysozyme
Plasminogen activator
Collagenase
Elastase
Angiotensin converting enzyme
Cysteine proteinase (Cathepsin L)
Proteases
Lipases
Deoxyribonucleases
Phosphatases
Glycosidases
Sulphatases
Arginase

PROTEINS
$Alpha_1$-proteinase inhibitor
$Alpha_2$-macroglobulin
Plasminogen activator inhibitor
Collagenase inhibitor
IL-1 inhibitor
Neutrophil migration inhibitor
Inhibitor of fibroblast growth
Lipomodulin
Glycoproteins
Fibronectin
Transferrin
Transcobalamin II
Apolipoprotein A and E

CYTOKINES
Interleukin-1 alpha and beta (IL-1α & IL-1β)
Interleukin-6 (IL-6)
Macrophage inflammatory protein-2 (MIP-2)
Interferon alpha and gamma (IFNα & IFNβ)
Transforming growth factor beta (TGFβ)
Tumour necrosis factor alpha (TNFα)
Neutrophil chemotactic factor
Colony stimulating factors (G-CSF, M-CSF & GM-CSF)

BIOACTIVE LIPIDS
Arachidonate metabolites
Prostaglandin E_2
Prostaglandin $F_{2\alpha}$
Cycloxygenase metabolites
Thromboxane A_2
Lipoxygenase metabolites
Leukotriene B_4, C_4, D_4, E
Platelet activating factors
Monohydroxyeicosatraenoic acids (5-, 12-, 15-)
Dihydroxyeicosatraenoic acids

REACTIVE OXYGEN METABOLITES
Superoxide anion
Hydrogen peroxide
Hydroxyl radical

ANTIOXIDANTS
Glutathione

COAGULATION FACTORS
Factor V
Factor VII
Factor IX
Factor X
1,25-dihydroxyvitamin D3
Thromboplastin
Prothrombin
Prothrombinase

Table 1.2 - Adapted from Fels & Cohn (1986) and Sibille & Reynolds (1990)

There are several other inflammatory mediators that also modulate the immune response during acute and chronic inflammation. IL-6, for example, is another cytokine with multiple activities such as B cell activation and induction of haematopoiesis. Studies have reported increased IL-6 release from macrophages as a result of air pollution particle exposure (Becker *et al.*, 1996 and Monn & Becker, 1999) and quartz exposure (Becher *et al.*, 2001). TGFβ is secreted by macrophages and has been described as a modulator of various cellular responses including cellular proliferation and differentiation, monocyte activation, cytokine release and leukocyte chemotaxis (Ashcroft, 1999). TGFβ has been shown to both activate and 'deactivate' monocytes and macrophages respectively (Wahl, 1992, Letterio & Roberts, 1998 and Ashcroft, 1999). TGFβ has also been shown to induce monocytes to release IL-6, IL-1 and TNFα, all regulators of acute inflammatory responses (Chantry *et al.*, 1989 and Turner *et al.*, 1990). With reference to TGFβ involvement in response to particle exposure, studies have demonstrated that TGFβ plays an important role in fibrogenesis and fibrosis in rat airways following ambient particulate exposure (Dai *et al.*, 2003). This group also demonstrated that inhibiting TGFβ receptors on airway cells prevented increases in the expression of genes involved in collagen production. Colony stimulating factors, including GM-CSF are involved in stimulating the growth and differentiation of cells such as granulocytes, eosinophils and macrophages. This cytokine therefore clearly plays an important role in allergic diseases such as asthma (Gormand *et al.*, 1995) where increased secretion of GM-CSF is observed. Studies such as that by Bayram *et al.*, (1998) and Boland *et al.*, (2000) have examined mechanisms by which diesel exhaust particles can stimulate GM-CSF release from epithelial cells.

The recruitment and subsequent migration of inflammatory cells to a site of particle deposition or inflammation is an important aspect of the immune response as it allows rapid removal of any foreign particles and a quick resolution of the inflammatory state. Chemokines, a family of chemoattractants, were first detected via the use of cytokine assays and, as such, were initially classified as members of the cytokine family. The primary function of macrophage derived chemokines is to act as chemoattractants to induce the recruitment of leukocytes to sites of infection or inflammation. There are generally two categories into which chemokines can be categorised based upon their molecular structure; CC chemokines and CXC chemokines. CC chemokines bind to CC chemokine receptors on cells and have two adjacent cysteine residues and CXC chemokines bind to the CXC receptors on cells and possess two cysteine residues separated by another amino acid. The less common C group of chemokines do not possess two of the possible four cysteine residues. (Janeway *et al.*, 1999). An example of a CXC chemokine would be IL-8 which is a chemoattractant for neutrophils whereas examples of CC chemokines include MIP-1α, MIP-1β, MCP-1 and RANTES which are all chemoattractants for monocytes.

Chemotaxins such as MIP-2 have been shown to be released from alveolar macrophages following exposure to air pollution particles (Dong *et al.*, 1996 and Ning *et al.*, 2000) and was reported to be present in increased concentrations in BAL fluid taken from rats exposed to quartz (Duffin *et al.*, 2001). Elevated MIP-2 levels were also found in BAL fluid of rats treated with various transition metals such as copper, zinc, manganese, iron, vanadium and nickel (Rice *et al.*, 2001). MIP-2 is a homologue of the human chemotaxin

IL-8 and is a potent chemoattractant for macrophages and neutrophils in rodents. It has also been reported that macrophages can release the complement protein C5, a pre-cursor to the macrophage and neutrophil chemoattractant C5a (Johnson & Hetland, 1988). Elevated levels of complement proteins have been described in individuals suffering from COPD and idiopathic pulmonary fibrosis (Lukacs & Ward, 1996). Warheit *et al.*, (1988, 1990) utilised hamster, rat, guinea pig and mouse models *in vitro* and *in vivo*, and suggested that alveolar macrophages were recruited to sites of particle deposition via a complement-mediated mechanism. This study referred to particles and fibres such as carbonyl iron, Zymosan, asbestos and fibreglass. The effects of particles on proteins of the complement system are discussed in greater detail in Chapter 3.

As can be seen from the studies conducted on macrophage secretory products and their role in both infection and particle induced inflammatory responses, the alveolar macrophage is an important mediator of the immune response. The macrophage not only removes particles from the lung but can also influence the migration of more inflammatory cells to a site of inflammation. Thus, further studies are warranted to determine the effects of inhaled particles on macrophage clearance mechanisms.

1.4 PARTICULATE AIR POLLUTION (PM_{10})

1.4.1 PM_{10} Characteristics and Components

The term PM_{10} is used to describe the mass of airborne particles collected by a method that has 50% efficiency for particles with an aerodynamic diameter of 10μm. The actual PM_{10} mixture comprises of a wide range of disparate materials sourced from various man-made and natural origins. The composition and toxicity of a given PM_{10} sample can vary enormously depending on a wide range of factors such as location, weather, wind direction and season (Schins *et al.*, 2004) or if the pollution is from indoor (gas cookers) or outdoor sources (Dick *et al.*, 2001). The PM_{10} components can be classified according to several different categories (table 1.3) (Stone *et al.*, 2003).

Method of Classification	Description	
Particle Size	Coarse	2.5 - 10μm diameter
	Fine	Less than 2.5μm diameter
	Nanoparticle	Less than 100nm diameter
Primary and Secondary	Primary	Remains in the form in which they were generated
	Secondary	Arise as a result of atmospheric chemical reactions
Organic and inorganic	Organic	Derived from living sources e.g. spores and pollen
Indoor and outdoor	Indoor	Generated by indoor sources such as cookers

Table 1.3 – PM_{10} component classification (adapted from Stone *et al.*, 2003)

Large particulate matter in the PM_{10} mixture, often called the coarse fraction, is predominantly composed of biological materials such as spores, pollen and small wind blown and soil particles. This component of the PM_{10} often has a basic pH. The fine and nanoparticulate (previously named the ultrafine fraction) components of PM_{10} are the fractions with the largest and most reactive surface area, most often having an acidic pH (Dockery and Pope, 1994). The coarse component of PM_{10} generally exists as single

particles while the fine and nanoparticle component can exist as single particles but can also exhibit a high degree of aggregation (Donaldson *et al.*, 2001 and Donaldson & MacNee, 2001). Approximately 50% of the particles in the fine and nanoparticle fractions are made of carbon and the rest of the particles are composed of metal salts as well as ammonium sulphates and nitrates (Harrison and Yin, 2000). The major contributing source to the small particulate mixture is traffic exhaust particles. A survey in London in 1990 ascribed approximately 87% of the mass of airborne particulate to diesel exhaust emissions (Bérubé *et al.*, 1999).

As well as the particulate component of air pollution there are also several other substances that contribute to the PM_{10} mixture. The interactions between each of these components and how they can contribute to the toxicological effects of air pollution as a whole have been widely studied and several hypotheses have been formulated to explain the toxicity of the PM_{10}. The transition metal content of PM_{10} has been implicated as a major factor in particle related toxicity. Exposures to metals have been assessed for their ability to cause pulmonary inflammation and exacerbation of disease. For example, it has been shown that exposure to metals can lead to pathological conditions such as COPD and pneumonia (Nemery, 1990 and Rice *et al.*, 2001). Obviously, the transition metal content of a given PM_{10} sample can differ from another depending on the source of the PM_{10}. Common metal components of PM_{10} include iron, zinc, copper, vanadium, cobalt, aluminium, manganese, titanium, silicon and sulphur (Tao *et al.*, 2003). The transition metals in PM_{10} can undergo Fenton chemistry to produce reactive oxygen species (See diagram 1.3). The redox-cycling of the metals can be accomplished due to the fact that

reducing agents such as glutathione, ascorbate and NADH are readily found in the lung (Smith and Aust, 1997). Adamson *et al.*, (2000) reported that zinc was the toxic factor in pulmonary responses to atmospheric air pollution. However, this study tested the toxic effects of individual metals and did not take into account mixtures of various metals or the interaction with other components of air pollution. Li *et al.*, (1996) showed that samples of PM_{10} demonstrated free radical activity both *in vivo* and *in vitro*. This was shown by the ability of the PM_{10} sample to deplete glutathione (GSH) levels *in vivo* and by the breakage of supercoiled DNA plasmid exposed to the PM_{10} sample *in vitro*. The depletion of the DNA plasmid could be prevented by the addition of mannitol, a hydroxyl radical scavenger. A study by Gilmour *et al.*, (1996) indicated that metals played an important role in the generation of the hydroxyl radical by PM_{10}. This was illustrated by the addition of a metal chelator, desferoxamine-B, which halted the depletion of supercoiled plasmid by PM_{10}. Donaldson *et al.*, (1997) examined the DNA cleaving potential of a PM_{10} solution that had been centrifuged to clarity and found that the supernatant exhibited the same potential as the uncentrifuged solution. This could indicate that that the free radical generating system had leached into the solution. It may also have been the case that the centrifugation of the solution did not completely remove all of the PM_{10} particles.

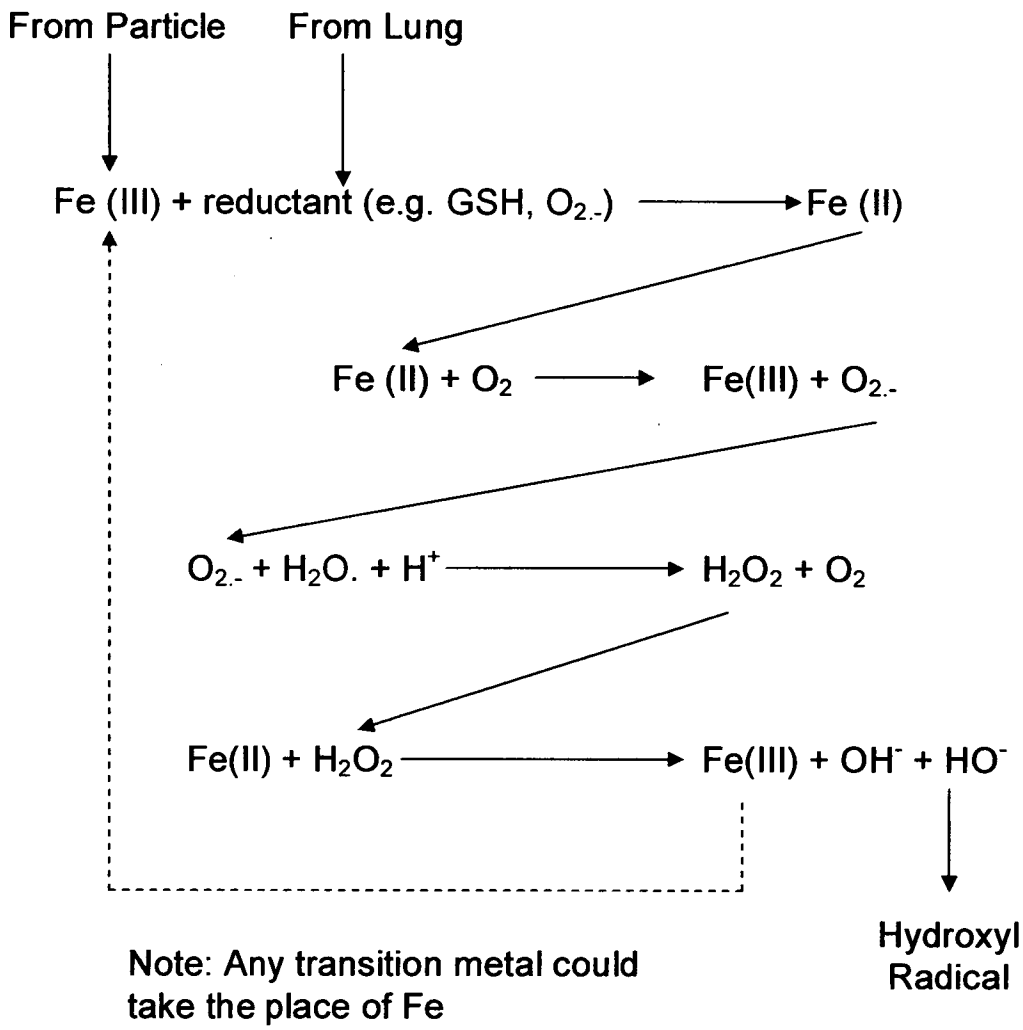

Figure 1.4 – The interaction of transition metal components with pulmonary reductants leading to free radical production (Diagram from Donaldson & Tran 2002).

Endotoxin is another component of PM_{10} that, in itself, is an inflammogenic substance which can induce the release of inflammatory mediators from macrophages and epithelial cells (Donaldson *et al.*, 2001b). Endotoxin or Lipid A, is the toxic part of lipopolysaccharide (LPS) which is a component of gram negative bacterial cell walls. It has been implicated as a factor in occupational respiratory diseases (Rylander & Haglind, 1984). Monn & Becker (1999), found that addition of lipopolysaccharide binding protein (LBP) to PM_{10} obtained from Chapel Hill, North Carolina prevented PM_{10} induced cytokine production by monocytes. This would indicate that the Chapel Hill endotoxin plays an important role in the induction of cytokine production by monocytes (Stone *et al.*, 2003).

Other components of $PM_{10,}$ which have received less attention than the particulates and metals, are the sulphates, nitrates and volatile organic compounds (VOCs) (Harrison and Yin, 2000). These substances may or may not interact with other PM_{10} components to play a role in pollution induced toxicity but this aspect of PM_{10} composition requires further study.

1.5 BIOLOGICAL EFFECTS OF PM_{10}

1.5.1 Background

The mammalian respiratory system has evolved many effective defence mechanisms to protect against foreign body entry into the airways and alveolar regions of the lungs. The airborne particle challenge that humans face today is different from that of 50 years ago, when sources of air pollution were dominated by particles from industrial and domestic burning of coal. These sources have decreased today, but the higher number of motor vehicles has increased the number of particles derived from traffic exhausts (Seaton *et al.*, 1995).

Mankind has been aware of diseases resulting from inhaled particles for hundreds of years and in this century, history demonstrates several air pollution 'disasters' (Donaldson *et al.*, 2001a and Folinsbee, 1993). In 1952, a smog enveloped London resulting in increased mortality as a result of cardiovascular and respiratory conditions. The UK Clean Air Act (1956) and subsequent amendment in 1993 reduced the level of air pollution and exposure standards for pollutants, but there continues to be great interest in air pollution particles due to changes in PM_{10} composition resulting from a decrease in industrial and domestic emissions but an increase in traffic emissions.

At least 200 epidemiological studies have been published on health effects of particulate air pollution. Airborne particle exposure, hospital admissions, health endpoints and mortality have all been well studied from different standpoints and since the 1970's, firm links have been established between particles and increased respiratory disease (Dockery

& Pope III., 1994). According to Donaldson *et al.*, (2000b) these health effects include the increased use of asthma medication, attacks of pre-existing lung diseases such as COPD and asthma, hospital admission attributed to cardiovascular disorders and deaths from heart attacks, strokes and respiratory disease. Whether these health effects are exclusively attributable to air pollution or whether other respiratory epidemics, such as those of influenza or pneumonia, are sometimes partially responsible for increased mortality is a potential cause for concern. A mathematical study conducted in the US by Braga *et al.*, (2000) showed that the association between air pollution and daily mortality was not affected by outbreaks of infectious respiratory disease. Schwartz (2001) developed an analysis, which was reported to differentiate between naturally occurring mortality and deaths that were induced by increased PM_{10} levels. The results indicated that during high pollution episodes, daily deaths and hospital admissions increased, but that there was no increase in deaths in hospitals, supporting the association between increased mortality and high levels of air pollution.

Some studies have focussed on the coarse and fine component of PM_{10} as being an important influence in the biological toxicity of PM_{10} (Englert., 2004) The debate as to which size fraction of PM_{10} can induce the greatest effect is a topic that is still under debate. The potential for fine and coarse particles to induce inflammation has been the subject of several studies. Hetland *et al.*, (2004) showed that the coarse and fine components in a sample of Norway PM_{10} were as effective as the nanoparticle fraction at inducing the production of IL-8 *in vitro* from the epithelial type II cell line A549. Schins *et al.*, (2004) found that the coarse component of rural and industrial PM_{10} samples from

Germany induced a higher degree of inflammation than the fine component *in vivo*. This increased inflammation was associated with the endotoxin component of the PM sample although it was suggested that other biological or chemical contaminants might have been involved. Monn & Becker (1999) found that monocyte secretion of IL-6 and IL-8 induced by the coarse fraction of North Carolina PM_{10} was 20 fold greater than that observed following treatment with the fine fraction. Cytotoxicity, as assessed by trypan blue exclusion, yielded similar results. Murphy *et al.*, (1998) concluded that, following an instillation study with several different types of fine particles, the surface chemistry of the fine particle was an important determinant of the particle effects on rat epithelial cells. Pope *et al.*, (2002) conducted an epidemiological study, which indicated that independent of coarse particle increases, elevation of fine particle concentration in the environment caused significant increases in cardiopulmonary and lung cancer mortality rate.

Many authors have suggested that the nanoparticle component plays the most important role in driving the health effects of PM_{10} (Seaton *et al.*, 1995, Donaldson & MacNee., 1998, Oberdorster *et al.*, 1995). Nanoparticles are the most numerous type of particle in PM_{10} as well as possessing the largest portion of the particulate surface area (Harrison & Yin, 2000). Many studies have demonstrated increases in cytokine concentration in the lavage fluid of animals treated with nanoparticles (Gilmour *et al.*, 2004 and Li *et al.*, 1999). Studies have also shown an increase in calcium levels in cells exposed to nanoparticles (Stone *et al.*, 2000a and Brown *et al.*, 2000). Other studies have demonstrated a direct toxicological effect on macrophages exposed to nanoparticles.

Lundborg *et al.*, (1999 and 2001) and Renwick *et al.*, (2001) showed impaired macrophage function following nanoparticle exposure. Möller *et al.*, (2002) further confirmed these results, indicating that the toxicological effect of the nanoparticles on the macrophages' cytoskeleton was critical in affecting macrophage movement and phagocytosis. As described in chapters 4 and 5, a reduction in the efficiency of clearance mechanisms could result in further damage in a lung that has encountered prolonged particle exposure.

Generally, cardiovascular factors such as increased blood coagulabilty caused by changes in fibrinogen and factor VII concentration (Seaton *et al.*, 1995) and changes in cardiac electrical activity (Utell & Frampton, 2000 and Dockery, 2001) have been reported as a result of increased particle exposure. It is possible that no one single component of PM_{10} is toxic enough to be responsible for the adverse health effects linked to air pollution and it is by examining the interaction of particulates in target organs such as the lung that we can hope to obtain a clearer picture of the events surrounding the toxicology of air pollution particles.

1.5.2 Particle Entry & Deposition in the Lung

Particle entry and site of deposition in the lung is determined by the particle size and degree of aggregation. The site of particle deposition is important as it determines the type of cells that will be exposed to the particles. The depth that particles enter into the lung airways is inversely proportional to their size i.e. smaller particles have access to a greater depth in the lung such as the alveolar areas (Adamson and Bowden, 1978).

Larger particles (diameter > 20μm) deposit in the upper respiratory tract and particles with a diameter of 5 – 15μm can deposit in the conducting airways and upper bronchial areas as well (Heyder *et al.*, 1986). Particles with a diameter of between 1 and 5μm can also access the terminal airways (Stahlhofen *et al.*, 1983,1989) and those with a diameter of less than 1μm may also deposit in the alveolar sacs (Heyder *et al.*, 1986). The deposition in the alveolar region occurs via diffusion or Brownian motion i.e. the bombardment of the particles with other molecules causing movement (Hofmann *et al.*, 2003). These figures describe individual particulates although particle collections with a high degree of aggregation can have an altered deposition pattern. However, the high lipid content of the surfactant lining the airways may change the aggregation properties of the particles.

Humans have a symmetrical pattern of respiratory zones which favours concentrated deposition of particles at bifurcations (Warheit and Hartsky, 1990). Focal deposition of particles may result in greater localised cellular trauma whereas an evenly distributed pattern of particulates may not be as damaging. Furthermore, humans may prefer to breathe through the mouth during exercise and vocal communication allowing greater particle entry into the lungs (Lippmann and Schlesinger, 1984). This is in comparison to rodents, which breathe through the nose, a factor that has to be taken into account when studying particle deposition using animal models. The particulate mass that is taken into the lungs is also dependant upon the ventilation rates of the individual (Miller, 2000).

An important study by Churg and Brauer, (2000) examined the deposition of ambient particulates in human airways. Examinations of particle deposition in subjects from Vancouver (a city with relatively low levels of PM) showed high concentrations of particles in the mucosa, and that increasing particle number correlated with decreasing airway diameter. Large numbers of particles were also observed in the respiratory bronchioles. It has been shown that the deposition fraction of nanoparticles in the lung is around 50% and that this figure can be higher in individuals with lung disease (Anderson *et al.*, 1990). Brown *et al.*, (2002) describe the deposition of particles in healthy individuals and those with obstructive lung diseases such as chronic obstructive pulmonary disease (COPD). The authors noted that COPD afflicted individuals may also receive an increased nanoparticle dose due to increased ventilation rate and resulting particle intake. Similar observations are noted in the increased ventilation responses of individuals undertaking exercise (Daigle *et al.*, 2003). The translocation of inhaled particles and subsequent deposition in other areas of the body are described in section 1.6.8.

1.5.3 Susceptibility to PM_{10} Induced Disease

Health effects influenced by PM_{10} exposure are frequently seen in individuals with pre-existing respiratory or cardiovascular conditions and very rarely seen in healthy individuals (Donaldson *et al.*, 2001b). Stone, (2000b) reviews several of the categories into which susceptibility to PM_{10} induced disease can be placed. Individuals who are *susceptible to exposure* are those that are exposed to airborne particulates as a result of lifestyle or occupational factors. Populations living in urban areas where traffic

emissions are high will be exposed to greater concentrations of combustion-derived particulate than those living in rural areas. Similarly, individuals who smoke or work in areas or trades that have a high airborne particulate content will also be exposed to a greater number of particles (Clouter *et al.*, 2001 and Lemiere *et al.*, 2000). A second category of susceptibility is the *susceptibility to response,* which describes individuals that have a pre-existing condition that could affect the inflammatory response to particles. Individuals with diseases such as asthma (Penttinen *et al.*, 2001 and Donaldson *et al.*, 2000b) and COPD (MacNee & Donaldson, 2000) or those that have experienced a viral infection (Gilmour *et al.*, 2001) may be primed to generate a magnified inflammatory response to particle exposure when compared to healthy individuals (Ning *et al.*, 2003). Studies have also shown that exposure to diesel exhaust particles can increase the susceptibility of the lung to subsequent viral or bacterial infection (Castranova *et al.*, 2001).

The final category of susceptibility deals with the *susceptibility to increased dose* where the clearance efficacy of macrophages dealing with deposited particles determines the dose to which the individual is exposed. This category also includes the physiological behaviour of the individual and the frequency of respirations, which can determine the ventilation volumes, and particle dose which is inhaled into the lungs. As described previously, COPD patients often have increased ventilation rate and deeper breaths, lending favour to increased particle exposure (Brown *et al.*, 2002). COPD patients and cigarette smokers often have damage to cilia, decreasing the effectiveness of the MCE in

clearing particle-laden macrophages and particles themselves (MacNee and Donaldson, 2000).

1.5.4 Particle Clearance Kinetics

In terms of the speed of particulate removal from the lung, MCE clearance is a fast process, which can very rapidly remove particles from the bronchial areas. However, alveolar macrophage mediated clearance is very slow. In a study by Oberdorster *et al.*, (1994) it was reported that rats inhaling nanoparticle TiO_2 showed increased retention half times compared to rats exposed to fine TiO_2 (117 days for fine compared to 541 days for nanoparticles). This illustrates both the length of time that particles can remain in the lung and the biopersistence of nanoparticles. Ferin *et al.*, (1992) reported similar figures following 12 week exposure studies to TiO_2 (501 days for nanoparticle TiO_2 compared to 174 days for fine TiO_2). Oberdorster (1995) reported that, the alveolar retention halftime of macrophage mediated clearance is around 70 days in the rat. Bailey *et al.*, (1985) reported alveolar retention halftimes of radiolabelled silicate nanoparticles upwards of 350 days in humans. Wanner (1977) reported that MCE clearance was fastest in the trachea and central bronchi where it is estimated that particles are moved up the MCE at a rate of around 1 cm per minute. Clearance in the peripheral bronchi is moderately slower. However, as described by Oberdorster *et al.*, (1994), the clearance time of a given particulate is dominated by the particle characteristics.

1.5.5 Overload

Dust overloading in the lungs is a hypothesis that has been used to account for pathogenic changes in the lungs induced by the inhalation of high concentrations of low toxicity dusts. Several studies have reported that large concentrations of dusts that have a low toxicity can cause a decrease in macrophage clearance resulting in pathological conditions such as fibrosis, cancer and epithelial cell hyperplasia (Morrow, 1988, Oberdorster 1994, 1995, Warheit *et al.*, 1997 and Lee *et al.*, 1985). As described previously, alveolar macrophages phagocytose particles and migrate out of the lung via the MCE without the release of large concentrations of pro-inflammatory mediators. If high numbers of particles are phagocytosed by the macrophages, it is thought that the phagocytic potential of the macrophage decreases and the macrophage appears to remain in the alveolar space instead of migrating out of the lung (Morrow, 1988). Morrow estimates that when 6% of the internal volume of the macrophage is occupied the clearance potential of the macrophage is affected. Dorger & Krombach (2000) report that when 60% of the macrophage volume is occupied by particles, the macrophage migratory mechanisms are completely retarded and the macrophage becomes unable to translocate to the MCE. This scenario would encourage more interaction of particulates with the epithelial cells in the alveolar space and would result in an increased pro-inflammatory mediator release. This would also increase the potential for transepithelial migrations of particles resulting in further epithelial permeability and interstitial inflammation. It is possible, however, that some of these problems could be countered by re-phagocytosis of the particulates that have been released from lysed macrophages. However, this would further increase the alveolar retention time of the particulate. Driscoll (1996) found that

when different types of instilled particles were compared, lung tumours were most commonly found with nanoparticles. This led to the hypothesis that lung overload is related to the particle surface area as opposed to the mass dose. Tran *et al.*, (2000) supported this by demonstrating that impairment of clearance mechanisms was dependent upon the surface area and not the mass of deposited particles. This was accomplished by allowing rats to inhale an equivalent mass of two poorly soluble dusts with different surface areas (TiO_2 and $BaSO_4$). It was found that the TiO_2 induced a greater amount of inflammation in the lung compared to the $BaSO_4$ at an equivalent mass. This inflammation was attributed to the larger surface area of the TiO_2. These studies support the hypothesis that increased surface area and free radical generation by nanoparticles is the primary cause of nanoparticle induced overload conditions.

1.5.6 Oxidative Stress

There are several different types of oxidants to which the lung can potentially be exposed. These can include molecular oxygen, ozone and reactive oxygen species (which in turn include hydrogen peroxide, hydroxyl radicals and superoxide) (Putman *et al.*, 1997). The term 'free radicals' describes a reactive species that can exist independently i.e. possessing at least one unpaired electron. When the term reactive oxygen species is used, this refers to reactive species with an oxygen centre such as superoxide and hydrogen peroxide. Reactive nitrogen species such as nitric oxide and the extremely toxic peroxynitrite can also be present although it should be noted that nitric oxide is relatively unreactive (Halliwell, 2001). Free radical species can react with the biological molecules present within an organism and change their biochemical properties

or cause severe damage (Putman *et al.*, 1997). The lung has evolved various mechanisms for dealing with these oxidant species. For example the epithelial lining fluid contains high concentrations of antioxidants and free radical scavengers such as vitamin E and glutathione (Freeman & Crapo 1982). As free radicals are essential for some biological processes and are produced as normal by-products of metabolism, the presence of radicals in the lung does not routinely cause large amounts of damage. However, the presence of reactive particles and transition metals in the lung can result in excess free radical release and pathological consequences for lung pneumocytes.

Free radicals can cause damage to several components in both living cells and their secretions and have implicated as disease causing agents for over 100 different pathological conditions. Freeman & Crapo (1982) provide a comprehensive review of the cellular targets that are susceptible to free radical damage. These include proteins such as enzymes, which can be denatured or inactivated by free radical exposure, DNA molecules and cellular membrane lipids (see table 1.5).

Target	Consequence
DNA	Cell cycle changes and mutations, strand scission, apoptosis
Carbohydrates	Cell surface receptor changes
Unsaturated Lipids	Cholesterol and fatty acid oxidation Changes in cell permeability Lipid peroxidation
Antioxidants	Decreased availability, oxidation, inactivation
Proteins	Denaturation and peptide chain scission
Tissue	Gross damage leading to fibrinogenesis and cancer

Table 1.5 - Biological targets of free radical damage (adapted from Freeman & Crapo, 1982)

As mentioned previously, there have been several studies demonstrating the potential for PM_{10} particles to generate free radicals and reactive oxygen species as a result of the particle surface chemistry and interaction with metals. Studies by Li *et al.*, (1996) and Gilmour *et al.*, (1996) demonstrated that PM_{10} could actively generate free radicals and that this phenomenon was potentially related to the iron content of the samples. Donaldson *et al.*, (1996) used a similar method to demonstrate that nanoparticle TiO_2 showed an enormous potential to damage a DNA plasmid in comparison to fine TiO_2, which induced only modest strand breakage. This evidence for reactive oxygen species involvement in nanoparticle toxicity was further enhanced by the addition of mannitol to the plasmid/particle mixture, which was found to ameliorate the effects of the nanoparticles. Carter *et al.*, (1997) reported that cytokine production by epithelial cells exposed to air pollution particles was inhibited by the addition of metal chelators or by free radical scavengers. Pritchard *et al.*, (1996) also noted that the surface metals of particulates could influence the potential for the production of ROS and subsequent inflammatory response in a rat model. Dick *et al.*, (2003) recently reported on the potential of four different nanoparticle types (carbon black, nickel, cobalt and TiO_2) to generate oxidant species. It was found that the cobalt, nickel and carbon black all generated high numbers of free radicals as indicated by depletion of supercoiled plasmid DNA. This was correlated with the potential of the more reactive particles to induce greater neutrophil recruitment into the lung following instillation into the rat lung. Donaldson *et al.*, (2003) recently reported that PM_{10} induced oxidative stress could activate pro-inflammatory signalling pathways in cells such as nuclear factor-kappa B

(NF-κB). Free radicals sourced from macrophages that have been activated by particle exposure could also potentially cause further damage (Freeman & Crapo, 1982).

The lung is an environment where the generation of oxidative stress can occur due to the high concentrations of oxygen and the presence of metals such as iron from inhaled particulates. As the human body does not possess mechanisms for the excretion of excess iron, the lung has therefore evolved effective methods for the regulation of metal content in order to minimise oxidative mechanisms that could potentially be damaging to cells. Turi *et al.*, (2004) lists several proteins including lactoferrin, ferritin and transferrin, which are involved in iron sequestering and regulation. Ferritin is an intracellular protein contained in the lung epithelium that sequesters iron that has been transported across the cell membrane. The potential therefore exists for particle induced cellular damage to allow more free iron to be released and allowed to react to form excessive reactive oxygen species. This could then lead to further damage via oxidant production.

1.5.7 Complement Activation by Particles

There have been many studies showing that asbestos can activate the alternative complement pathway (i.e. antibody independent), resulting in the generation of C5a proteins, a known chemoattractant. Saint-Remy *et al.*, (1980), Wilson *et al.*, (1977) and Warheit *et al.*, (1985) have all demonstrated that asbestos fibres have the capacity to activate the alternative complement pathway. Kanemitsu *et al.*, (1998) reported that diesel exhaust particles could activate complement. In a more recent publication by

Governa *et al.*, (2002), crystalline silica was also found to have the potential to cleave the complement protein C5 to produce a C5a-like product. This was hypothesised to be due to oxidative stress taking place via redox-active iron present on the silica surface. This obviously has important implications for silica-induced lung disease as well as stimulating questions regarding particulates and their potential to activate the alternative complement cascade. Donaldson & Tran., (2002) suggest that as PM_{10} is reported to contain endotoxin, it is likely that PM_{10} would initiate the complement cascade. Warheit *et al.*, (1988) concluded that alveolar macrophages are attracted to sites of deposition via complement activation and that the clearance of a given particulate depends on its potential to activate complement.

As mentioned previously in section 1.5.6, there have been several studies showing that the large surface area of fine and nanoparticles demonstrates a high potential for the generation of reactive oxygen species and their subsequent cytotoxicity following inhalation or instillation into the alveolar space. For example, in a study by Li *et al.*, (1996), it was shown that PM_{10} generated free radical activity *in vitro*, and induced oxidative stress *in vivo* resulting in pulmonary inflammation. A study by Gilmour *et al.*, (1996) supported these findings, stating that hydroxyl radicals were generated by PM_{10} and that, this too occurred via an iron-dependant mechanism. Governa *et al.*, (2002) demonstrated that silica had the capacity to induce the generation of a C5a-like protein, perhaps due to the oxidative stress generated on the silica surface.

1.5.8 Particle Translocation into Interstitium and CV System

Although the epithelium of the lung appears to be the target tissue when examining airborne particle exposure through inhalation, it has been shown that particles have the potential to breach the epithelial barrier and migrate into the interstitium and cardiovascular circulation (Ferin *et al.*, 1992; Frampton, 2001 and Nemmar *et al.*, 2002). This creates the possibility that other tissues may be exposed to airborne particulates.

When particles deposit in the alveolar space, the primary mechanism of clearance is via phagocytosis by alveolar macrophages. However, if large numbers of particles are deposited and allowed to interact with the epithelial cells before phagocytosis can take place or if particle numbers are too high for macrophages to deal with, as in the case of particle overload, the epithelial cell function and integrity could be compromised as a result of particle exposure. This could result in increased inflammation, epithelial permeability and a chronic inflammatory state (Mauderly, 1996). When the epithelial layer has been damaged, it is possible for deposited particles, as well as inflammatory mediators produced in the lung, to enter the interstitium, lymph nodes and systemic circulation (Lehnert *et al.* 1986 and Donaldson *et al.*, 2001b) as the numerous studies detailed below have shown.

Ferin *et al.*, (1992) exposed rats to airborne fine and nanoparticle TiO_2 for 12 weeks and noted increased inflammation with the nanoparticles. It was also noted that there was an increase in the transfer of nanoparticles to the interstitium compared to the fine particles. This was attributed to the inflammation caused by the nanoparticles as well as the fact

that the type I cells in the rat lung had taken up the unphagocytosed particles. Previous studies had noted transepithelial migration to hilar or pleural lymph nodes (Adamson & Bowden, 1981, Ferin & Feldstein, 1978 and Lippmann *et al.*, 1980). Lee and colleagues (1985) found TiO_2 deposits in the lymphatic vessels and trace amounts in the systemic circulation in rats exposed by inhalation for 2 years. Nemmar *et al.*, (2001) noted that intratracheal instillation of radiolabelled nanoparticles into hamsters resulted in the particles being observed in the systemic circulation. It was subsequently determined by Nemmar *et al.*, (2002) that, in humans, inhaled radiolabelled particles could quickly pass into the systemic circulation (within 1 minute of inhalation). Rahman *et al.*, (1996) indicated that, in a study of smokers and individuals with COPD and asthma exacerbations, systemic antioxidant activity was decreased indicating an increased susceptibility to oxidative stress induced by particles. Very recently, Oberdorster *et al.*, (2004) demonstrated carbon nanoparticle entry into the cerebrum and cerebellum of rats exposed to the particles by inhalation. This suggested that translocation of these particles into the olfactory bulb region of the brain could bypass the blood-brain barrier and that further studies are warranted to determine the health effects of central nervous system (CNS) exposure to inhaled particles

In terms of health effects of particle translocation, these are determined by the particle properties (i.e. potential for reactive oxygen species generation), the number of particles and the areas to which translocation has taken place. It has already been established that smaller particles display a greater potential for epithelial damage and subsequent translocation due to their small size and reactive surface. Stone *et al.*, (1998)

demonstrated that nanoparticle carbon black induced greater oxidative stress in epithelial type II cells than an equivalent dose of fine CB. When taking into account the studies by Ferin *et al.*, (1992) and Rahman *et al.*, (1996), the potential for nanoparticles to cause systemic damage via oxidative stress is high. Dockery & Pope (1994) observed that total mortality increases by 1% per $10\mu g/m^3$ increase in PM_{10} levels. A stronger association for cardiovascular mortality is also observed (1.4% per $10\mu g/m^3$ increase in PM_{10}), illustrating the potential for extrapulmonary effects of inhaled particles. Seaton *et al.*, (1995) suggested that increased coagulabilty of the blood may be a causal agent and Peters *et al.*, (1997) supported this hypothesis by demonstrating an increased plasma viscosity in a population exposed to an incidence of increased atmospheric particulate matter. Salvi *et al.*, (1999) showed an increase in the number of circulating platelets in the blood of humans exposed to diesel exhaust particles. Donaldson & MacNee (2001) hypothesised that production of procoagulants from the liver could also occur via IL-6 and TNFα release into the circulation by pulmonary inflammatory cells. Together with increases in cardiac arrhythmias and heart rate (Dockery, 2001) it is likely that increases in blood coagulabilty and plasma viscosity could lead to incidents involving thromboses and a resulting increase in mortality from particle induced cardiovascular conditions.

1.6 SURROGATE AIR POLLUTION PARTICLES

The surrogate particles utilised in this study were fine and nanoparticle forms of carbon black and titanium dioxide. The particle characteristics are outlined below in Table 1.6

DUST	GEOMETRIC DIAMETER (nm)	SURFACE AREA (m^2/g)
Fine TiO_2	250	6.6
Nanoparticle TiO_2	29	49.78
Fine carbon black	260.3	7.9
Nanoparticle carbon black	14.3	253.9

Table 1.6 Particle Characteristics (From Brown *et al.*, 2000)

1.6.1 Carbon Black

Carbon black is a paracrystalline carbon compound that is utilised in a wide variety of industrial processes (Degussa Technical Bulletin 15, 1986). It is utilised primarily by the rubber industry for the production of tyres although it is also used in printing inks, plastics, fibres, paper and in the construction (cement pigment) and electrical (carbon electrodes) industries. There are several methods that are employed for generating carbon black, all of which involve thermal or thermal-oxidative (partial combustion) decomposition (IARC Monographs, 1996). Approximately 98% of all industrial carbon black produced (6 million tonnes annually) is via the furnace black process. The raw materials used in this process include oils with a high hydrocarbon content and bituminous coal tar. The particles that are produced by this industrial process are between 10 and 100nm in size although various specifications of the particles can be altered including the surface area and aerodynamic diameter depending on the destined

application of the particles. The particles can also form long branching aggregates depending on the chemical composition (Degussa Technical Document – What is Carbon Black?).

The composition of carbon black can vary depending on its type, but it is essentially 95 – 99% colloidal carbon. Several other elements such as hydrogen, oxygen, nitrogen and sulphur are also bound to the carbon atoms. Depending upon the production method and type of carbon black, there are also some negligible traces of metals which can be extracted from the surface of the carbon particles. These include common elements such as iron, calcium and magnesium as well as more uncommon heavy metals such as barium, lead, cadmium, chromium and zinc (Degussa Technical Document – What is Carbon Black?). The presence of extractable carbon black components was also examined by Degussa by boiling carbon black in toluene and it was determined that extraction residues from the carbon black was minimal. These results were supported in a study by Brown *et al.*, (2000) which indicated that inflammation induced by nanoparticle carbon black was not caused by the presence of soluble component leaching from the surface of the particles.

The carbon blacks utilised in this study were fine and nanoparticle forms produced by the thermal black and furnace black processes respectively. The average diameter of the individual primary particles of fine carbon black was around 260nm and for the nanoparticle, 14nm as described by Renwick *et al.*, (2001) and Stone *et al.*, (1998). These particles were chosen as surrogate air pollution particles as they are well

characterised in terms of physical properties and composition and have the potential to induce a high degree of biological reactivity (Wilson *et al.*, 2002; Stone *et al.*, 1998).

1.6.2 Biological Effects of Carbon Black

The biological reactivity of carbon black has been investigated in several studies as a surrogate particle representing the particulate component of atmospheric air pollution. However, it is important when assessing these studies to highlight the distinction between the biological effects of the fine and nanoparticle forms of carbon black. Many *in vivo* investigations have been conducted which compare and contrast the inflammatory effects of the two types of carbon black (Driscoll *et al.*, 1996a, Li *et al.*, 1999, Brown *et al.*, 2000, Donaldson *et al.*, 2001a). The IARC has classified carbon black as a group 2B carcinogen, surmising that it could possibly be carcinogenic in humans. The occupational exposure limits for workers in the UK in an industry where carbon black is present is 3.5mg/m^3 (Degussa Technical Safety Bulletin 25, 1990). This does not take into account the size of particles in question, for example, an exposure metric of nanoparticles assessed by weight would contain a considerably higher number of individual particulates and a larger surface area than the equivalent mass of fine particles.

A study by Driscoll *et al.*, (1996a) examined the effects of short term inhalation exposures of rats to carbon black particles in the nanoparticle size range and illustrated several adverse inflammatory responses. It was observed that increased inflammation, fibrosis and increased chemokine expression were all associated with the particulate exposure. A higher incidence of gene mutation also occurred in alveolar epithelial cells

in rats that had been exposed to the higher doses of the carbon black. Li *et al.*, (1999) also compared the rat inflammatory response as a result of carbon black exposure, using both fine and nano-sized forms of the particle. This study supported the results of Driscoll *et al.*, in that instillation with nanoparticle carbon black induced pulmonary inflammation at a relatively low dose. The inflammation brought about by the nanoparticle exposure was also greater in intensity compared to the fine particles, as demonstrated by a greater neutrophil influx, increased LDH levels and a marked decrease in glutathione. Li *et al.*, (1996) had previously compared the effects of nanoparticle carbon black to those of fine carbon black and PM_{10}. This study illustrated that nanoparticle carbon black induced a greater neutrophil influx, decreased glutathione and increased epithelial permeability 6 hours post-exposure, than both the fine carbon black and PM_{10}. Increased epithelial damage and neutrophil influx as well as glutathione reduction was also reported by Donaldson *et al.*, (2001a).

Investigations were also conducted to determine the cellular basis for the increased inflammatory response to nanoparticle carbon black in rats. As mentioned previously in section 1.5.1 Lundborg *et al.*, (1999), Renwick *et al.*, (2001) and Möller *et al.*, (2002)also reported decreased phagocytic ability and cytoskeletal toxicity in macrophages exposed to nanoparticle carbon black. Investigations have also focused on the reactive oxygen species production by nanoparticles and the possibly detrimental effects on pulmonary function. In 1998, Stone *et al.*, demonstrated that oxidative stress was involved in the toxicological effects exerted on epithelial cells by nanoparticle carbon black. It was shown that fine carbon black could decrease the metabolic competence of epithelial cells

at a timepoint of 24 hours but that this had recovered to control levels at 48 hours. In contrast, the group found that nanoparticle carbon black caused a decrease in metabolic competency at 48 hours compared to the control. The study by Wilson *et al.*, (2002) indicated that, *in vitro* and in the rat lung, nanoparticle carbon black can react with transition metals in a potentiative manner to produce reactive oxygen species which would be potentially damaging in a biological environment such as the lung.

1.6.3 Titanium Dioxide

Titanium is an extremely common element and can form over 40 different minerals when it combines with other elements. In industry it can be converted to metal titanium, or can be utilised in the production of other useful compounds (Lee *et al.*, 1985). Titanium dioxide (TiO_2) is a dust that is used widely in the manufacturing and cosmetics industries having replaced white lead and zinc white due to the fact that TiO_2 is regarded as being relatively biologically inert. TiO_2 is formed mainly from ilmenite ($FeTiO_3$) and is used to produce paint, paper, plastic ceramics, inks and other products (IARC Monograph, 1989 and Chen & Fayerweather, 1988). It commonly exists in one of three crystal lattice forms; tertragonal rutile, tetragonal anatase or rhombic brookite. Anatase and rutile are produced in large amounts on an extensive industrial scale by wet processes (Degussa Technical Bulletin 64, 1992).

Exposure of workers to TiO_2 can occur in an industrial setting, especially when titanium dioxide pigment is ground to a finer dust, where atmospheric concentrations can be up to 400mg/m^3 (Elo *et al.*, 1972). As TiO_2 is generally regarded as a nuisance dust with low

biological activity, many countries have not set a specific exposure limit, deciding instead to use the general limit for exposure to dust in the workplace which is $10mg/m^3$ in the UK (Rehn *et al.*, 2003 and Degussa Technical Bulletin 64, 1992).

In this study, both fine and nanoparticle forms of titanium dioxide were utilised. The fine TiO_2, obtained from Tioxide Ltd, has a diameter of 250nm. The nanoparticle form, obtained from Degussa, has a primary particle diameter of 29nm. The surface areas of the two forms of TiO_2 used in this study are 6.6 and 49.78 m^2/g for the fine and nanoparticles respectively (Renwick *et al.*, 2001). As well as existing as single particulates, the TiO_2 particles may also exist as branching aggregates with a marginally lower surface area than that of polydispersed non-agglomerated TiO_2 particles.

1.6.4 Biological Effects of Titanium Dioxide

The biological and toxicological effects of TiO_2 exposure have been well established by many independent studies in that most have concluded that it is a relatively inert dust with a low biological reactivity (IARC Monographs, 1989, Chen & Fayerweather., 1988, Elo *et al.*, 1972, Lee *et al.*, 1985, Driscoll *et al.*, 1990). The IARC classified TiO_2 as a group 3 carcinogen, meaning that there is very little evidence for TiO_2 exposure resulting in cancer in humans. The IARC also examined animal studies with various exposure routes (oral, intratracheal instillation, inhalation and subcutaneous injection) and found that only very high doses given by inhalation increased the incidence of adenomas and carcinomas within the lungs of the animals. Many other studies have focussed on animal models to establish pulmonary responses to TiO_2, most commonly utilising the rat as the

test subject. Lee *et al.*, (1985) conducted a chronic inhalation study exposing rats to TiO_2 for two years. This group showed that no abnormal clinical manifestations or increased mortality occurred in the test animals and that only very high doses ($250mg/m^3$) induced the occurrence of bronchioalveolar adenoma and squamous cell carcinomas.

Ferin *et al.*, (1992) conducted an investigation looking at the retention of TiO_2 particles in the lung and recorded several observations. It was noted that the nanoparticle forms of the TiO_2 entered the interstitium much more readily and rapidly than the larger particles and that this was attributed to the particle size and a trend in increased interstitialisation as a result of increased dose. The numbers of lavaged neutrophils were higher in the nanoparticle TiO_2 rats than those in the rats exposed to fine TiO_2 indicating a higher level of inflammation. Creating a clear picture of the response of rats to high doses of TiO_2, Warheit *et al.*, (1997) examined the effects of high doses of TiO_2 over a period of 4 weeks. This investigation resulted in the observation that inflammation, as well as impairment of macrophage clearance mechanisms could occur when even a relatively innocuous dust is given in high doses. The deficiencies in the clearance mechanisms were ascribed to the *in vitro* examination of the decrease in phagocytic ability and chemotactic potential of the macrophages from the particle treated animals.

Another two studies, which examined the effects of the surface coating of titanium dioxide particles in inflammatory responses in rats, also raised issues regarding TiO_2 toxicity. A key paper by Höhr *et al.*, (2002) suggested that the surface area of TiO_2 was responsible for the level of inflammation displayed in treated rats as opposed to the

surface coating of the particles. The group used hydrophobic (surface treated) and hydrophilic forms of fine and nanoparticle TiO_2. After examining the inflammatory effects of both the surface treated and the untreated forms of the TiO_2, the group suggested that it was, in fact, the surface area of the dust that determined the inflammatory response rather than the surface coating. These findings were supported in an instillation study by Rehn *et al.*, (2003) who examined the inflammatory effects of surface treated TiO_2. The results indicated that the rats instilled with surface treated TiO_2 samples (silanized with a hydrophobic surface) showed a similar low level of inflammation and DNA damage as the rats instilled with untreated (hydrophilic surface) TiO_2.

Studies concerned with the effects of titanium dioxide exposure in man have also been conducted both from an epidemiological and pathological standpoint. Elo *et al.*, (1972) compared the levels of TiO_2 found in lung tissue samples from normal individuals to those from factory workers exposed to TiO_2 pigments on a daily basis. The study found titanium present in the tissue as well as in the interstitium and lymphatic vessels of the factory workers. This was accompanied by the presence of a mild amount of lung fibrosis. An epidemiologic study by Chen and Fayerweather (1988) investigated whether workers exposed to TiO_2 demonstrated higher levels of lung cancer, fibrosis or chronic respiratory disease. This investigation suggested that exposure to TiO_2 did not increase the risk associated with developing pulmonary fibrosis or any other pathogenic respiratory condition.

1.7 AIMS

The aim of this thesis was to investigate the effects of particulates on clearance mechanisms present within the lung. The influence of particles on the primary clearance functions of macrophages, such as phagocytosis and chemotaxis was assessed, together with peripheral factors affecting particle clearance such as complement activation and chemotaxin secretion by epithelial cells. The interaction between nanoparticles and zinc was also examined with a view to determining the consequences on macrophage phagocytosis.

The aim of the first data chapter (chapter 2) was to assess the potential for particles to induce chemoattractant release from type II cells and the potential for the chemoattractant to affect macrophage migration. It was hypothesised that exposure to fine and nanoparticles will result in the secretion of chemotactic proteins from type II cells and that these proteins play a key role in the recruitment of pulmonary macrophages to sites of particle deposition and inflammation.

The aim of chapter 3 was to assess the potential for fine and nanoparticles to activate the alternative complement cascade in blood serum is investigated using the macrophage chemotaxis assay described in chapter 1. It was hypothesised that, due to their reactive surface chemistry, that nanoparticles will activate the alternative complement cascade and induce the generation of the chemotactic complement protein C5a. It was also hypothesised that exposure of blood serum to PM_{10} extracts or a pure oxidant such as tert-butyl hydroperoxide (tBHP) will also result in C5a production.

The aim of chapter 4 was to investigate the effects of PM_{10} extracts on the pulmonary macrophage clearance functions of phagocytosis and chemotaxis using an animal model. Biochemical measurements of pro-inflammatory cytokines present in the bronchoalveolar lavage fluid were also conducted with a view to assessing any lung damage that had occurred. It was hypothesised that the PM_{10} samples would decrease macrophage phagocytic and chemotactic potential and cause increases in the concentrations of pro-inflammatory cytokines and proteins present in the bronchoalveolar lavage fluid.

The final data chapter (chapter 5) aimed to investigate the interaction between carbon black nanoparticles and zinc salts. The consequences on the phagocytic potential of a macrophage cell line exposed to zinc and nanoparticle carbon black was assessed. This chapter forms part of a larger study which aims to determine the effects of zinc and nanoparticles on various aspects of macrophage function including cytokine production and cytoskeletal changes. It was hypothesised that, when mixed together and added to a macrophage cell line, the zinc and nanoparticles will interact in a synergistic manner to decrease the ability of a macrophage cell line to perform phagocytosis.

CHAPTER 2

MACROPHAGE MIGRATION INDUCED BY TYPE II EPITHELIAL CELLS EXPOSED TO FINE AND NANOPARTICLES

2.1 INTRODUCTION

2.1.1 Type II Cells and Inflammation

Chemotaxis is the movement of leukocytes towards a chemotactic substance i.e. where the direction of movement is determined by the concentration gradient of a chemotactic substance. Chemotaxis is important for the migration and accumulation of inflammatory cells at sites of inflammation (Wilkinson, 1998 and Warheit *et al.*, 1988).

Type II cells have been shown to produce chemoattractants such as monocyte chemoattractant protein-1 (MCP-1) and RANTES. It has also been shown that granulocyte monocyte colony stimulating factor (GM-CSF) can be released by type II cells. This is a glycoprotein growth factor involved in stimulating the growth of macrophages (O'Brien *et al.*, 1998). Type II cells can also release cytokines such as IL-8 (Simon and Paine III, 1995). As well as chemokines, type II cells have been shown to produce complement proteins such as C5a, which is a potent macrophage chemoattractant (Strunk *et al.*, 1988). This indicates that type II cells can act as important mediators of pulmonary inflammation and leukocyte influx into the alveolar space.

There are several ways in which type II cells can participate in the modulation of inflammatory processes in the lung following particle inhalation. As mentioned above, the type II cells can release pro-inflammatory proteins such as cytokines, complement proteins and growth factors and may also act as antigen presenting cells to lymphocytes (Simon & Paine III, 1995). In terms of particle induced macrophage recruitment, studies have shown that α-quartz can cause an increase in MIP-2 (the rat equivalent of IL-8)

mRNA in type II cells (Driscoll *et al.,* 1996b). This is consistent with a pro-inflammatory chemotactic response. Driscoll *et al.,* (1997b) has also demonstrated that TNFα, produced by macrophages exposed to particles, can induce type II cells to release chemokines such as MIP-2. Barrett *et al.*, (1999) showed that the production of MIP-2 and MCP-1 by a murine type II cell line following silica exposure was mediated by TNFα which, together with silica exposure, could induce ROS production by the type II cells. Becher *et al.*, (2001) also demonstrated that type II release of IL-6, TNFα and MIP-2 differed depending on the type of stone particle that the cells were exposed to.

In terms of chemotaxis of alveolar macrophages towards signals from type II cells, O'Brien *et al.,* (1998) showed that macrophages migrated towards conditioned medium obtained from type II cells treated with IL-1α. This was in response to chemokines in the conditioned medium such as RANTES, MCP-1 and GM-CSF. Eosinophil and lymphocyte chemotaxis in response to IL-16 and eotaxin secretions by type II cells stimulated with TNFα and IL-1 have also been demonstrated (Cheng *et al.*, 2001). Stimulation of type II cells with bradykinin has also been shown to induce the production of proteins that are chemotactic for neutrophils and monocytes (Koyama *et al.*, 1998). Paine III *et al.*, (1993) also observed increased MCP-1 production by type II cells stimulated with IL-1 and TNFα. It has also been shown that surfactant protein A (SP-A), secreted by type II cells, can enhance the release of reactive oxygen species from alveolar macrophages (Weissbach *et al.*, 1994).

We hypothesise that exposure of a type II cell line to various fine and nanoparticles will result in the release of chemotactic proteins from the type II cells. We further hypothesise that these proteins play an important role in the recruitment of macrophages towards sites of inflammation.

This chapter describes a study in which two cell lines are used as a model to look at the effects of fine and nanoparticle carbon black on type II cells, and their potential to induce macrophage migration. The toxicity of the particles on both cell lines was examined via the measurement of lactate dehydrogenase (LDH) release into the cell culture medium. Optimisation of an *in vitro* chemotaxis assay enabled investigation of alveolar macrophage migration towards conditioned medium obtained from particle treated type II cells. Following testing in the chemotaxis chamber, several other techniques such as differential centrifugation, SDS-PAGE electrophoresis and antibody blocking were employed with a view to determining the primary mediators of macrophage migration present in the conditioned medium.

2.2 MATERIALS AND METHODS

2.2.1 Chemicals and Reagents

L-Glutamine (200mM); penicillin-streptomycin (1000μg/ml) and foetal bovine serum (FBS) were obtained from Invitrogen, UK. RPMI 1640 (without L-glutamine), Zymosan A and Bovine Serum Albumin (BSA) were obtained from Sigma Chemicals Company, Dorset, UK. The Rapi Diff 2 (Romanowsky) stain set was obtained from Raymond A Lamb, London. All other chemicals and reagents were purchased from Sigma Chemicals Company, Dorset, UK unless otherwise stated.

2.2.2 Culture of L-2 Type II Epithelial Cell Line

The rat alveolar type II cell line L-2 was obtained from the European Collection of Animal Cell Cultures (Salisbury, England). The cells were grown in 25cm^2 tissue culture flasks in RPMI 1640 medium supplemented with 1% L-glutamine, 1% penicillin/streptomycin and 10% heat inactivated FBS. Cultures were incubated in a humidified incubator at 37°C / 5% CO_2. Cell counts were performed using 0.3% trypan blue exclusion (1:1 dilution with cells) and an improved Neubauer haemocytometer. Cells were removed from the flask by adding 1 x trypsin / EDTA in Hanks balanced salt solution (HBSS) and incubating for 5 minutes, then centrifuged at 900 g for 2 minutes and resuspended in RPMI 1640 supplemented with 10% FBS.

2.2.3 Culture of J774.2 Macrophage Cell Line

The adherent murine monocytic-macrophage cell line J774.2 was obtained from the European Collection of Animal Cell Cultures (Salisbury, England). The cells were

grown in 25cm^2 tissue culture flasks in RPMI 1640 medium supplemented with 1% L-glutamine, 1% penicillin/streptomycin and 10% heat-inactivated FBS. Culture flasks were stored in a humidified incubator at 37°C and 5% CO_2. Cell counts and viability were assessed using an improved Neubauer haemocytometer and trypan blue exclusion. All cells that were found to be non-adherent in the culture flasks were discarded by washing prior to use.

2.2.4 Particles

The particles used in these experiments were fine carbon black (H.Haeffner & Co Ltd., Chepstow, UK), fine titanium dioxide (Tioxide Ltd.) and nanoparticle carbon black and titanium dioxide (Degussa, UK). The particle diameter and surface area are shown in table 1.5.

2.2.5 Treatment of Cells

Cells were seeded at 40,000 cells per well in a 96 well plate and incubated for 24 hours in RPMI 1640 supplemented with 10% FBS. Serial dilutions (62.5 – 2000μg/ml by mass dose) of each type of particle were prepared in serum-free RPMI and sonicated for 5 minutes before use. After 24 hours, the medium was removed from the cells and replaced with appropriate concentrations of particle before incubation for a further 24 hours. Following particle treatments, the medium was removed from the cells and centrifuged for 30 minutes at 15000 g to remove the particles. The supernatants were removed and stored in separate tubes at -80°C for use in the LDH assay.

2.2.6 LDH Assay Controls

Control samples for the LDH assay were prepared by lysing cells with 50µl of 0.1% Triton X-100 dissolved in phosphate buffered saline (PBS). The solutions were then centrifuged at 11,000 g for three minutes and 10µl of the supernatant was used as a positive control to indicate total releasable LDH. A negative control was obtained by incubating the cells with serum-free medium.

To create a standard curve, pyruvate standards were prepared (using distilled H_2O and 1mg/ml NADH dissolved in 0.75mM sodium pyruvate), ranging in concentrations equivalent to 0 – 2000 Units/ml of LDH. One unit of LDH activity is defined as the amount of LDH that reduces 4.8 x 10^{-4} µmol of pyruvate in 1 minute at 25°C. The standards were transferred (60µl) in triplicate, to a 96-well plate. Into all of the remaining wells of the plate, 50µl of NADH was added. The samples were incubated at 37°C / 5% CO_2 for 5 minutes.

The test and control samples (10µl) were added to the relevant wells on the plate containing the NADH solution. The plate was incubated at 37°C, 5% CO_2 for 30 minutes. Following incubation, 50µl of 2, 4-dinitrophenylhydrazine (0.2mg/ml dissolved in 1M HCl) was added to all of the wells and the plate was left for 20 minutes at room temperature. Sodium hydroxide (50µl of 4M concentration) was then added to each well and the plate was left at room temperature for 5 minutes. The plate was shaken for 5 seconds and the absorbance of all the wells was measured at 540nm with a Dynex MRX microplate reader.

2.2.7 Chemotaxis Chamber - Overview

The chemotaxis apparatus utilised in these studies was a re-usable 96-well Neuroprobe chemotaxis chamber (Receptor Technologies, UK) consisting of an upper and lower half. The samples being tested for potential to induce macrophage migration (30µl) are pipetted into wells on the bottom half of the chamber, overlaid with a polycarbonate filter, which is then covered by the top half of the chamber. Macrophages are then loaded into the top wells of the chamber and allowed to migrate through. The non-migrated macrophages are washed off the top of the filter with PBS and the filter stained with Romanowsky stain (5 washes in each solution followed by 5 washes in distilled water). Once the staining is complete, the optical density of each well can be read using a multiwell plate reader. Increasing absorbance correlates with the increasing number of macrophages moving through the filter.

2.2.8 Chemotaxis Protocol

Each sample (30µl) was loaded, in triplicate, into the bottom wells of the chamber. A Neuroprobe polycarbonate filter (pore size 5µM) was inserted between the layers. J774.2 macrophages (2×10^5) in 200µl of serum-free RPMI 1640 were added to the top of each well. The chamber was incubated at 37°C in 5% CO_2 for 6 hours and the filter was removed, washed and stained with a Romanowsky stain as described in section 2.2.7. The absorbance of the filter was read at 540nm in a Dynex multiwell plate reader.

2.2.9 Zymosan Activated Serum (ZAS)

ZAS is a known activator of C5a in blood serum and, as such, has been utilised in numerous studies as a positive control in chemotaxis assays. A stock solution of Zymosan A in saline (10mg/ml) was prepared and sonicated for 5 minutes to ensure adequate dispersal of the Zymosan particles. The stock Zymosan solution (100µl) was added to 900µl of FBS. To prepare a control solution, 100µl of sterile saline was added to 900µl serum. Both solutions were incubated in a shaking water bath at 37°C for 2 hours and then at 56°C for 30 minutes. The solutions were centrifuged for 5 minutes at 2000 g then aliquoted and stored at –80°C until use. For use in the chemotaxis assay, both solutions were diluted to the appropriate concentration using serum-free RPMI 1640.

Experiments were conducted to determine the optimum incubation times and ZAS concentrations to use in the chemotaxis assay. A solution of ZAS (1mg/ml) and a negative control were prepared as detailed above. For the concentration response experiments, both solutions were diluted to 2%, 5%, 10% and 20% with RPMI 1640 medium. Solutions were then tested using the chemotaxis protocol as described in section 2.2.8. For the time course experiments, 10% ZAS solution was prepared and tested in the chemotaxis chamber as detailed above. The cells were incubated in the chamber for 45 minutes, 90 minutes, 3 hours or 6 hours before the filter was removed and stained.

2.2.10 Exposure of L-2 Cells to TNFα

L-2 cells were seeded in a 96-well plate at a cell count of 40,000 cells per well and incubated overnight. Rat TNFα (Biosource, UK) was prepared at three different concentrations; 0.1, 1 and 10ng/ml using sterile PBS containing 0.1% bovine serum albumin. The medium from the L-2 cells was removed and replaced with 200µl of TNFα at the required concentration. TNFα was also added at an equivalent concentration to wells that did not contain any L-2 cells in order to provide a cell-free comparison. Negative controls were prepared by adding serum-free RPMI to both the L-2 cells and the cell-free wells. The plate was incubated in a humidified incubator at 37°C and 5% CO_2 for 6 hours. Following incubation, the supernatants were removed and tested for potential to induce macrophage migration using the chemotaxis assay protocol as described previously.

2.2.11 L-2 Cells and Particles

A 96-well plate was seeded with L-2 cells (40,000 cells per well) and incubated overnight in a humidified incubator at 37°C and 5%CO_2. Suspensions of fine and nanoparticle carbon black and titanium dioxide were prepared in serum-free RPMI at a concentration of 125µg/ml. The suspensions were sonicated for 10 minutes prior to use. A 1ng/ml solution was also prepared in 0.1% BSA in PBS. The dust suspensions and TNFα were added to the relevant wells in the 96-well plate with L-2 cells. A duplicate cell-free 96-well plate was also prepared using identical solutions of TNFα and dust suspensions. Both 96-well plates were subsequently incubated in a humidified incubator at 37°C and 5% CO_2. After 24 hours incubation, the two plates were removed and the supernatants

were extracted and stored in eppendorf tubes. The eppendorf tubes were centrifuged at 15,000 g for 15 minutes and the supernatants transferred to fresh tubes. The samples were stored at –80°C prior to analysis.

2.2.12 Preparation of L-2 Conditioned Medium

Trypsin in HBSS (1x) was added to a flask of L-2 cells at approximately 80% confluency and incubated for 5 minutes at 37°C / 5% CO_2. Serum-free RPMI culture medium (10mls) was added to the cells and the cells were centrifuged at 900 g for 2 minutes. The supernatant was decanted and the cells were resuspended in normal culture medium. Cell counts were assessed and adjusted to 1 million cells per ml. The cells were seeded in a 6 well plate at 1 million cells per well and incubated overnight.

To prepare particle suspension, fine and nanoparticle carbon black was weighed out and suspended in serum-free RPMI. The suspension was sonicated for 10 minutes and diluted to 125µg/ml of particles. The particle suspensions (200µl) were added to the 6-well plate and incubated for 24 hours. Cells were also incubated with serum-free RPMI for 24 hours. Following incubation, the conditioned medium was removed and centrifuged at 15,000 g for 15 minutes and the supernatants were pooled and stored at –80°C until use.

2.2.13 SDS-PAGE Gel Electrophoresis of L-2 Conditioned Medium

A 15% separating gel was prepared by mixing 23% distilled H_2O, 50% Acrylamide mix, 25% Tris HCl (1.5 M, pH 8.8), 1% sodium dodecyl sulphate (SDS, 10%) and 1%

ammonium persulphate (APS, 10%). TEMED was added at a concentration of 0.04% immediately prior to pipetting the gel into the casting apparatus. A stacking gel was prepared by mixing 68% H_2O, 17% Acrylamide mix, 12.5% Tris HCl (0.5 M, pH 6.8), 1% SDS (10%) and 1% APS (10%). TEMED was added at a concentration of 0.1% immediately prior to adding the gel to the separating gel in the casting apparatus. Immediately following addition of the stacking gel to the casting apparatus, 1µl of bromophenol blue was added to the stacking gel.

To prepare the samples, 20µl of L-2 conditioned medium was pipetted into an eppendorf. For the non-reducing gel, 30µl of sample buffer was added to the conditioned medium. For the reducing gel, 27µl of sample buffer and 3µl of DTT was added to each of the samples. Both sets of samples were then incubated on a heating block; 1 minute incubation for non-reducing samples and 2 minutes for reducing samples. After heating, the samples were immediately stored on ice.

Once cast, the gels were transferred to an electrophoresis tank and immersed in 1 x buffer. Samples (20µl) as well as coloured molecular weight markers were added to the gels and the electrophoresis was run at 40mA for 45 minutes. Both gels were stained with the Coomassie blue stain overnight and destained by microwaving (3 x 1 minute) the gels in fresh distilled water.

2.2.14 Differential Centrifugation of L-2 Conditioned Medium

Conditioned medium obtained from L-2 cells treated with nanoparticle carbon black according to the protocol in section 2.2.12 was separated according to molecular weight using Vivaspin 2 centrifuge filters (supplier) operated according to manufacturers' instructions. A 30kDa filter was used first, followed by a 10kDa filter and finally a 5kDa filter. Supernatants were stored at –80°C until tested for potential to induce macrophage migration using the chemotaxis protocol outlined in section 2.2.8.

2.2.15 Statistical Analysis

Results are expressed as the mean ± SEM. All figures are the results of three separate experiments with three observations in each unless otherwise stated. Statistical analysis was accomplished by a one-way ANOVA with Tukey's multiple comparison.

2.3 RESULTS

2.3.1 LDH Release by J774.2 Cells Following Treatment with Fine & Nanoparticle Carbon Black and Titanium Dioxide

Figures 2.1 and 2.2 show LDH concentrations in conditioned medium obtained from J774.2 cells treated for 24 hours with either fine or nanoparticle carbon black or titanium dioxide. The graphs indicated that, in this study, all types of particle tested showed cytotoxic effects towards the cells. The results also suggested that the nanoparticles induced a slightly cytotoxicity at the same mass dose of particles but this was not significant. The higher doses (1-2mg/ml) of all types of particle induced what appeared to be maximum LDH release. The dose-dependant increases in LDH concentration should be noted following doses up to and including 1mg/ml although no further increase was noted with the dose of 2mg/ml.

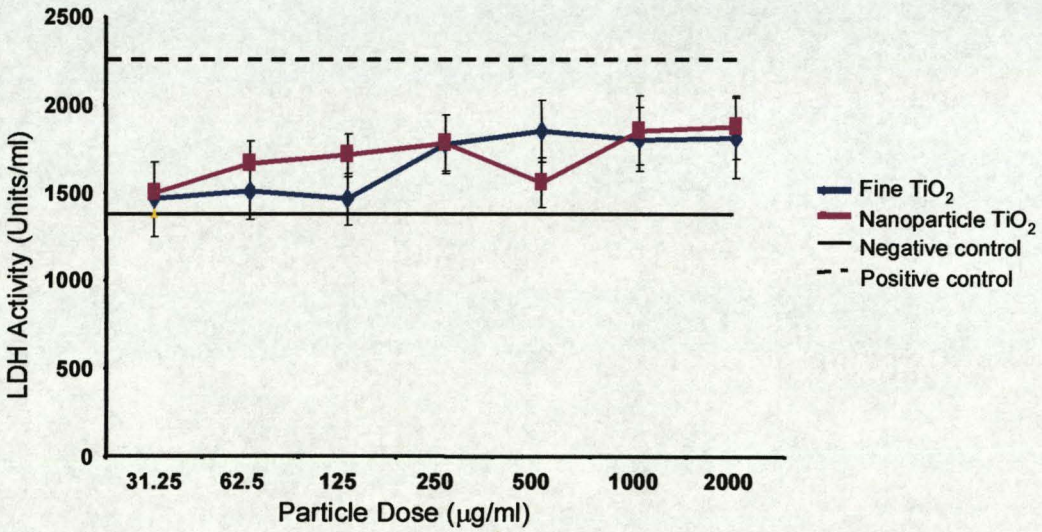

Figure 2.1 LDH release from J774.2 cells following exposure to varying doses of fine and nanoparticle TiO_2 for 24 hours. All values are the mean of three experiments conducted in triplicate ± SEM.

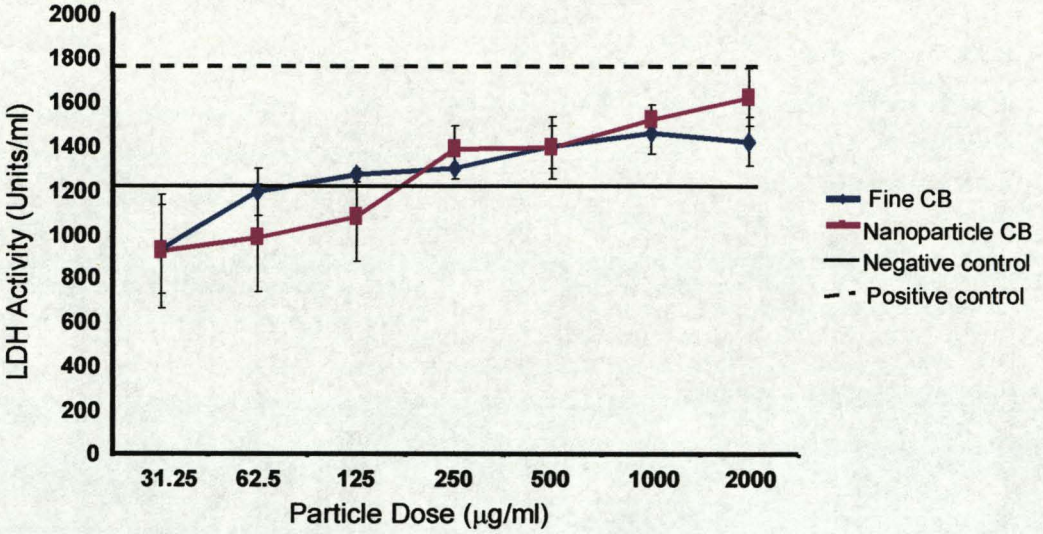

Figure 2.2 LDH release from J774.2 cells following exposure to varying doses of fine and nanoparticle carbon black for 24 hours. All values are the mean of three experiments conducted in triplicate ± SEM.

2.3.2 LDH Release by L-2 Cells Following Treatment with Fine & Nanoparticle Carbon Black and Titanium Dioxide

LDH release from untreated L-2 cells was inherently lower than that of the J774.2 cells (figures 2.3 and 2.4). Treatment with 1mg/ml fine and nanoparticle titanium dioxide resulted in the detection of high concentrations of LDH. Fine and nanoparticle carbon black treatment of L-2 cells resulted in similar effects to those induced by TiO_2 particles. Doses of 1 and 2mg/ml of nanoparticle carbon black resulted in a significant increase in LDH release compared to the negative control ($p<0.05$). As with the J774.2 cells, LDH release from the L-2 cells increased in a dose dependant manner until a maximum was reached at a particle concentration of around 1mg/ml. However, this was noted to be marginally lower than the LDH concentrations observed following cell lysis with Triton X-100 (positive control).

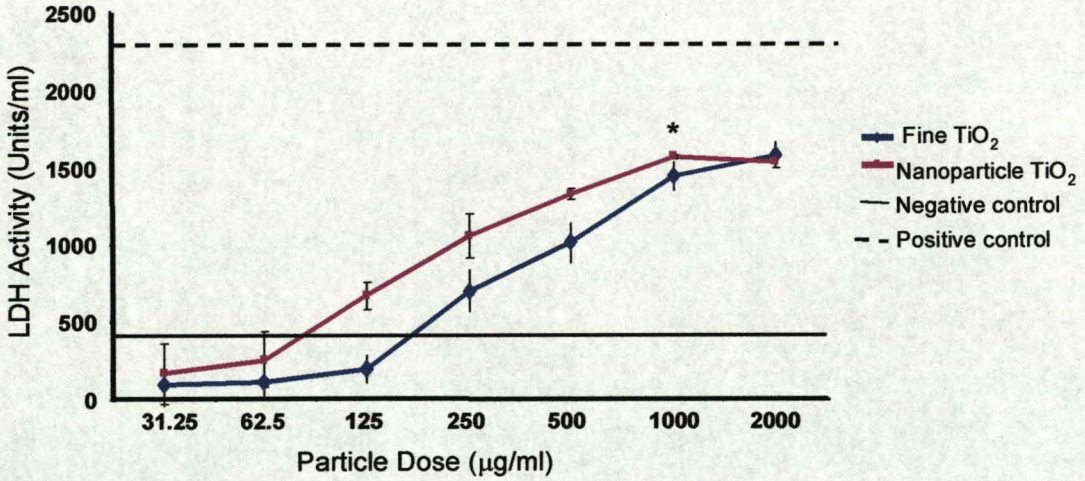

Figure 2.3 LDH release from L-2 cells following exposure to varying doses of fine and nanoparticle TiO_2 for 24 hours. All values are the mean of three experiments conducted in triplicate ± SEM. Asterisks denote a significant difference from the negative control (* $p<0.05$).

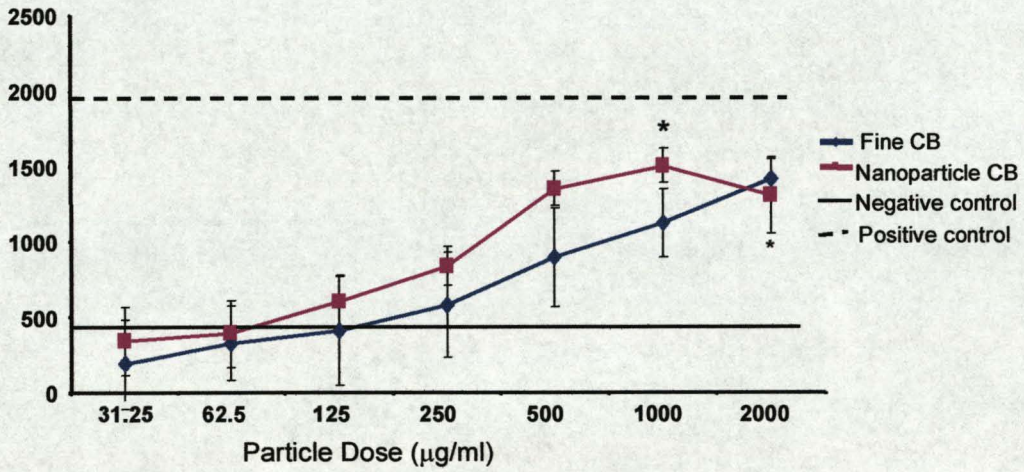

Figure 2.4 LDH release from L-2 cells following exposure to varying doses of fine and nanoparticle carbon black for 24 hours. All values are the mean of three experiments conducted in triplicate ± SEM. Asterisks denote a significant difference from the negative control (* $p<0.05$).

2.3.3 Concentration and Time Course Studies with ZAS and J774.2 Macrophages

Figure 2.5 shows the effects of varying concentrations of ZAS on macrophage migration following a 6 hour incubation period. The graph shows that the absorbance of the

chemotaxis filter increases as the concentration of ZAS increases from 2-20%. An increasing absorbance correlates with increasing numbers of macrophages moving into or through the polycarbonate filter. Significant increases in macrophage migration were observed at both 10% and 20% dilutions of ZAS. This was compared to the negative control of FBS incubated with sterile saline which indicated that no significant increases in macrophage migration were taking place.

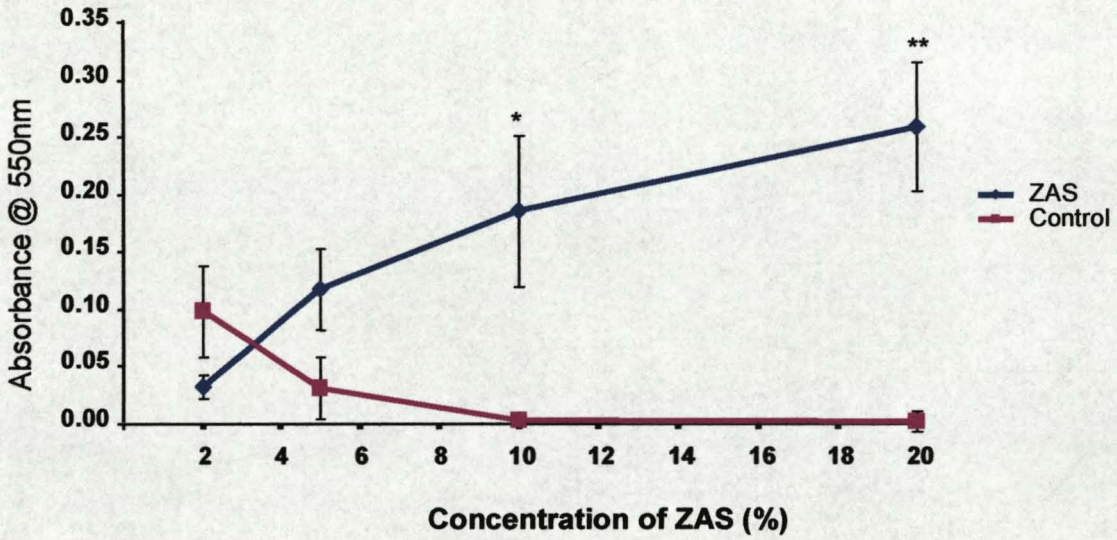

Figure 2.5 – The effect of varying concentrations of zymosan activated serum (ZAS) on macrophage migration compared to a negative control of non-activated serum. (6 hour incubation time). Asterisks denote a significant difference from the control (* $p<0.05$ and ** $p<0.01$).

ZAS induced significant increases ($p<0.001$) in macrophage migration at both the 3 hour and 6 hour time points (Figure 2.6). The highest level of macrophage migration was found at the 6 hour time point where macrophage migration was found to be 8 fold greater than that of the negative control. The negative control did not display any

potential for inducing macrophage migration and thus may serve as an indicator that random macrophage migration was minimal.

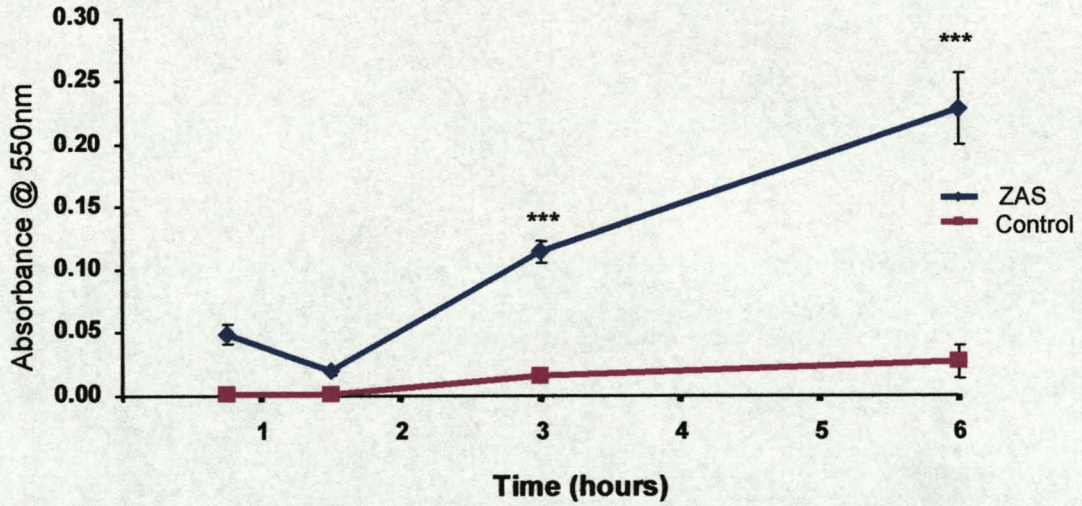

Figure 2.6 – A time course examination of macrophage migration towards 10% zymosan activated serum (ZAS) compared to a negative control of non-activated serum. Asterisks denote a significant difference from the control (*** $p<0.001$)

2.3.4 Macrophage Migration Stimulated by Conditioned Medium from L-2 Cells Exposed to TNFα

L-2 cells were exposed to TNFα in order to induce the secretion of pro-inflammatory mediators such as chemotactic proteins. TNFα, at a concentration of 1ng/ml, induced a significant increase in macrophage migration ($p<0.05$) compared to the negative control (figure 2.7). However macrophage migration was also noted at both the lower and higher TNFα concentrations although this was not significant. TNFα alone, at comparable concentrations to those used for cell treatments, induced minimal macrophage migration.

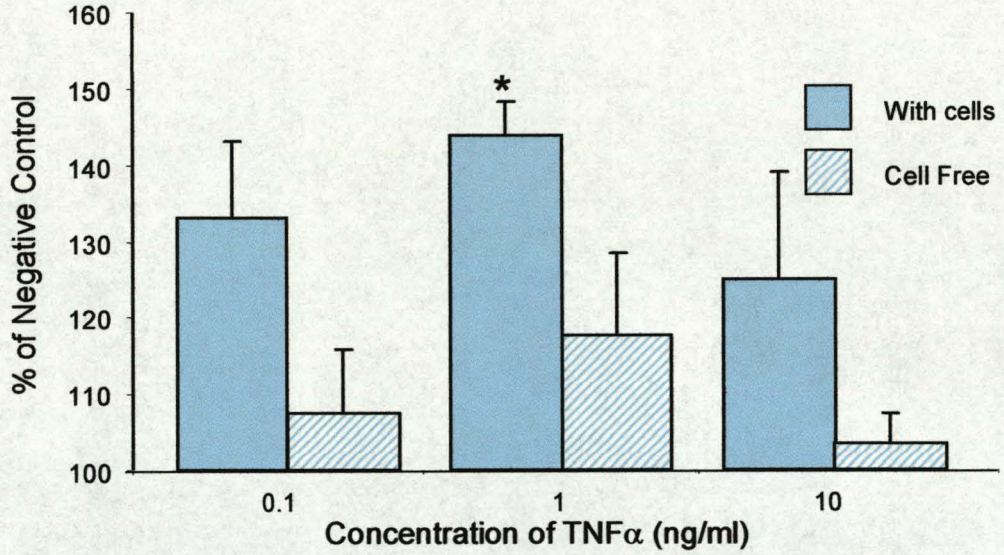

Figure 2.7 – The chemotactic effect of conditioned medium from L-2 cells exposed for 6 hours to varying doses of TNFα compared with TNFα alone. Asterisks denote a significant change from the cell free TNFα treatment (* $p<0.05$). Graph shows the result of one experiment with three replicates.

2.3.5 Macrophage Migration Stimulated by Conditioned Medium from L-2 Cells Exposed to Fine and Nanoparticle Carbon Black and TiO_2

When compared to the negative control, nanoparticle carbon black treatment of L-2 cells generated a conditioned medium that induced a significant increase ($p>0.01$) in the stimulation of macrophage migration (Figure 2.8). In comparison, conditioned medium from L-2 cells treated with fine TiO_2, CB and nanoparticle TiO_2 did not induce any significant increases in macrophage migration. It should also be noted that both fine and nanoparticle carbon black treatment of L-2 cells did induce significant increases in macrophage migration compared to medium incubated with the particles alone ($p<0.01$ and $p<0.001$ for fine and nanoparticle carbon black respectively).

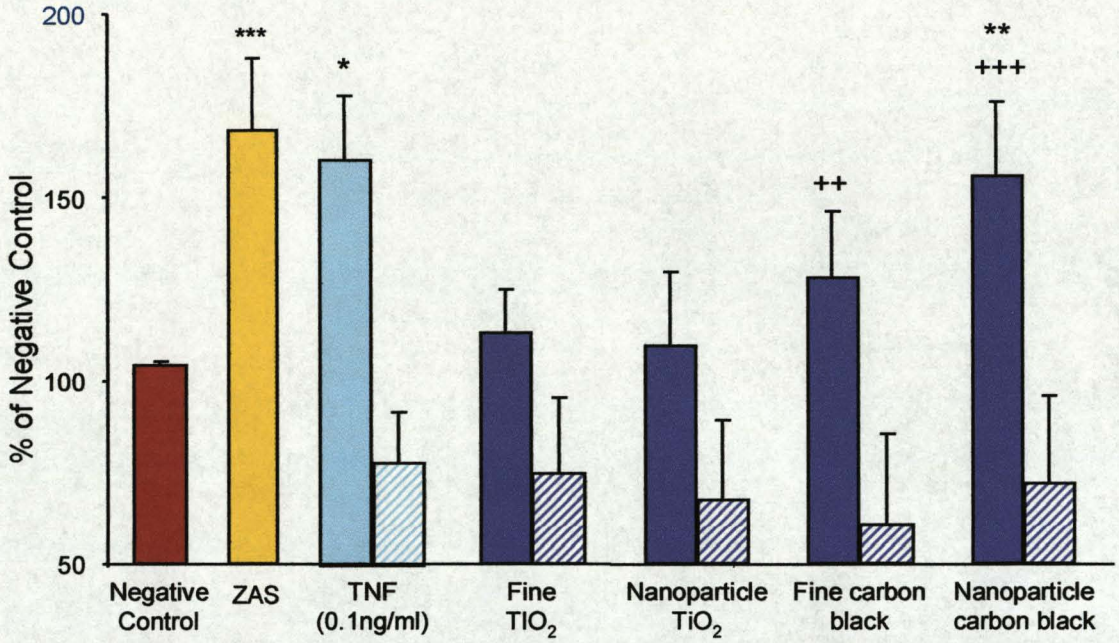

Figure 2.8 – Macrophage migration induced by L-2 cell supernatant following treatment for 6 hours with 125µg/ml fine and nanoparticle TiO_2 and carbon black (striped bars indicate cell free treatments). Asterisks denote a significant increase compared to the negative control (* $p<0.05$, ** $p<0.01$ and *** $p<0.001$). Significant increases from the appropriate cell-free treatments are denoted by a cross (++ $p<0.01$ and +++ $p<0.001$).

2.3.6 SDS-PAGE Electrophoresis of Conditioned Medium from L-2 Cells Treated with a Sub-Toxic Dose of Nanoparticle Carbon Black

Figures 2.9.1 and 2.9.2 show photographs of non reducing SDS-PAGE gels which were run with conditioned medium obtained from L-2 cells treated for 24 hours with either fine or nanoparticle carbon black (125µg/ml). Cells were also incubated with serum-free medium for 24 hours and this conditioned medium was run together with other two treatments as a negative control. As can be seen from both gels, no protein bands were present following the treatments used.

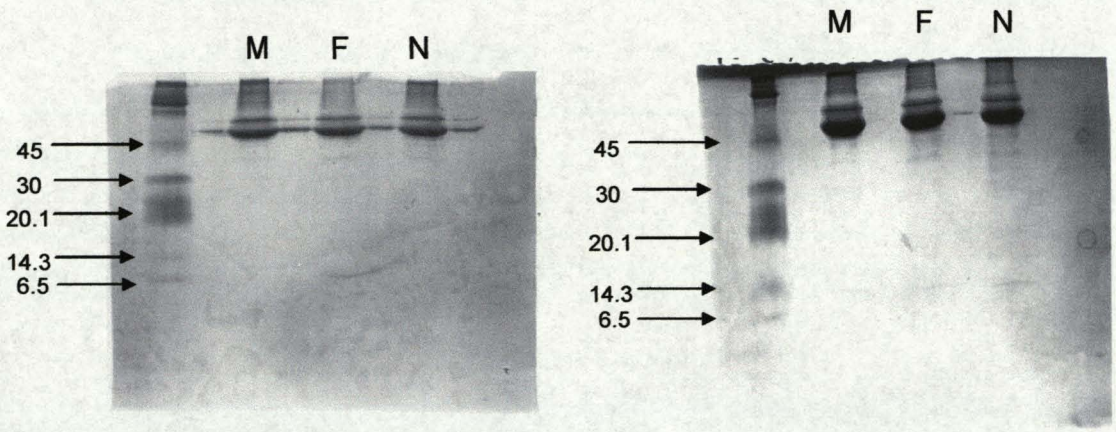

Figure 2.9.1 and 2.9.2 – SDS-PAGE gels of conditioned medium from untreated L-2 cells and L-2 cells treated with 125µg fine or nanoparticle carbon black for 24 hours. Gels were both run in non-reducing conditions. Marker bands and corresponding molecular weights (kDa) are indicated at the left hand side of each gel.

M= Medium Only, F=Fine carbon black treatment, N=Nanoparticle carbon black treatment

Figures 2.10.1 and 2.10.2 show conditioned medium obtained from similar particle treatments but run under reducing conditions. As can be seen from both gels, bands are present in all three treatments. It should be noted that figure 2.10.1 shows an especially clear representation of these bands. As can be seen from figure 2.10.1, an increased density and number of protein bands are observed in the lane containing the conditioned medium obtained from cells that have been treated with nanoparticle carbon black. Very clear bands are noted around the 14kDa weight and, as can be seen from the photograph, the density of this band is increased in the lane containing the nanoparticle treated conditioned medium.

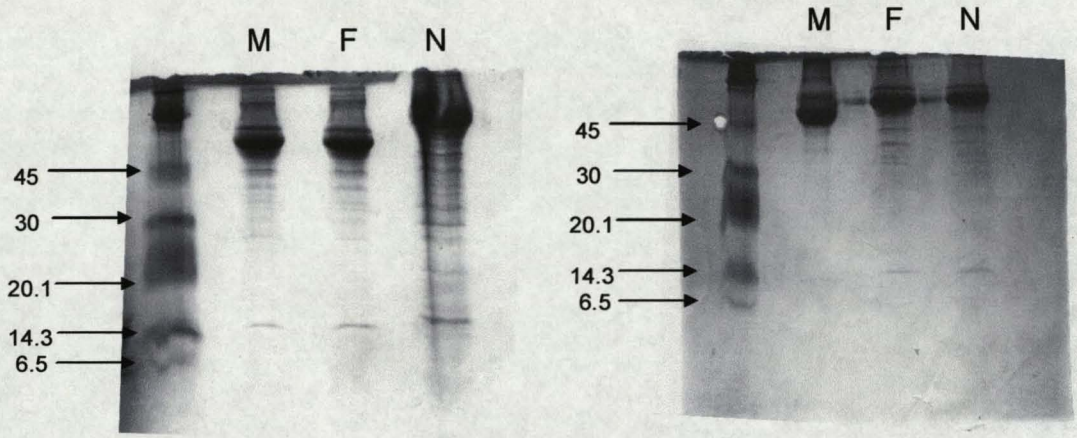

Figure 2.10.1 and 2.10.2 – SDS-PAGE gels of conditioned medium from L-2 cells treated with 125µg fine or nanoparticle carbon black for 24 hours. Gels were both run in reducing conditions via the addition of DTT . Marker bands and corresponding molecular weights (kDa) are indicated at the left hand side of each gel.

M= Medium Only, F=Fine carbon black treatment, N=Nanoparticle carbon black treatment

2.3.7 Differential Centrifugation and Macrophage Migration Studies of Conditioned Medium Obtained from L-2 Cells Treated with a Sub-Toxic Dose of Nanoparticle Carbon Black

The conditioned medium generated by nanoparticle carbon black treatment (125µg/ml) of L-2 cells was fractionated by centrifugation through size selective filters. It was found that the fraction sizes of 5-10 kDa and 10-30 kDa both induced a significant increase in macrophage migration ($p<0.01$) when compared to the negative control. The other two fractions (0-5 and >30 kDa) did not induce a significant increase in macrophage migration (Figure 2.11).

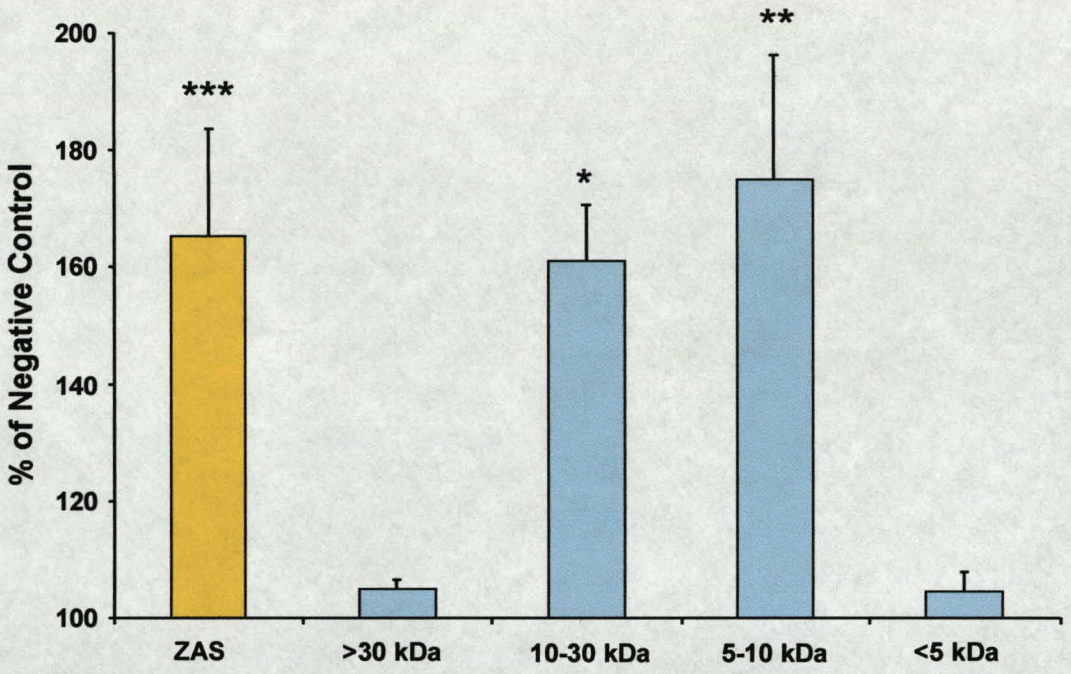

Figure 2.11 – Macrophage migration induced by centrifuge fractions of conditioned medium from L-2 cells treated with nanoparticle carbon black (125μg/ml) for 24 hours. Asterisks denote a significant increase compared to the negative control (* $p<0.05$, ** $p<0.01$, *** $p<0.001$).

2.4 DISCUSSION

2.4.1 Particle Toxicity

Studies have shown that nanoparticles can be more toxic than an equivalent mass dose of fine particles (Stone *et al.*, 1998). This is hypothesised to be due to the larger surface area of the particles and resulting oxidative stress. Figures 2.1 and 2.2 show LDH release from J774.2 cells treated with varying doses of fine and nanoparticle carbon black and titanium dioxide. Although the results suggest that the nanoparticles exhibit a slightly higher toxicity than the fine particles, this effect was not significant.

The concentration of LDH detected in the J774 conditioned medium increased in a dose dependant manner correlating with the increased dose of particulates. The maximal LDH release was obtained when cells were treated with 1-2 mg/ml of either fine or nanoparticles TiO_2 or carbon black particles. At lower doses of both fine and nanoparticle carbon black, it was noted that the LDH concentrations detected in the conditioned medium were lower than that observed in the conditioned medium that had been obtained from untreated cells.

The cytotoxicity that was observed when treating J774.2 cells with fine particles and nanoparticle was further confirmed when similar treatments were conducted with the alveolar type II epithelial cell line L-2. Figures 2.3 and 2.4 indicate that, at the doses tested in this study, the nanoparticles appeared to demonstrate a moderately increased toxicity towards the cells. Indeed, at a dose of 1mg/ml of both types of nanoparticle tested, there was a significant increase in the concentration of LDH detected compared to

the negative control. While the results of these experiments may provide an accurate representation of particle cytotoxicity by measuring LDH concentrations, it is possible that LDH may have been adsorbed on the surface of the particles following release from the cells. Desai and Richards (1978) and Jones *et al.,* (1972) both noted how different types of biological molecules could be adsorbed on to the surface of inorganic and mineral dusts. Brown *et al.*, (2000) also showed extensive binding of BSA to the surface of nanoparticle carbon black. This may occur when measuring LDH concentrations, especially when taking into account the large surface area of the nanoparticles and potential for protein adsorption.

It should be noted that the J774.2 cells released an inherently high concentration of LDH even when no particles were used in the treatments. This may be attributed to the minor physical trauma induced during the scraping procedure by which the cells were removed from the culture flask prior to seeding in the microplate. Inter-species differences (i.e. rat versus murine) in the intracellular LDH content may also account for the differences in resting LDH concentration, as well as differences between two types of cells i.e. type II epithelial and macrophage. Certainly, differences in species-related responses to the same particulate have indeed been noted (Donaldson & Tran, 2002), and this may have had some influence on the results displayed here. Primary isolated cells may also behave in a different manner to those cell lines utilised in this study and this may be a worthy area of comparison to study.

2.4.2 Macrophage Migration

Dose and time response experiments were conducted with J774 macrophages with a view to optimising the chemotaxis assay. Zymosan activated serum has been used a positive stimulatory agent to induce macrophage chemotaxis in numerous studies (Donaldson *et al.*, 1989, 1990 and Warheit *et al.*, 1985). Zymosan A is a polysaccharide extracted from yeast cell walls and generates large quantities of the macrophage chemoattractant C5a when added to serum (Snyderman *et al.,* 1971). Figure 2.5 shows macrophage migration towards ZAS and non-activated serum that was diluted to a range of concentrations from 2-20%. Increases in macrophage migration correlated with increases in the concentration of ZAS with significant increases in macrophage migration observed at ZAS concentrations of 10% and 20% ($p<0.001$). Therefore, it was decided, based upon a review of the relevant literature and the results indicated in Figure 2.5, that 10% ZAS would be an adequate concentration to use as a positive control in future studies using the chemotaxis chamber.

Figure 2.6 shows the effects of chamber incubation time on the level of macrophage migration. Other macrophage chemotaxis studies have routinely allowed at least 3 hours incubation time to allow macrophages to complete shape change and migration (Milanowski *et al.*, 1995, Warheit *et al.*, 1985 and Donaldson *et al.*, 1989, 1990). While 3 hours incubation appeared to allow for a significant level of macrophage migration to take place, it was felt that 6 hours would provide more opportunity for the macrophages to migrate through the filter. This decision took into consideration the fact that future chemotaxis studies would be testing a very dilute conditioned medium and as such,

macrophages responses could possibly be slower than those observed with Zymosan activated serum. Previous investigations in the research group using primary alveolar macrophages had encountered problems in measuring macrophage migration and it was not understood if shorter incubation times had contributed to these observations.

2.4.3 Macrophage Migration in Response to Signals from Particle Treated Type II Cells

Prior to conducting particle treatments on L-2 cells, a preliminary experiment was conducted to determine if stimulation by a potent pro-inflammatory cytokine such as TNFα could induce the type II cells to release macrophage chemoattractants. Figure 2.7 shows the results of an experiment where L-2 cells were treated with varying concentrations of recombinant rat TNFα for 6 hours. The cells were also exposed to TNFα at equivalent concentrations for 24 hours (data not shown) but macrophage migration towards these conditioned medium samples did not display any significant changes. As can be seen from the graph, a significant increase in macrophage migration was observed when the L-2 cells were treated with TNFα at a concentration of 1ng/ml for 6 hours. A similar macrophage response was not observed in the cell free supernatants i.e. TNFα at equivalent concentrations that had been incubated for 6 hours in cell-free wells. The results from this experiment indicate that the L-2 cells were capable of releasing macrophage chemoattractants following pro-inflammatory stimulation. The fact that similar increases in macrophage migration were not observed with the TNFα alone indicated that the TNFα did not exert a chemotactic influence on the macrophages and that any chemoattractants present in the conditioned medium that were influencing

macrophage migration were released by the L-2 cells into the medium. It was decided that a TNFα treatment (1ng/ml) would also be used in experiments examining L-2 responses to particle treatments. This correlates well with results published by Standiford *et al.*, (1991), Paine III *et al.*, (1993) and O'Brien *et al.*, (1998) which state that TNFα is able to induce the secretion of chemoattractants from type II epithelial cells. Studies have also shown that other cytokines such as IL-9 induce the release of chemoattractants from bronchial epithelial cells (Little *et al.*, 2001). However, TNFα has been shown to be present in the BAL fluid of particle treated animals in many *in vivo* studies (Schins *et al.*, 2004, Becher *et al.*, 2001 and Li *et al.*, 1999) as well as being detected in *in vitro* studies (Jimenez *et al.*, 2002). As such, TNFα was considered to be a better candidate to induce epithelial cell inflammatory processes and was used in subsequent experiments as an additional positive control.

Based on the results shown in figures 2.4 and 2.5, it was decided that 125ug/ml would act as a sub-toxic dose for all particles tested. Figure 2.8 shows the results of an experiment where L-2 cells were treated with four different types of particles for 24 hours and the conditioned medium that was generated was tested for potential to induce macrophage migration. As can be seen from the graph, the nanoparticle carbon black treatment of the L-2 cells generated a conditioned medium that induced a significant increase in macrophage migration compared to the negative control, whereas none of the other particle treatments had a significant effect on macrophage migration. This would indicate that the carbon black nanoparticles, as well as showing increased cytotoxicity, are able to stimulate the release of macrophage chemoattractants when exposed to L-2

cells at sub-toxic doses. Cell-free treatments were also conducted to determine whether any soluble substances present on the surface of the particles had the potential to directly induce macrophage migration. This took into consideration studies by Milanowski *et al.*, (1995) which showed macrophage chemotaxis towards bacterial and fungal products extracted from organic dust samples.

Following the experiments using four different particle types, it was decided that further experiments should focus upon the effects of the nanoparticle carbon black on the L-2 cells and the elucidation of the products that were released from the type II cells as a result of particle exposure. Figures 2.9.1 and 2.9.2 show SDS-PAGE gels of conditioned medium obtained from L-2 cells treated with 125μg of either fine or nanoparticle carbon black. As can be seen from the gels, no bands were visible below the 45kDa molecular weight. Figures 2.10.1 and 2.10.2 are gels with the same treatments but with the addition of the reducing agent DTT. As can be clearly seen from figure 2.10.1, a higher number of protein bands are present in the nanoparticle carbon black conditioned medium compared to the medium obtained from the fine carbon black and untreated cells. This indicates that an increased number and concentration of proteins were released from the type II cells into the conditioned medium as a result of the nanoparticle carbon black exposure. This may account for the increased macrophage migration observed when exposing macrophages to conditioned medium obtained from cells exposed to nanoparticle carbon black. The increased bands are present in the molecular weight range of approximately 14 – 35 kDa. A subsequent experiment where the conditioned medium was centrifuged through molecular weight filters and then tested in the

chemotaxis chamber indicated that the substance(s) that induced macrophage migration was located in the 5 – 30 kDa weight range. This is based on the observation that the 5-10 kDa and 10-30 kDa fractions of the conditioned medium induced a significant increase in macrophage migration compared to the negative control. Antibody blocking experiments using antibodies for rat C5a, MIP-2 and RANTES were attempted but were unsuccessful (data not shown).

The regulation and stimulation of leukocyte recruitment in the lung is an important factor in the regulation of inflammation and several mechanisms exist to ensure that a homeostatic environment exists (Fantone & Ward, 1983). The response of macrophages to signals derived from other cells is a topic that has generated a lot of interest. Indeed, studies have been conducted which investigate macrophage chemotactic responses to signals from neutrophils (Donaldson *et al.*, 1989), from type II cells (O'Brien *et al.*, 1998) and from other macrophages (Brieland *et al.*, 1995). Other studies have focussed on the inhibition of macrophage chemotaxis induced by molecules such as the lymphocyte-derived macrophage migration inhibitory factor (MIF), described by Hermanowski-Vosatka *et al.*, (1999) which inhibits macrophage movement. As described previously in section 2.1.1., several studies have demonstrated that type II cells can secrete a wide range of pro-inflammatory mediators capable of inducing macrophage migration to sites of inflammation. It is likely that, due to the highly toxic nature of carbon black nanoparticles, an increased amount of proteins designed to induce macrophage recruitment are secreted by the type II cell line utilised in this study. This may indicate an adaptive response of lung epithelial cells which would aid in the rapid

recruitment of inflammatory cells to sites of particle deposition and the subsequent removal of the particles by phagocytic cells such as macrophages and neutrophils.

Future studies in this area could focus on the identity of the substances released by the type II cells in response to particle exposure. This study indicates that the factors inducing macrophage migration are of a molecular weight that is between 5 and 30kDa. However, due to the wide range of substances released by the type II cells, it is likely that no one single substance is responsible for inducing macrophage recruitment and, as such, further experiments in this area may involve deciphering the complex mixtures of chemotactic molecules released by the type II cells to ascertain their specific cellular targets. Other investigations may attempt to examine the effects of other forms of particles as well as various components of particulate air pollution.

CHAPTER 3

THE EFFECTS OF NANOPARTICLES ON SERUM-INDUCED MACROPHAGE MIGRATION

3.1 INTRODUCTION

3.1.1 The Complement System

It has long been accepted that the complement system is an integral part of the innate immune system involved in mediating inflammatory responses to foreign organisms and particulates. The complement system itself has evolved over a period of around 700 million years to aid in the removal of any foreign or pathogenic substances from the body (Sahu & Lambris, 2000 & Sunyer & Lambris, 1999). There are several ways in which the complement system can accomplish this.

Firstly the complement system recognises foreign material, and labels it for removal by phagocytes. The process is known as opsonisation. The complement system is also involved with removing self-reactive B cells from circulation as well as primary production of the 'membrane attack complex', a bacteriolytic complement arrangement (Barrington *et al.*, 2001). Finally, the complement system is capable of generating localised inflammation via release of anaphylatoxins into specific tissues. This is the concept which is most important in this chapter and one which deals with the understanding of macrophage migration (Barrington *et al.*, 2001, Sunyer & Lambris 1999 and Sahu & Lambris, 2000).

The principles behind macrophage migration were dealt with in the previous chapter, focusing on pulmonary macrophagic responses to inhaled particulates using an *in vitro* model. In this chapter, the ability of fine and nanoparticles to activate the complement cascade is studied, utilising a similar *in vitro* model as used in the previous chapter.

3.1.2 Chemotactic Complement Proteins

Complement proteins are circulating components of normal plasma which are produced by the spleen, the liver and by cells such as macrophages (Johnson & Hetland, 1988). The proteins circulate in the blood until the cascade is activated, either by antibody binding to an antigen or a complement component binding to the surface of a pathogen. These two common pathways of complement activation are the 'classical' pathway (Arlaud and Colomb, 1998) and the 'alternative' pathway, both culminating in the cleavage of the complement protein C3 (Janeway & Travers, 1999, Zipfel, 1999 and Ward, 2004).

When the alternative pathway of the complement cascade is activated (Figure 3.1), C3 is cleaved and two anaphylatoxins (C3a and C5a) are produced (Sahu & Lambris, 2000). C5a is a potent chemoattractant for macrophages and neutrophils and acts, therefore, as a primary mediator for macrophage recruitment and subsequent particle clearance. Therefore, the toxicity of a given particulate may depend on the particulate potency in activating the alternative complement cascade (Warheit *et al.*, 1988).

3.1.3 Complement in the Lung

Studies have shown that complement proteins are present in the lung, on the surface of the alveolar epithelium and in the alveolar lining fluid (Watford *et al.*, 2000). Strunk *et al.*, (1988) demonstrated that lung epithelial cells could secrete complement proteins from both the alternative and classical pathways. Cole *et al.*, (1983) showed that human bronchoalveolar macrophages could secrete complement proteins C2 and C3, but that this

can be affected by disease state. Johnson and Hetland (1988) reviewed several studies, and illustrated that macrophages possessed the ability to produce a complete set of complement proteins. The presence of complement proteins in the lung fluid and on the tissues may act as an early defence mechanism to facilitate phagocytosis and clearance of foreign particles.

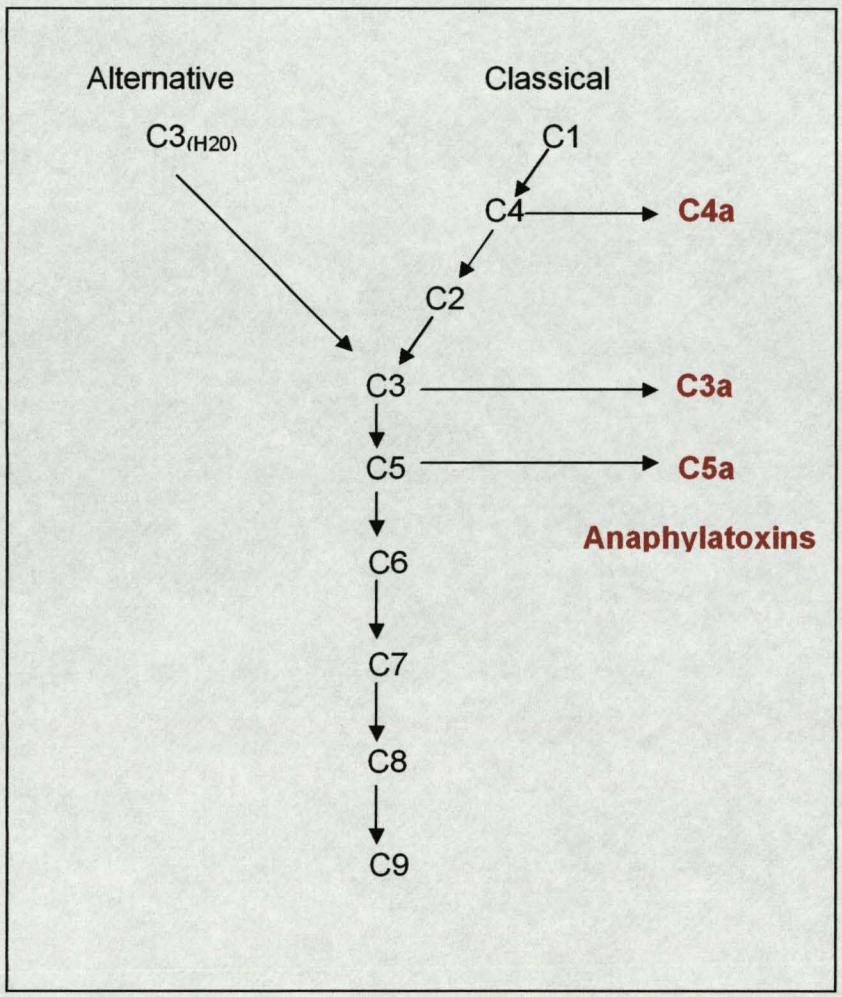

Figure 3.1 – The Complement Cascade

3.1.4 Complement Activation by Particles and Fibres

There have been many studies showing that asbestos can activate the alternative complement pathway, resulting in the generation of C5a proteins. Saint-Remy *et al.*, (1980), Wilson *et al.*, (1977) and Warheit *et al.*, (1985) have all demonstrated that different types of asbestos fibres have the capacity to activate the alternative complement pathway in serum both *in vivo* and *in vitro*. Kanemitsu *et al.*, (1998) reported that diesel exhaust particles could also activate complement. In a more recent publication by Governa *et al.*, (2002), crystalline silica was also found to have the potential to cleave the complement protein C5 to produce a C5a-like product. This was hypothesised to be due to oxidative stress taking place via redox-active iron present on the silica surface. This obviously has important implications for silica-induced lung disease as well as stimulating questions regarding particulates and their potential to activate the alternative complement cascade. Warheit *et al.*, (1988) concluded that alveolar macrophages are attracted to sites of deposition via complement activation and that the clearance of a given particulate depends on its potential to activate complement.

3.1.5 Particles and Free Radicals

As mentioned previously, there have been several studies showing that the large surface area of fine and nanoparticles demonstrates a high potential for the generation of reactive oxygen species and their subsequent cytotoxicity following inhalation or instillation into the alveolar space. For example, in a study by Li *et al.*, (1996), it was shown that PM_{10} generated free radical activity *in vitro*, and induced oxidative stress *in vivo* resulting in

pulmonary inflammation. A study by Gilmour *et al.*, (1996) supported these findings, stating that hydroxyl radicals were generated by PM_{10} and that, this too occurred via an iron-dependant mechanism. Greenwell *et al.*, (2002) demonstrated that the oxidative stress induced by PM_{10}, as measured by damage to supercoiled DNA, could be decreased by the addition of antioxidants. Governa *et al.*, (2002) demonstrated that silica had the capacity to induce the generation of a C5a-like protein which may have been due to the oxidative stress generated on the silica surface.

With regard to the particles utilised in this study, Stone *et al.*, (1998) demonstrated that nanoparticle carbon black displayed higher levels of free radical activity than that of fine carbon black. This is hypothesised to play an important role in increased nanoparticle toxicity as it is well known that nanoparticles are more inflammogenic than an equivalent mass of fine particles when deposited in the lung (Donaldson & Tran, 2002). This may indeed be due to nanoparticle initiation of the complement cascade and subsequent chemotactic influx of macrophages and neutrophils into the alveolar space.

3.1.6 Particle Induced Inflammation Hypothesis

We hypothesise that the reactive oxygen species present on the surface of nanoparticles may have the capability to stimulate C5a generation via cleavage of precursor complement proteins. This could induce macrophage recruitment towards sites of nanoparticle deposition and result in increased inflammation.

This chapter describes an investigation looking at the specific effects of particulates with regard to activating the alternative complement pathway, using the *in vitro* macrophage chemotaxis assay described in chapter 2 as an indication of C5a generation and complement activation. The study compares both fine and nanoparticles in the forms of carbon black and titanium dioxide. It has been hypothesised that nanoparticle carbon black would induce the generation of chemotactic complement proteins as a result of the reactive oxygen species present on the particle surface.

With regard to the hypothesis that reactive oxygen species generated on the nanoparticle surface play an integral role in the generation of chemotactic factors in serum, an experiment was also conducted using the oxidant tert-butyl hydroperoxide (tBHP) to determine if this treatment would have the potential to induce the generation of chemoattractants in the serum. The effects of low doses of particulate air pollution (PM_{10}) extracted from filters was also assessed.

3.2 MATERIALS AND METHODS

3.2.1 Chemicals and Reagents

Non-heat inactivated foetal bovine serum (FBS) was obtained from Invitrogen, UK. All other chemicals and reagents used were purchased from Sigma Chemicals Company, UK.

3.2.2 Cell Culture and Chemotaxis Assay

The cell culture of J774.2 cells was conducted as described in section 2.2.3. The macrophage migration experiments were conducted according to the protocol described in section 2.2.8. As described in Chapter 2, ZAS was used as a positive control.

3.2.3 FBS Particle Treatments

FBS was exposed to fine and nanoparticle carbon black and titanium dioxide (doses 5mg/ml, 1.5mg/ml and 1mg/ml) by incubation in a shaking water bath at 37°C for 2 hours. Following incubation, the treated serum was centrifuged at 15000 g for 30 minutes to remove the particles. The supernatants were stored at -80°C prior to use in the chemotaxis assay.

3.2.4 Serum Heat Inactivation

FBS was treated with particles as described above. Samples were then split into two separate tubes and half of the samples were heat inactivated by incubation in a shaking water bath at 56°C for 30 minutes. Both sets of samples were then centrifuged at 15000 g for 30 minutes to remove the particles. The supernatants were stored at -80°C prior to use in the chemotaxis assay.

3.2.5 Diluted Serum

In order to examine the effect of diluting serum on the stimulation of macrophage migration, FBS, generated by treatment with fine and nanoparticle carbon black at doses of 5 and 10 mg/ml as described previously, was diluted to 50% and 20% using serum-free RPMI 1640 medium. The diluted serum was then tested for chemotactic potential using the chemotaxis protocol.

3.2.6 Antioxidants

In order to determine the role of ROS in chemotactic factor generation in serum, FBS was exposed to nanoparticle carbon black (5 and 10 mg, 37°C for 2 hours) in the presence and absence of the antioxidants nacystelin (500μM) or Trolox (25μM), before heat inactivation at 56°C for 30 minutes in a shaking water bath. Following incubation, the serum was centrifuged at 15000 g for 30 minutes to remove the particles. The supernatants were stored at -80°C until use in the chemotaxis assay. Particle treated serum was diluted to 20% with serum-free RPMI 1640 for use in the chemotaxis assay using the protocol described in Chapter 2.

3.2.7 Serum and Oxidant Exposure

FBS was exposed to tBHP at final concentrations of 0.1, 0.2 and 0.3mM. The samples were incubated at 37°C for two hours in a shaking water bath and then stored at -80°C until use in the chemotaxis assay. Samples were diluted to 20% prior to use in the chemotaxis assay utilising the protocol described in Chapter 2

3.2.8 PM_{10} exposure

FBS was exposed to PM_{10} at a final dose of 1mg/ml. PM_{10} was obtained from 3 TEOM filters which had been used to collect particulate matter in the area of North Kensington, London at the DEFRA Automated Urban Network monitoring site. Each filter had been used to sample PM_{10} for 2 weeks particulate content present on the surface. The PM_{10} was extracted from the filter into 500µl of sterile saline by vortexing for 10 minutes. Turbidometry assays were conducted by preparing serial dilutions of nanoparticle carbon black standards ranging from 15µg/ml to 2mg/ml and measuring optical density using a Dynex multiwell plate reader. The concentration of PM_{10} was determined to be approximately 2 mg/ml. The PM_{10} extract was added to FBS to give an estimated final dose of 1 mg/ml PM_{10}. For comparison, the FBS was also exposed to 10 mg/ml of nanoparticle carbon black and both sets of samples were incubated in a shaking water bath at 37°C for 2 hours. Following incubation, the treated serum was centrifuged at 15000 g for 30 minutes. The serum was then tested for potential to induce macrophage migration. PM_{10}-treated serum diluted to 20% was also tested but due to limitations in the PM_{10} available for study, this could only be tested in one experiment (data not shown).

3.2.9 Statistical Analysis

Results are expressed as the mean ± SEM. All figures are the results of three separate experiments with three observations in each unless otherwise stated. Statistical analysis was by means of a one-way ANOVA with Tukeys multiple comparison.

3.3 RESULTS

3.3.1 Effects of Particle Treated Serum on Macrophage Migration

The results obtained indicate that treatment of serum with fine carbon black, fine TiO_2 or nanoparticle TiO_2 at all concentrations tested did not induce the production of any substance able to stimulate a subsequent migratory response by macrophages (Figure 3.2). Similarly, the 1 and 1.5 mg/ml concentrations of nanoparticle carbon black had no significant effect on serum-induced macrophage migration. In contrast, the highest dose of nanoparticle carbon black tested (5 mg/ml) did stimulate the production of an agent(s) in the bovine serum that induced a significant increase in the level of macrophage migration measured ($p<0.001$).

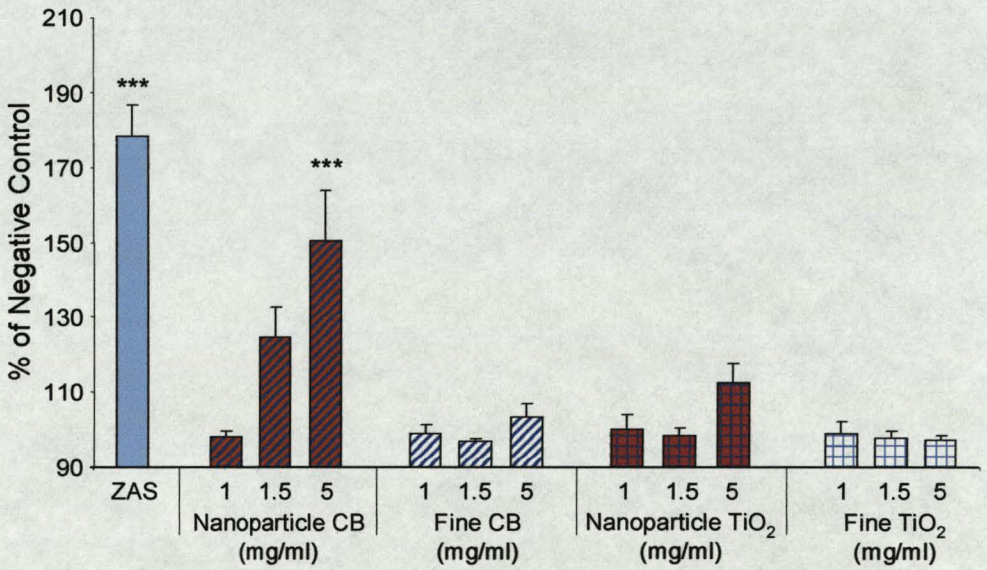

Figure 3.2 – Migration of J774.2 cells stimulated by FBS exposed to either fine and nanoparticle carbon black or TiO_2. Asterisks denote a significant change from the negative control (*** $p<0.001$)

3.3.2 The Effects of Dilution on the Potential for Particle Treated Serum to Induce Macrophage Migration

To date, many studies have utilised dilutions of ZAS as a positive control in chemotaxis experiments (Warheit *et al.*, 1988 and Donaldson *et al.*, 1990). Other studies have found that macrophage migration towards samples increases when samples are diluted (O'Brien *et al.*, 1998, and Warheit *et al.*, 1985). Therefore, dilutions of the treated serum were prepared to examine this observation (Figure 3.3). In contrast to the previous experiment, serum exposed to nanoparticle carbon black at a dose of 5 mg/ml did not induce a significant increase in macrophage migration at dilutions of 50% and 20% when compared to the negative control. Similarly, no increase was shown when the serum was treated with 10mg/ml nanoparticle CB and diluted to 50%. However, a significant increase in macrophage migration was found when serum was exposed to 10mg/ml of nanoparticle carbon black and diluted to 20% ($p<0.001$). There was no significant effect on migration as a result of exposure to serum incubated with any of the fine carbon black doses and dilutions tested.

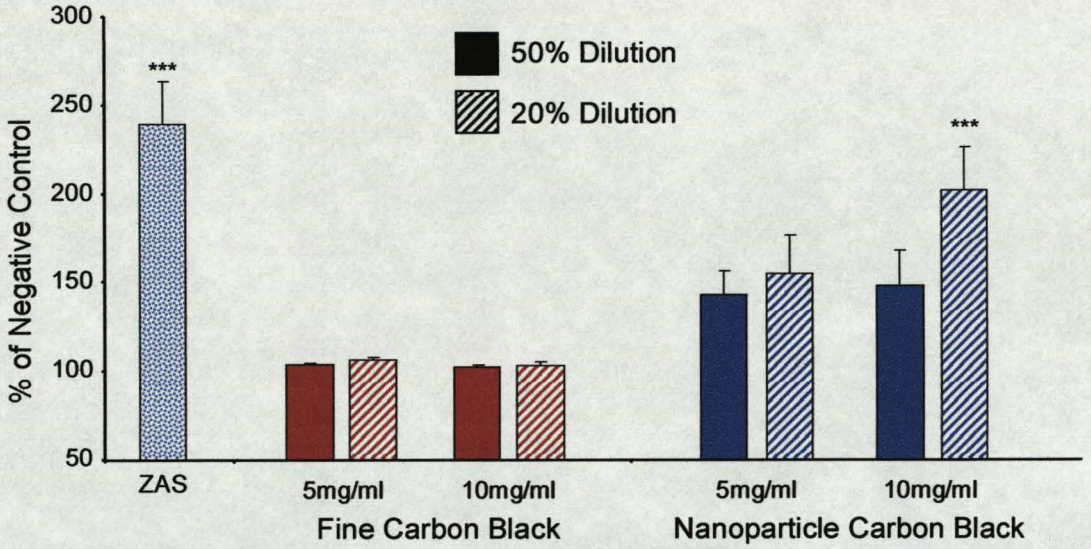

Figure 3.3 – Migration of J774.2 cells towards FBS exposed to fine or nanoparticle carbon black and subsequently diluted to 50% (1 in 2 dilution with RPMI) and 20% (1 in 5 dilution with RPMI). Asterisks denote a significant difference from the negative control. (*** $p<0.001$)

3.3.3 The Effect of Heat Inactivation on the Potential for Dilutions of Particle Treated Serum to Induce Macrophage Migration

In order to determine whether heat-labile components of the particle-treated serum were involved in stimulating macrophage migration, serum was treated with particles and subsequently heat-inactivated (Figure 3.4). Serum that had been exposed to nanoparticle carbon black (5mg/ml and 10mg/ml) and diluted to 20% demonstrated a significant increase in macrophage migratory potential compared to the negative control ($p<0.01$). When the serum was heat inactivated, the migration was decreased to a level that was no longer significantly different from the negative control.

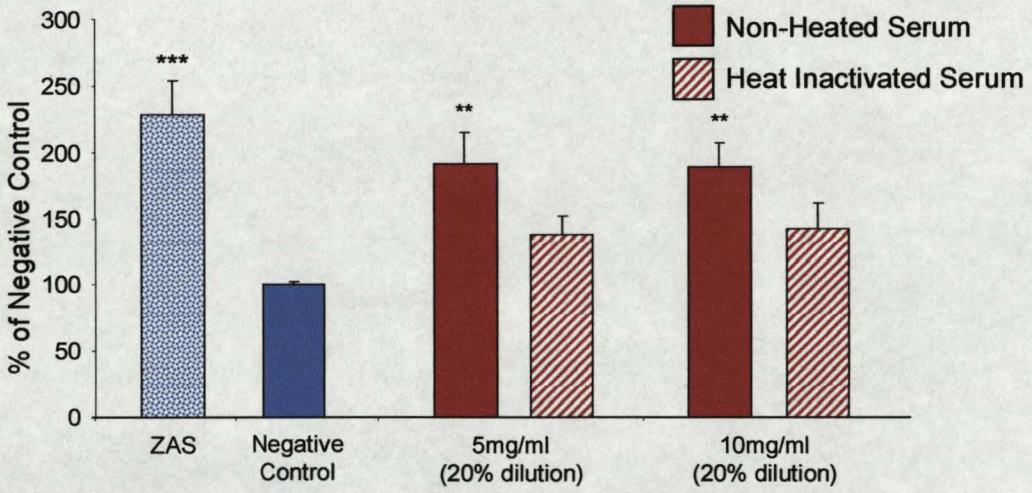

Figure 3.4 – Migration of J774.2 cells towards FBS treated with nanoparticle carbon black. Treated FBS was then heat inactivated and compared to non-heat inactivated FBS utilising a 20% dilution of each sample in the chemotaxis chamber. Asterisks denote a significant difference from the negative control. (**$p<0.01$).

3.3.4 The Effects of Serum Exposed to the Oxidant tBHP on Macrophage Migration

Serum was exposed to three different doses of the oxidant tBHP in order to determine whether oxidative stress can increase the potential of serum to induce macrophage migration. Serum exposed to tBHP demonstrated no significant increase in the induction of macrophage migration at any dose tested compared to the untreated serum control (Figure 3.5).

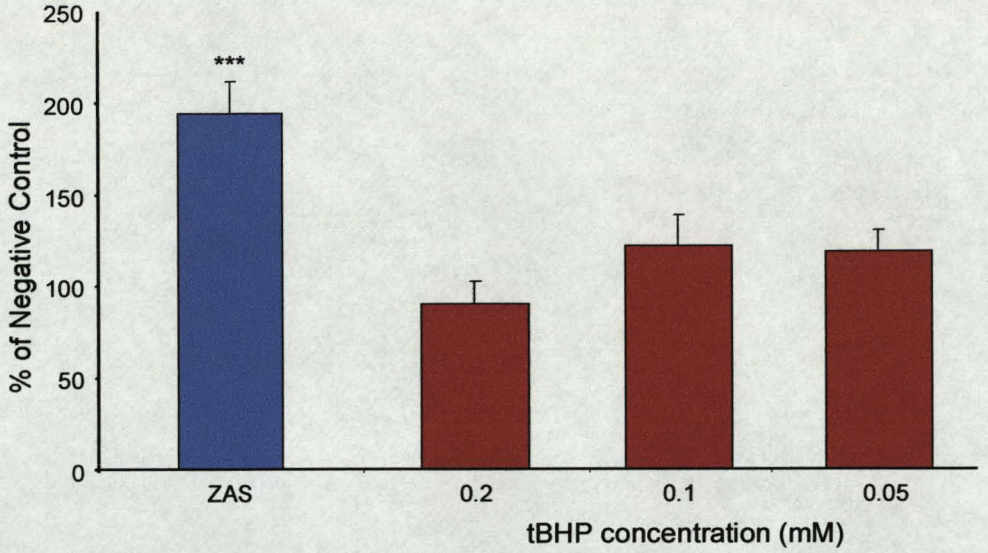

Figure 3.5 – Migration of J774.2 cells towards FBS that has been treated with varying concentrations of tBHP. Asterisks denote a significant change from the negative control (***$p<0.001$).

3.3.5 Serum Exposed to Particles in the Presence of Antioxidants – Effects on Macrophage Migration

As shown previously, serum exposed to nanoparticle carbon black (10 mg/ml) when diluted to 20%, demonstrated a significant increase in inducing macrophage migration ($p<0.01$). Following co-exposure of serum with nanoparticle carbon black and either the antioxidant Trolox or nacystelin, the effect on macrophage migration was ameliorated and was no longer significant (Figure 3.6). In contrast to the results shown in figure 3.2, the 5mg/ml dose of nanoparticle carbon black did not induce the production of substances which could significantly influence macrophage migration.

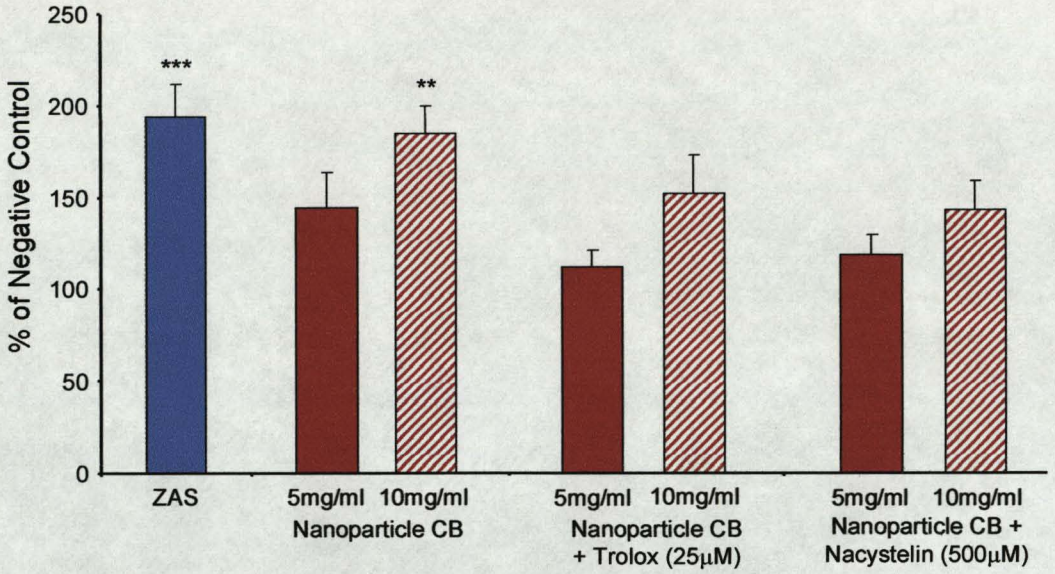

Figure 3.6 – Migration of J774.2 cells towards FBS that has been treated with nanoparticle carbon black (5 & 10mg/ml) in the presence and absence of the antioxidant Trolox or nacystelin. Asterisks denote a significant change from the negative control (** $p<0.01$ and *** $p<0.001$).

3.3.6 Serum Exposed to PM_{10} Extracts

Serum was exposed to extracts of PM_{10} suspended in sterile saline at a final concentration of 1 mg/ml. Serum was also exposed to sterile saline to control for the particle suspension medium. A significant increase in the potential of the serum to induce migration of macrophages was not observed with either the PM_{10} or sterile saline treatments at the doses used (Figure 3.7). As expected, the 10 mg/ml dose of nanoparticle carbon black induced a significant increase in the migration of macrophages towards the serum. PM_{10} exposed serum that had been diluted to 20% was also examined in a single experiment but did not induce any increase in macrophage migration (data not shown).

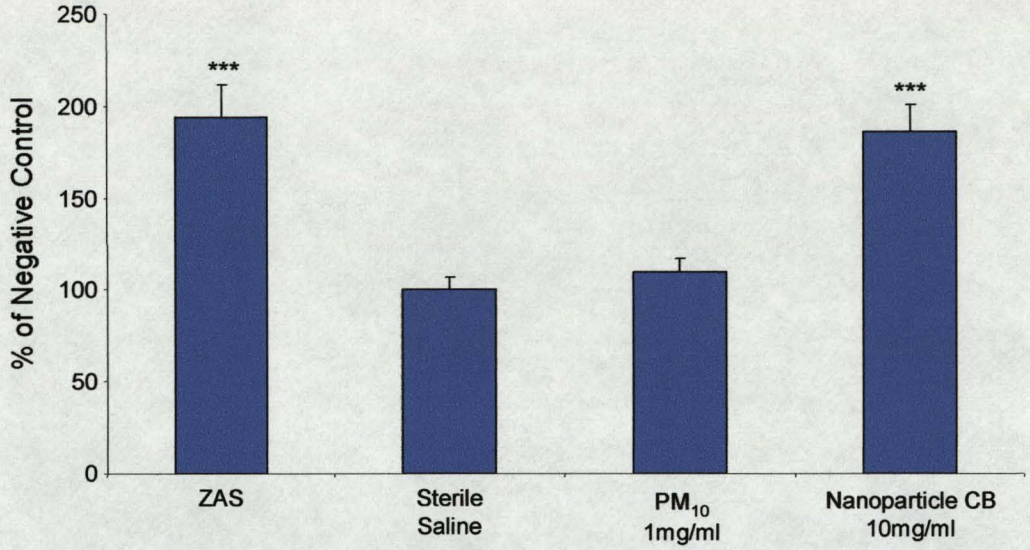

Figure 3.7 – Migration of J774.2 cells towards FBS that has been treated with sterile saline, PM_{10} (1mg/ml) and nanoparticle carbon black (10mg/ml). Asterisks denote a significant change from the negative control (*** $p<0.001$).

3.4 DISCUSSION

To date, the majority of the research that has been conducted on the potential for various occupational and environmental materials to activate the complement cascade in serum has focussed on asbestos (Hasselbacher, 1979, Warheit *et al.*, 1984, 1985, 1986 & 1988, Donaldson *et al.*, 1990 and Saint-Remy & Cole, 1980). These investigations have been worthwhile as they have established that different forms of asbestos (chrysotile and crocidolite) have the potential to activate the complement cascade and potentially induce macrophage migration to sites of fibre deposition. Other studies have shown that silica could also display this potential by cleaving pre-cursor complement proteins to produce anaphylatoxins that are potent macrophage and neutrophil chemoattractants (Governa *et al.*, 2002). Thus, the topic of this study is particularly relevant as ambient air pollution nanoparticles have attracted considerable attention with respect to their potential to cause toxicity and inflammation leading to disease exacerbation (Donaldson *et al.*, 2001a). Engineered nanoparticles have engendered a new discipline of 'nanotoxicology' to address the lack of knowledge in this area.

The results from this study indicate that nanoparticle carbon black, when exposed to blood serum at high doses (5-10mg/ml), induces the generation of a serum component which can cause significant increases in macrophage migration *in vitro*. Following nanoparticle carbon black treatment at a concentration of 5mg/ml, undiluted serum was found to have the potential to induce significant increases in macrophage migration. However, if the serum was diluted following treatment with particles, the dose of nanoparticle carbon black required to induce a significant increase in macrophage

migration was 10mg/ml in serum that had been subsequently diluted to 20%. The 50% dilution of serum at this dose of particles did not appear to induce significant increases in macrophage migration. This could indicate that a Gaussian-shaped balance exists between the concentrations of chemoattractant generated and the macrophage migration induced by the chemoattractant i.e. too little or too much of the chemoattractant does not cause any change in the potential for the serum to induce macrophage migration.

Subsequent concentration response studies indicated that the most potent chemotactic response of the macrophages was found when the treated serum was diluted to 20%. When the serum was heat inactivated following particle treatment, the migratory effects of the diluted serum were reduced to a level that was no longer significantly different compared to the negative control. It was noted that the effect of the 20% dilution of particle treated serum was decreased when co-exposing the serum to particles in the presence of antioxidants. It should also be noted, however, that when serum was exposed to the oxidant tBHP or low doses of PM_{10}, there is no increase in the potential of the serum to induce macrophage migration.

Several studies have described the interactions of various organic and inorganic substances with the complement system. Wilson *et al.*, (1977) utilised an *in vitro* haemolysis assay to demonstrate that five different types of asbestos fibres activated the alternative complement pathway. An investigation of chrysotile asbestos by Saint- Remy & Cole (1980) showed a potential to activate the alternative pathway *in vitro*. These studies were supported by in an investigation by Yano *et al.*, (1984), which showed the

generation of chemotactic factors in serum by both chrysotile and crocidolite asbestos. Warheit *et al.*, (1985 and 1986) also demonstrated that chrysotile asbestos fibres activated complement in rat serum both *in vitro* and *in vivo* and noted that complement activation was the primary chemotactic stimulus for macrophage mediated clearance of fibres; there was also a suggestion that iron chemistry might be involved in these effects. Hill *et al.*, (1982) demonstrated fly ash particle induced complement activation while Olenchock *et al.*, (1978) described activation of the alternative pathway by grain dust *in vitro*.

Based on the results generated by this study it is possible that, should the nanoparticles activate the alternative complement cascade, the anaphylatoxin C5a could be generated via cleavage of the pre-cursor protein C5. C5a is known to be a potent macrophage and neutrophil chemoattractant (Shin *et al.*, 1968 and Snyderman *et al.*, 1971) and is involved in enhancing functional responses of phagocytes (Ward, 2004). The enhanced migration of macrophages towards serum that has been exposed to nanoparticle carbon black indicates that such a generation of C5a may have taken place.

The mechanism by which asbestos fibres and particles such as silica activate the complement cascade is, as yet, unclear but several hypotheses have been formed to explain this finding. In the study by Governa *et al.*, (2002), it was proposed that hydroxyl radicals present on the surface of the silica were involved in C5 (the pre-cursor to C5a) cleavage and that the extent to which the C5 was cleaved was dependent on C5 adsorption onto the surface of the silica particles. The adsorption of serum proteins on to the surface of coal dust and asbestos has been investigated, and it was determined that

selective binding of proteins took place on the surfaces of both the asbestos and silica (Jones *et al.*, 1972 and Hasselbacher, 1979). Desai & Richards, (1978) demonstrated that the incubation of FBS with asbestos, quartz and TiO_2 samples resulted in the binding of serum proteins to the surface of the mineral dusts. Nanoparticles have been shown to have a much larger surface area than an equivalent mass of fine particles. Brown *et al.*, (2000) has demonstrated binding of bovine serum albumin (BSA) to nanoparticles in concordance with studies by Wilson *et al.*, (personal communication) and Lightbody *et al.*, (DEFRA report EPG1/3/147) which showed cytokine binding to the surface of nanoparticles and PM_{10} samples. It may be that this increased potential for protein binding could provide an indication as to the potential of a given particulate to activate the complement cascade by surface binding.

Governa *et al.*, (2002) also suggested that iron, a common contaminant on the surface of silica, assisted the reaction via Fenton or Haber-Weiss chemistry. The study by Warheit *et al.*, (1985) also supported the theory that iron played an important role in the surface chemistry of the reactions involved in complement activation. Wilson *et al.*, (2002) noted that when nanoparticle carbon black was co-incubated in the presence of iron salts, ROS production increased in a potentiative manner. The summation of these studies would indicate that iron is a key component in potentiating surface chemistry, and that complement activation studies conducted with nanoparticle carbon black and iron salts may provide an interesting insight into the interaction between metals and particles.

When the serum was exposed to nanoparticle carbon black in the presence of antioxidants, the chemotactic potential of the serum was less than that of serum treated with only nanoparticle carbon black. This would further support the hypothesis that the activation of the complement cascade is oxidant mediated. However, when testing serum that has been exposed to varying concentrations of the oxidant tBHP to induce macrophage migration, it was found that, with an oxidant alone, there was no significant increase in the level of macrophage migration towards the treated serum. This could indicate that there were no complement proteins present that could cause macrophage migration. This could indicate that pure oxidants, such as tBHP, do not possess the pre-requisites to activate complement. However, these results are not conclusive as it is entirely possible that further studies conducted with other oxidants such as H_2O_2, $O_2^{\bullet-}$ or $ONOO^-$ could yield different results. The observations in this study indicate that another factor could be involved in C5a generation. Vogt *et al.*, (1989) demonstrated that C5 cleavage by radicals of H_2O_2 could form a C5b-like protein that was not chemotactic itself, but could be split by the proteolytic 'kallikrein-kinin' plasma system to form C5a (Regoli *et al.*, 2001). This would suggest that ROS play a key role in the generation of chemotaxins in serum, but that further steps are required to complete the production of functional chemotactic serum components.

The complement protein C5a is known to be heat stable when heated to 56°C as opposed to other serum proteins that are heat labile (Georgsen *et al.*, 1990). When serum was heat inactivated following particle treatment it was found that the potential for the serum to induce macrophage migration was decreased. This is contrary to the hypothesis that C5a

is the complement component responsible for inducing macrophage migration in our studies. However, there could be several explanations for this. The first fact to take into account is that the serum tested in this set of experiments did not have a high potential for inducing macrophage migration when incubated with nanoparticle carbon black. It is possible that C5a was not the only component of serum to attract macrophages, therefore, when the serum was heat inactivated, a portion of the potential may have been lost through the destruction of a heat-labile serum protein. It may also be possible that following removal of the particles from the serum, residual complement activation may still have been occurring. The heating process prevents any further complement activation and as such may have halted this process.

The results indicate that the most potent macrophage response to the particle treated serum was found when the serum was diluted to 20% with RPMI 1640. This is a higher concentration than with serum that has been incubated with Zymosan A. Zymosan is a potent activator of C5 and as such is hypothesised to generate a large amount of C5a in blood serum. Therefore, it could be suggested that nanoparticle carbon black, is not as potent an activator and, as such, a higher concentration of activated serum is required to induce a significant amount of macrophage migration. Renwick *et al.*, (2004) found that a 10% dilution of ZAS acted as an adequate positive control for a macrophage chemotaxis study. Warheit *et al.*, (1985) also found that a 10% dilution of asbestos and Zymosan activated sera induced the highest level of macrophage migration. Lower dilutions of ZAS were also used by Geiser *et al.*, (1998) where it was found that a ZAS dilution of 1:256 induced a high level of macrophage migration. It may be the case that

high concentrations of ZAS could also prove to be toxic to macrophages or that much lower dilutions of particle treated serum could induce levels of macrophage migration measured in this study.

PM_{10} has been shown to induce inflammatory responses when instilled into the lung. Li *et al.*, (1996) demonstrated that PM_{10} exhibited free radical activity and that this activity may play a role in the pro-inflammatory effects of PM_{10}. It has been shown that PM_{10} contains a mixture of nanoparticles and transition metals as well as other components that have a potential for inducing inflammation (Stone *et al.*, 2003 and Gilmour *et al.*, 1996). In this study, low doses of PM_{10} did not appear to induce the generation of factors that could induce macrophage migration. This could be attributed to several factors; firstly, the PM_{10} dose utilised in this study may have been too low to induce any measurable effects in the serum. The PM_{10} mass that could be used in this investigation was limited by the number of filters available for use and the mass of PM_{10} that could be extracted from each filter. Further studies using higher doses of PM_{10}, together with various dilutions of PM_{10} treated serum may yield different results to those expressed here. Secondly, the composition of PM_{10} has been shown to be highly variable depending upon a number of factors such as the location of the sampler, wind direction and other anthropogenic factors (Schins *et al.*, 2004). The PM_{10} in this study was sourced from North Kensington, London, an urban background area, and was analysed for inflammatory potential by Lightbody *et al.*, (2004 – manuscript in preparation). Treatment of serum with a PM_{10} sample that has been reported to have a higher concentration of nanoparticles or transition metals per unit of mass may display different

results but due to the limitations of the PM_{10} samples available for this study, this avenue of investigation could not be pursued. Similarly, the endotoxin content of the PM_{10} may have some bearing on the potential of the sample to activate the complement cascade in the serum. Endotoxin has been shown to be present in airborne particulate samples (Soukup and Becker, 2001) and has been shown to activate complement based chemotactic components in serum (Snyderman *et al.*, 1969 and Horn *et al.*, 1984). Finally, the particulate component of the PM_{10} may have adsorbed some of the chemotactic proteins onto the particle surface, similar to the adsorption phenomenon observed by Jones *et al.*, (1972) and Lightbody *et al.*, (DEFRA report EPG1/3/147). This may render the proteins non-functional in terms of influencing macrophage migration.

In conclusion, the fact that complement proteins are found in lung lining fluid at biologically active concentrations may indicate that an early complement-based clearance mechanism for particles depositing in the alveolar regions of the lung. Complement activation can occur within minutes (Śladowski *et al.*, 2001) and activation of complement cascades resulting in the generation of chemotactic proteins could induce recruitment of leukocytes prior to opsonisation and phagocytosis of the particulates. This could result in a rapid removal of particles from the alveolar region and decrease the potential damage that can be caused by deposited nanoparticles. The increased potential of nanoparticles in activating the alternative complement cascade compared to fine particles may actually aid in the clearance of these particles and, as such, help prevent nanoparticle induced toxicity.

CHAPTER 4

THE EFFECTS OF PM_{10} ON ALVEOLAR MACROPHAGE CLEARANCE MECHANISMS *EX VIVO*

4.1 INTRODUCTION

The alveolar macrophage is the primary mediator of particle clearance in the alveolar space. It is hypothesised that the volumetric loading of the macrophage can have deleterious effects on the cells phagocytic and chemotactic ability. Morrow (1988) indicated that macrophages showed an impaired ability to migrate towards the mucociliary escalator (MCE) when approximately 6% of the internal volume of the macrophage was occupied by phagocytosed particles. Investigations by Tran *et al.*, (2000) with two low toxicity, low solubility dusts implied that impaired clearance was in fact driven by the surface area metric rather than the mass metric. This supported data previously published by Oberdörster *et al.*, (1994) which illustrated prolonged macrophage mediated clearance of nanoparticle TiO_2 from the lung compared to fine TiO_2. Renwick *et al.*, (2001) also demonstrated that exposure to high concentrations of nanoparticles of TiO_2 and carbon black *in vitro*, could impair the phagocytic ability of a macrophage cell line. Hoet and Nemery (2001) also suggested that the results of Renwick *et al.*, demonstrated that low concentrations of particles could also stimulate phagocytosis and that further investigation was needed to establish a clearer picture. However, these effects of alveolar macrophage overloading may only be relevant at very high or overload dose exposures (Oberdörster, 1995).

The consequences of impaired clearance mechanisms can be severe. As exposure to particles continues, there is a build up of dose, which can lead to direct macrophage and epithelial cell damage. There is also increased potential for the translocation of particles into the cardiovascular system as well as systemic cytokine release and increased blood

coagulabilty (Seaton *et al.*, 1995). Nemmar *et al.*, (2001, 2002) demonstrated how both instilled and inhaled nanoparticles could rapidly pass into the blood circulation. Oberdorster *et al.*, (2004) showed translocation of inhaled radioactive carbon nanoparticles to the cerebrum and cerebellum in a rat model. Conversely, Kreyling *et al.*, (2002) found limited evidence of nanoparticle iridium translocation from the lungs.

The aim of this study was to use an animal model to investigate the effects of PM_{10} on pulmonary macrophage clearance mechanisms. The ability of alveolar macrophages, isolated from rats treated with PM_{10} particles, to phagocytose indicator latex beads was assessed as well as the potential for PM_{10} treated macrophages to migrate towards a positive chemoattractant *ex vivo*. Biochemical measurements of proteins present in the bronchoalveolar lavage (BAL) fluid were also conducted with a view to ascertaining the extent to which the cellular integrity of the lung had been affected. It is hoped that the results presented in this chapter contribute to the understanding of the toxicological effects of particulate air pollution on macrophage mediated clearance mechanisms.

4.2 MATERIALS AND METHODS

4.2.1 Chemicals and Reagents

All chemicals and materials were purchased from Sigma Aldrich, UK, unless otherwise specified.

4.2.2 Particle Preparation

PM_{10} collected over 2-week intervals at kerbside TEOM samplers located in North Kensington, London between 1998 and 2001 were used in this study. To extract the particulates, the filters were immersed in 0.5 ml of sterile saline and vortexed for 10 minutes. The suspended particulate mass was then estimated using turbidometry and adjusted to 125μg and 250μg doses suspended in 0.5ml of sterile saline. Solutions were sonicated for 20 minutes to ensure particle suspension prior to instillation.

4.2.3 Instillations of PM_{10}

Male Wistar rats, weighing between 200-300g were anaesthetised with halothane. One rat was utilised for each PM_{10} or control treatment i.e. 3 rats per experiment. Control rats were instilled with 0.5ml of sterile saline. Particle treated animals were instilled with either 125μg or 250μg of PM_{10} filter extracts in 0.5ml of saline. Rats were subsequently sacrificed by an intra-peritoneal injection of pentobarbitone 18 hours after particle instillation. The lungs were lavaged 5 times with 8 ml sterile saline and the first lavage was stored at -80°C for cell-free biochemical analysis. The other four lavages were pooled and then centrifuged at 900 g to isolate the bronchoalveolar lavage (BAL)

leukocytes, which were then pooled with the leukocytes isolated from the first lavage. The remaining BAL fluid was discarded.

The BAL cell pellet was resuspended in RPMI 1640 medium supplemented with 1% L-glutamine and 1% Penicillin/Streptomycin. Total cell counts and viability were assessed using 0.3% trypan blue exclusion and an improved Neubauer haemocytometer. To ascertain the numbers of neutrophils that had migrated into the lung, cytospin slides were also prepared and stained with Diffquik stain. (Raymond A Lamb, London), before counting using light microscopy. The remaining BAL cells were employed in the phagocytosis (section 4.2.6) and chemotaxis (section 2.2.8) assays.

4.2.4 Cytotoxicity & Lung Damage

Total BAL lactate dehydrogenase (LDH) levels were determined as follows (Brown *et al.*, 2001). To create a standard curve, pyruvate standards were prepared (using distilled H_2O and 1mg/ml NADH dissolved in 0.75mM sodium pyruvate), ranging in concentrations equivalent to 0 – 2000 Units/ml of LDH. One unit of LDH activity is defined as the amount of LDH that reduces 4.8×10^{-4} µmol of pyruvate in 1 minute at 25°C. The standards were transferred (60µl) in triplicate, to a 96-well plate. Into all of the remaining wells of the plate, 50µl of NADH was added. The samples were incubated at 37°C / 5% CO_2 for 5 minutes.

The test and control samples (10µl) were added to the relevant wells on the plate containing the NADH solution. The samples were incubated at 37°C, 5% CO_2 for 30 minutes. Following incubation, 50µl of 2, 4-dinitrophenylhydrazine (0.2mg/ml dissolved

in 1M HCl) was added to all of the wells and the samples were left for 20 minutes at room temperature. Sodium hydroxide (50µl of 4M concentration) was then added to each well and the samples were left at room temperature for 5 minutes. The plate was shaken for 5 seconds and the absorbance of all the wells was measured at 540nm with a Dynex MRX microplate reader.

BAL protein levels were assessed using Coomassie Blue G250. Coomassie Blue protein reagent (Bio-Rad) was diluted 1 in 5 with distilled water and added to each well on a 96 well plate (200µl). BAL samples were then added (5µl) and incubated for 15 minutes. The absorbance of each well was read at 450nm.

BAL albumin was measured using Bromocresyl green reagent substrate prepared with 0.66mM of Bromocresyl green in 100mM of succinate buffer at pH 4.2. Samples (100µl) were added to the reagent substrate and the absorbance was read at 630nm.

4.2.5 TNFα & MIP-2 ELISA

BAL TNFα and MIP-2 protein concentrations were determined by an ELISA cytoset kit (Biosource, UK), according to manufacturer's instructions. Briefly, 96-well plates (Scientific Laboratory Supplies, UK) were coated with coating antibody and incubated for 18 hours at 2-8°C. Between each step of the protocol the plates were washed with wash buffer (PBS + 0.1% Tween 20). The plates were then blocked with 0.35g BSA dissolved in 70ml PBS for 2 hours. Standards and samples were then added and incubated for 90 minutes at room temperature. The biotinylated detection antibody was

added and the plate was incubated for a further 1 hour at room temperature. The streptavidin-horse radish peroxidase (S-HRP) conjugate (0.16%) was added (100µl) and incubated for 45 minutes at room temperature. The chromagen tetramethylbenzidine (TMB) was added (100µl) and the plate was incubated for 30 minutes in the dark. A stop solution of 2M sulphuric acid was added to develop the colour and the optical density of each well was read at a dual wavelength absorbance of 450/650nm.

4.2.6 Phagocytosis Assay

BAL cells were suspended in normal culture medium at a concentration of 2×10^5/ml and 1ml was added to each well in Labtek chamber slides. The chamber slides were incubated overnight in a humidified incubator at 37°C and 5% CO_2. The medium from the slides was aspirated and the slides were washed twice with normal culture medium to remove any non-adherent cells. The medium was replaced with 1ml of culture medium containing 2µm latex beads at a bead to cell ratio of 5:1. Following incubation for 18 hours the slides were washed twice with PBS, stained with a Diffquik stain and then counted using a fluorescent microscope (Carl Zeiss). The counting procedure for each chamber slide involved randomly counting 300 cells from each treatment, establishing whether PM_{10} was visible inside the cell or not, and counting the number of latex beads visible inside each cell.

4.2.7 Chemotaxis Assay

The chemotaxis assay was conducted according to the protocol described in section 2.2.8. Macrophages that had been isolated from the PM_{10} treated rats were tested for their ability to migrate towards positive (ZAS) and negative (HIS) chemoattractants.

4.2.8 Statistical Analysis

Results are expressed as the mean ± SEM. All figures are the results of three separate experiments with three observations in each experiment unless otherwise stated. Statistical analysis was by a one-way ANOVA with Tukeys multiple comparisons.

4.3 RESULTS

4.3.1 Inflammatory Responses to PM_{10}

Figure 4.1 illustrates the number of neutrophils identified in the BAL 18 hours after instillation of the PM_{10} samples. Treatment with 250μg of PM_{10} induced a significant increase in BAL neutrophil number compared to the saline control ($p<0.05$). In contrast the 125μg dose of PM_{10} did not induce a significant change in neutrophil numbers. Treatment of the rats with 250μg PM_{10} for 18 hours also induced a significant decrease in macrophage number observed in the BAL compared to the control ($p<0.05$) (Figure 4.2). Again, the 125μg treatment induced a modest decrease in macrophage numbers that was not statistically significant.

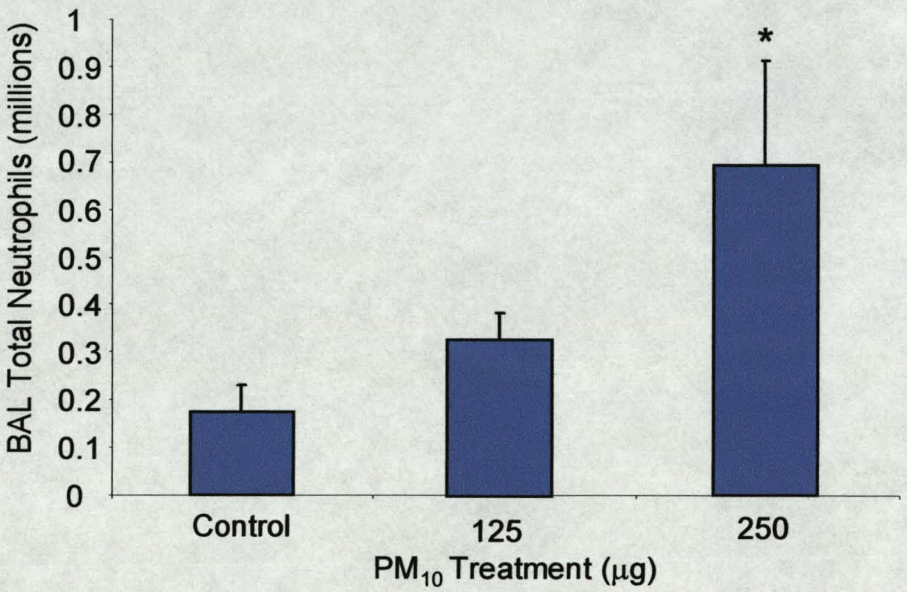

Figure 4.1 – Total neutrophil count in BAL fluid of rats 18 hours after instillation with either sterile saline (control), 125μg or 250μg of PM_{10}. Results are the mean ± SEM of three separate experiments. * indicates a significant difference from the control ($p<0.05$).

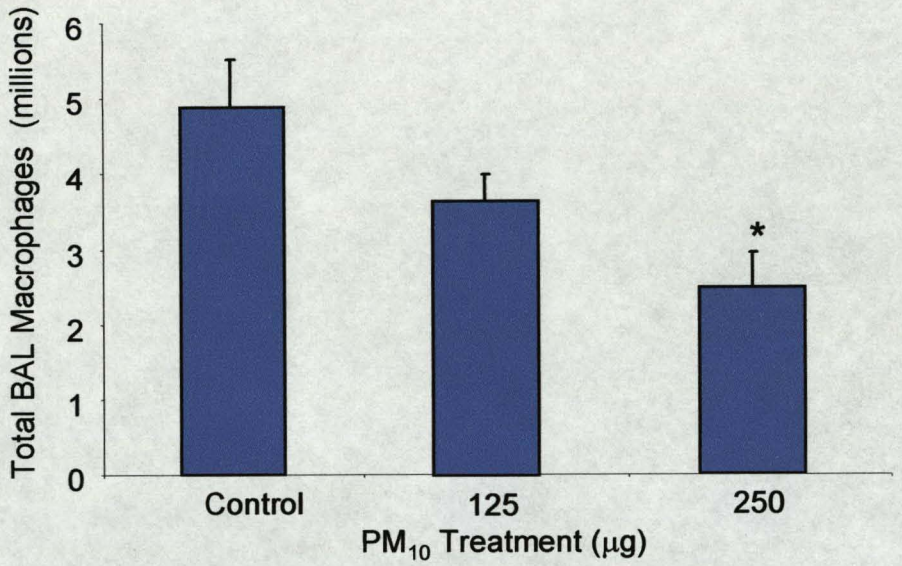

Figure 4.2 – Total macrophage count in BAL fluid of rats 18 hours after instillation with either sterile saline (control), 125μg or 250μg of PM_{10}. Results are the mean ± SEM of three separate experiments. * indicates a significant difference from the control ($p<0.05$).

4.3.2 Cytotoxicity

LDH levels in BAL were measured with a view to assessing the extent of the cellular damage caused by the PM_{10} particles. The data showed that there was no change in BAL LDH compared to the saline control for both PM_{10} doses (Figure 4.3). This was supported by data obtained by measuring the total protein concentration in the BAL as an indicator of lung permeability. As was seen with the LDH measurements, there was no significant change in BAL protein compared to the control (Figure 4.4).

The albumin concentration in the BAL was also measured to determine whether the lung vasculature had been damaged. The results indicated that there was also no significant change in the concentration of albumin in the BAL after treatment with either PM_{10} dose (Figure 4.5).

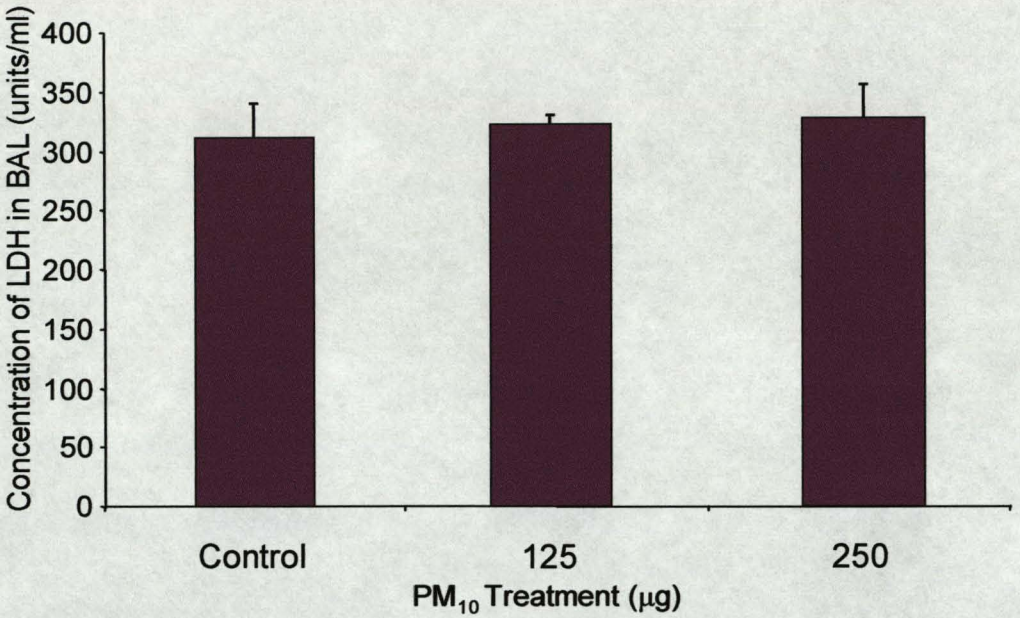

Figure 4.3 – Concentration of lactate dehydrogenase (LDH) in BAL fluid of rats 18 hours after instillation with either sterile saline (control), 125μg or 250μg of PM_{10}. Results are the mean ± SEM of three separate experiments.

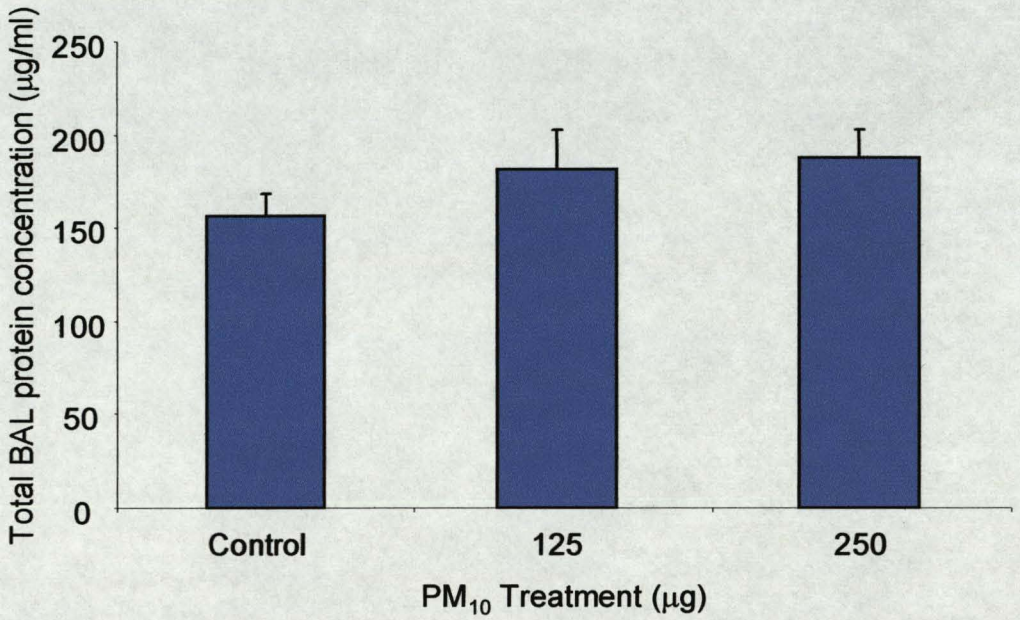

Figure 4.4 – Total protein concentration in BAL fluid of rats 18 hours after instillation with either sterile saline (control), 125μg or 250μg of PM_{10}. Results are the mean ± SEM of three separate experiments.

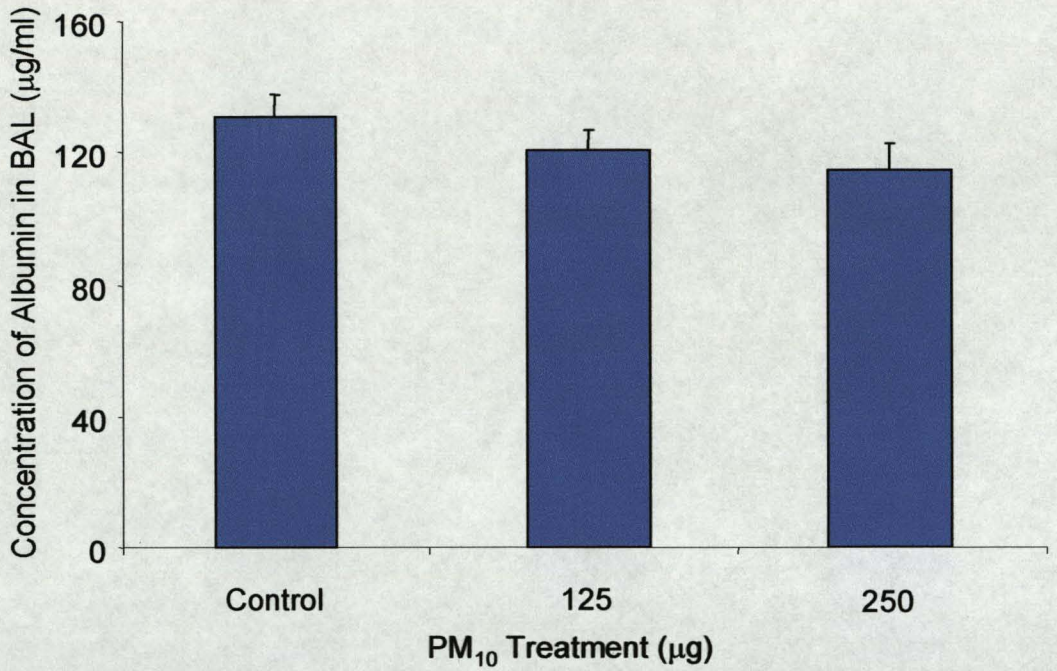

Figure 4.5 – Albumin concentration in BAL fluid of rats 18 hours after instillation with either sterile saline (control), 125µg or 250µg of PM_{10}. Results are the mean ± SEM of three separate experiments.

4.3.3 Cytokine release

The concentrations of the two pro-inflammatory cytokines MIP-2 and TNFα in the BAL fluid were measured by ELISA. Both the 125µg and the 250µg dose of PM_{10} induced a significant increase in the concentration of TNFα in the BAL compared to the saline control ($p<0.01$ and $p<0.001$ respectively) (Figure 4.6). In contrast, the concentration of MIP-2 in the BAL remained unchanged (Figure 4.7).

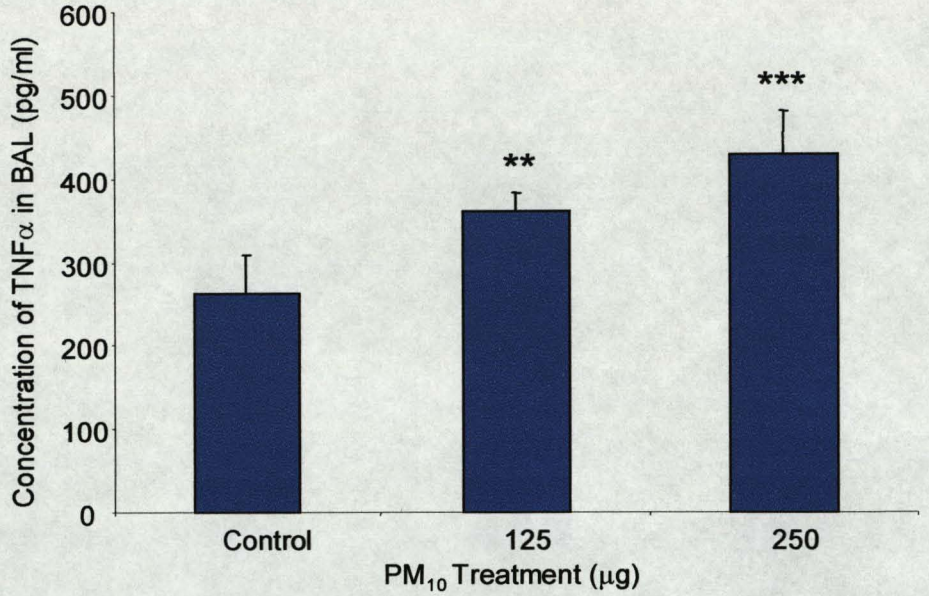

Figure 4.6 – Concentration of TNFα in BAL fluid of rats 18 hours after instillation with either sterile saline (control), 125μg or 250μg of PM_{10}. Results are the mean ± SEM of three separate experiments. *** denotes a significant difference from control ($p<0.001$), ** denotes a significant difference from control ($p<0.01$).

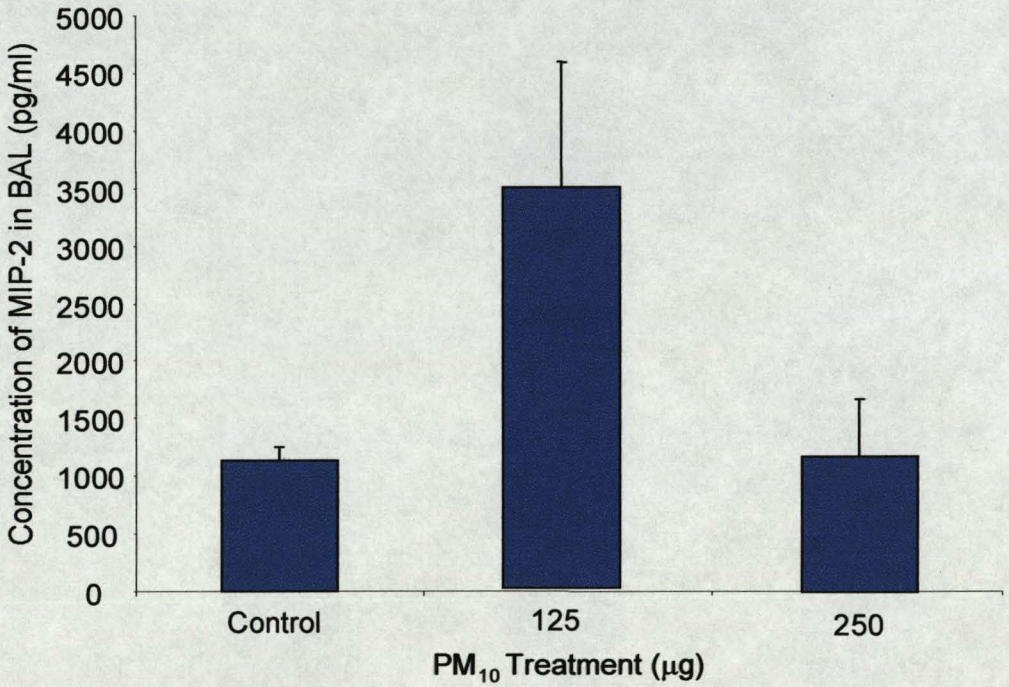

Figure 4.7 – Concentration of MIP-2 in BAL fluid of rats 18 hours after instillation with either sterile saline (control), 125μg or 250μg of PM_{10}. Results are the mean ± SEM of three separate experiments.

4.3.4 Phagocytosis

Figure 4.8 is a microscope image of macrophages obtained from a rat 18 hours after instillation of 250μg of PM_{10}. The white arrow points towards a latex bead and the black arrow points towards PM_{10} that has been phagocytosed by the macrophage. Figure 4.9 shows the percentage of alveolar macrophages that had phagocytosed indicator beads and/or PM_{10} after treatment of the rats with saline or PM_{10}. Cells that had visibly phagocytosed PM_{10} particles, indicator latex beads or both as determined by microscopy were termed 'phagocytic'. Cells that did not visibly phagocytose either PM_{10} or latex beads were termed 'non-phagocytic'. Treatment of the animals with 125μg of PM_{10} significantly decreased the number of non-phagocytic cells present in BAL ($p<0.001$). There was no significant change in the number of non-phagocytic cells from the animals treated with 250μg PM_{10}. The number of phagocytic cells was slightly increased following treatment with particles but this was not statistically significant.

Treatment of the rats with either 125 or 250μg PM_{10} resulted in a BAL alveolar macrophage population that visibly contained PM_{10} and exhibited a significant decrease in the number of latex beads that they could phagocytose per cell *ex vivo* ($p<0.05$ and $p<0.01$ respectively) (Figure 4.10). The alveolar macrophages that did not visibly contain PM_{10} appeared to also phagocytose fewer latex beads than the control but this was not statistically significant.

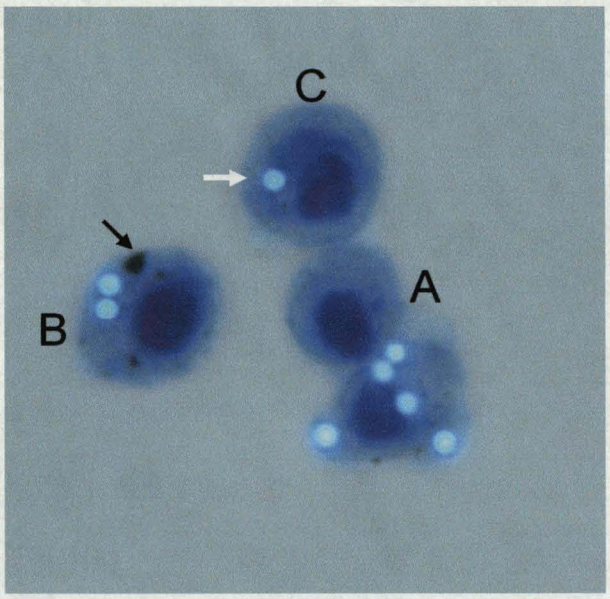

Figure 4.8 - Microscope image of macrophages obtained from rats treated for 18 hours with PM_{10} or saline (control). 'Non'phagocytic' macrophages (A), cells that have visibly phagocytosed indicator beads and PM_{10} (B) as well as cells that have only phagocytosed indicator beads are illustrated (C). The white arrow indicates a latex bead and the black arrow points towards PM_{10} (Magnification x1000).

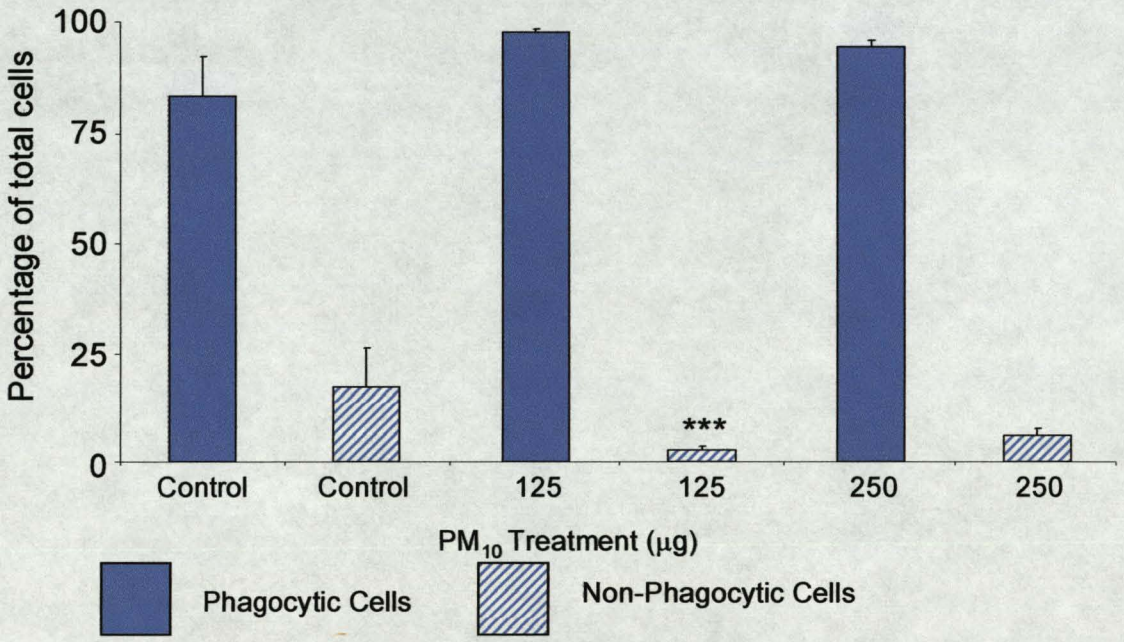

Figure 4.9 – The number of macrophages exhibiting phagocytosis as indicated by PM_{10} or latex bead uptake. Macrophages were lavaged from rats 18 hours after instillation with either sterile saline (control), 125µg or 250µg of PM_{10}. Results are the mean ± SEM of three separate experiments. *** denotes a significant change from the non-phagocytic control ($P<0.001$)

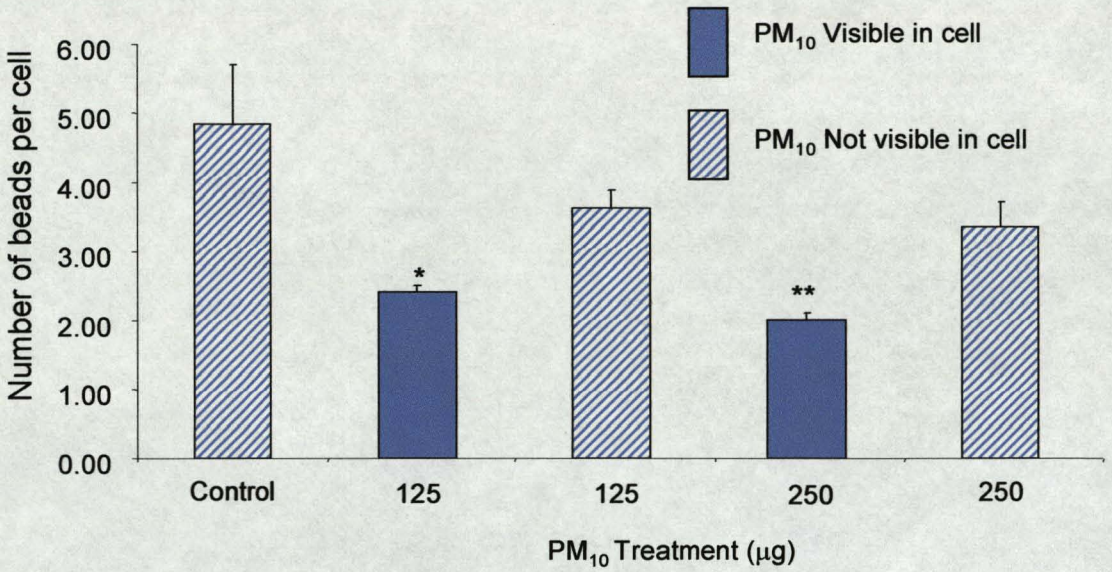

Figure 4.10 – Phagocytic potential of macrophages from rats instilled with sterile saline (control), 125μg or 250μg of PM_{10}. Phagocytic potential is indicated by the number of latex beads phagocytosed per macrophage *ex vivo*. Results are the mean ± SEM of three separate experiments. ** denotes a significant change from the non-phagocytic control ($P<0.01$), * denotes a significant change from the control cells ($p<0.05$)

4.3.5 Macrophage Migration Studies

The ability of the lavaged macrophages to migrate towards the known chemoattractant ZAS is shown in figure 4.11. Instillation of both doses of PM_{10} resulted in a significant decrease in macrophage migration towards ZAS ($p<0.001$). The negative control involved assessing migration of macrophages from control animals towards heat-inactivated serum, and indeed this was significantly less than towards ZAS. Migration towards heat-inactivated serum was not altered by PM_{10} treatment of the rats ($p<0.001$) indicating that the effect of PM_{10} on ZAS-induced migration was a specific effect.

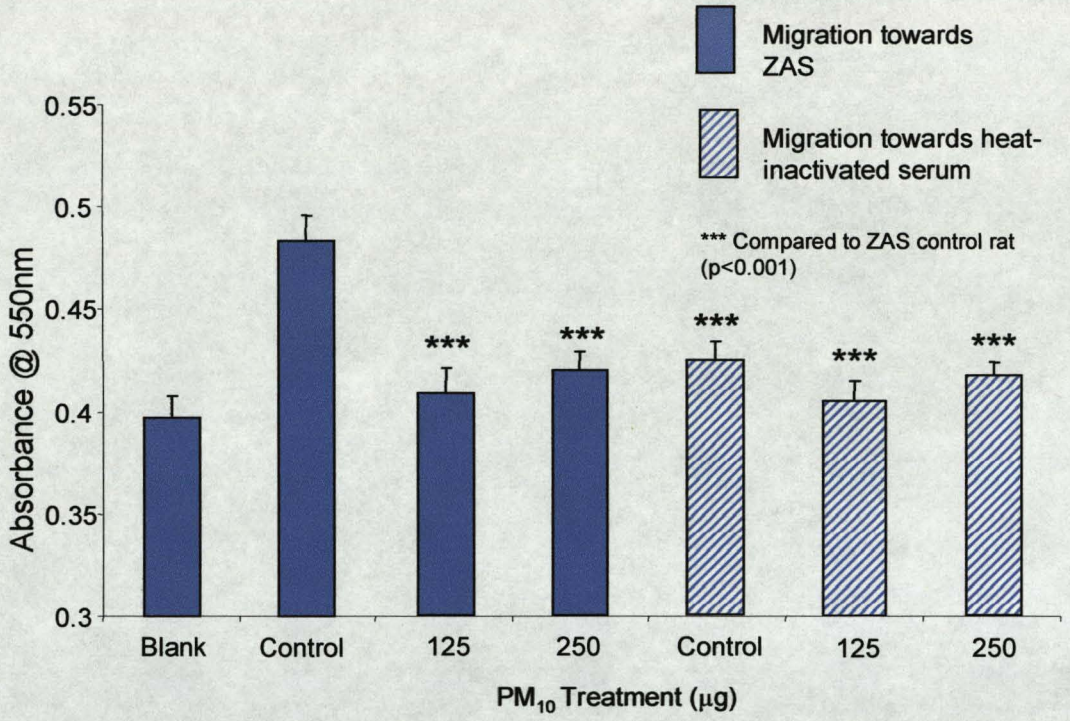

Figure 4.11 – Migration of macrophages obtained from rats 18 hours after instillation with either PM_{10} (125 or 250μg) or saline (control) towards positive (ZAS) and negative (heat-inactivated serum) chemoattractants. Results are the mean ± SEM of three separate experiments. *** denotes a significant difference from the positive control ($p<0.001$)

4.4 DISCUSSION

As mentioned in chapter 1, increases in environmental PM_{10} levels have been implicated as a causal agent in inducing exacerbations of disease and increased mortality from cardiovascular and respiratory conditions (Seaton *et al.*, 1995). This chapter examined the effects of PM_{10} collected in North Kensington, London, on inflammation in the rat lung and the subsequent effects on alveolar macrophage phagocytosis and chemotactic capability *ex vivo*.

The highest dose of PM_{10} utilised in this study (250μg/rat) caused an increase in the number of neutrophils present in the BAL fluid indicating that neutrophilic inflammation was present in the lung. This is comparable with many other studies that have also reported neutrophil influx as a result of ambient particle exposure (Li *et al.*, 1996, Schins *et al.*, 2004). It should also be noted that macrophage numbers were decreased in the lavages obtained from the PM_{10} treated animals. This decrease in macrophage number may be due to the migration of the macrophages, with their particle burden, from the lung via the MCE. Alternatively, the particle-laden macrophages may have undergone apoptosis (Soukup & Becker, 2001 and Obot *et al.*, 2002).

Cytotoxicity assessments (LDH, total protein and albumin measurement) conducted in this study indicated that no significant cellular or lung damage was induced by the PM_{10} treatments compared with the control animals. Therefore, this indicated that the inflammatory responses evoked were specific to the particle treatment rather than being a consequence of gross lung damage.

TNFα and MIP-2 have previously been described to play important roles in particle induced lung inflammation. As mentioned previously, TNFα is a potent pro-inflammatory cytokine that is involved in stimulating the production of chemotactic cytokines such as MIP-2 (Driscoll, 2000). In this study, it was noted that the concentration of TNFα in BAL fluid increased as a result of PM_{10} treatment at either dose. Jimenez *et al.*, (2002) noted that macrophages exposed to PM_{10} produce TNFα and that this TNFα is capable of stimulating lung epithelial cells to release pro-inflammatory cytokines for the recruitment of leukocytes.

As described in chapter 1, MIP-2, the rat homologue of IL-8 is a chemotactic cytokine involved in the recruitment of neutrophils and monocytes to localised sites of inflammation (Driscoll, 2000). In this study the concentration of MIP-2 was modestly increased following PM_{10} treatment at a dose of 125μg but this was not statistically significant compared to MIP-2 levels found in the BAL from the control rat. This may have been due to large variations in the concentrations detected by the ELISA method, but may also be attributed to the dilute nature of the BAL fluid.

As noted previously, the impairment of macrophage mediated phagocytosis following particle uptake could be an import factor in determining the pathogenicity of particle-induced disease. Renwick *et al.*, (2001) described a study in which high doses of ultrafine particles significantly impaired the ability of a macrophage cell line to subsequently phagocytose latex beads, whilst Hoet & Nemery (2001) observed that in the data of Renwick *et al.*, low concentrations of particles could be interpreted as actually

stimulating the phagocytic ability of the macrophages. In the present study, a decrease in the number of non-phagocytic cells was observed when examining macrophages treated with the lower dose of PM_{10}. This means that in the presence of PM_{10}, more cells could phagocytose latex beads or PM_{10} particles. However, when examining the phagocytic ability of the macrophages in terms of the number of latex beads the macrophages could phagocytose following particle treatment, this number actually decreased in cells that visibly contain PM_{10}. This suggests that PM_{10} uptake by macrophages diminishes the ability to further phagocytose other particles. This decrease in phagocytic ability could be attributable to several factors. The PM_{10} or specific components of the PM_{10} such as the ultrafine particles or transition metals may inhibit cell function, essentially decreasing the phagocytic ability of the macrophages. The decreased phagocytic ability of the macrophages when visibly loaded with PM_{10} also invites the question of dust overloading as described by Morrow (1988) and Oberdörster (1995). The presence of PM_{10} inside the cells, could overload the macrophages to such an extent that they are not able to subsequently phagocytose large numbers of latex beads. Monn *et al.*, (2002) noted similar observations when conducting a study with PM_{10} and a macrophage cell line *in vitro*. It should be noted however, that one of the limitations of this study is the use of a light microscope to determine the presence of PM_{10} inside the cells. Due to the resolution limitations of light microscopy, nanoparticles could only be seen as aggregates and, as such, it is possible that non-aggregated nanoparticles could be present in cells classed as non-phagocytic.

The alveolar macrophages isolated from animals treated with PM_{10} showed a decreased potential to migrate towards the positive chemoattractant ZAS. This was in contrast to results published by Renwick *et al.*, (2004) where it was shown that rat macrophages exposed to carbon black nanoparticles showed increased sensitivity to the chemoattractant C5a. This decrease in mobility may be due to the toxicity of the PM_{10} particles and/or overload which would both restrict macrophage movement via the cytoskeleton (Möller *et al.*, 2002). Other pathogenic particles have been found to inhibit macrophage chemotactic activity following *in vivo* exposure (Donaldson *et al.*, 1990). Neutrophils closely situated to macrophages in the bronchoalveolar space during inflammation may release factor(s) that inhibit macrophage membrane related functions such as phagocytosis, chemotaxis and spreading and this may provide an explanation (Donaldson *et al.*, 1988, 1989).

In the lung, inhibition of macrophage phagocytosis and chemotaxis may result in particles remaining in contact with the epithelium for a protracted period and particle-laden macrophages remaining in the alveolar region instead of migrating out of the lung via the MCE or lymphatic system. Both of these eventualities would allow the dose of particles to build up, leading to chronic inflammation, which may further exacerbate respiratory conditions, as well as increasing the potential for particles to move into the interstitium and the circulation.

This study suggests that acute PM_{10} exposure has an effect on macrophage phagocytosis and chemotaxis that may prove deleterious to particle clearance within the alveolar region of the lung. This may represent one mechanism that promotes inflammation following

increases in ambient PM levels. Further investigation is warranted to determine the effects of chronic PM_{10} exposure on macrophage clearance mechanisms as well as establishing the molecular mechanisms behind decreased macrophage mobility and phagocytic potential as a result of ambient air particle exposure.

CHAPTER 5

THE EFFECTS OF ZINC AND NANOPARTICLE CARBON BLACK ON MACROPHAGE PHAGOCYTOSIS

5.1 INTRODUCTION

Zinc is a physiologically essential element required for the development of animals and microorganisms. Zinc plays an extremely important role in the development of the immune system in animals (Rink and Gabriel, 2000 and Beisel, 1982) and, consequently, several studies have examined the effects of zinc deprivation on leukocytes. Tone *et al.*, (1991) found that murine phagocytes showed reduced phagocytic potential in zinc deficient animals. Ercan & Bor, (1991) also reported similar results with rat macrophages. Allen *et al.*, (1983) and Keen & Gershwin, (1990) reported that reduced zinc concentrations could inhibit macrophage and neutrophil phagocytosis as well as cause reductions in the phagocytic burst.

Other studies have looked at zinc from a toxicological standpoint and observed impaired cell function and toxicity when exposing cells to increased concentrations of zinc. Chvapil *et al.*, (1977a) conducted a key study reporting decreases in the phagocytic ability of dog PMN cells following treatment with 50μM zinc. Increased intracellular concentrations of zinc were also described together with decreases in the oxidative metabolism of the cells. Chvapil *et al.*, (1977b) also specifically looked at the effects of zinc on rat peritoneal macrophages and showed that oxygen consumption decreased in activated macrophages exposed to 0.4mM zinc, but that no effect was observed in resting macrophages.

Due to the fact that zinc is known to be a common component of PM_{10} samples, a number of studies have examined the relationship between zinc and the onset of inflammation

following entry of PM_{10} into the lung. Adamson *et al.*, (2000) reported that zinc induced high toxicity in a sample of atmospheric air pollution but did not appear to take into account any interactions of zinc with other components of air pollution such as the particles or the other metals. A similar result was obtained in a study by Prieditis & Adamson, (2002) using the same atmospheric dust sample, EHC-93. Rice *et al.*, (2001) compared the abilities of six transition metals, including zinc, to induce lung inflammation in a rat model. Zinc sulphate (10μmol/kg) induced significant increases in BAL total protein levels and neutrophil influx. However, this study did not conduct any experiments that examined the interactions of different metals. A human inhalation study using zinc oxide showed increases in several cytokines such as IL-8 and TNFα in the BAL fluid (Kuschner *et al.*, 1997). Skornik and Brain, (1983) examined the uptake of colloidal gold particles by hamster macrophages and showed that 1 hour exposures to zinc sulphate ($3.1mg/m^3$) and zinc ammonium sulphate ($10mg/m^3$) aerosols significantly inhibited macrophage endocytosis. The summation of these studies indicates that zinc can be a potential inflammatory agent even without interacting with the particulate portion of air pollution.

This chapter is part of a study being undertaken by members of the Biomedicine Research Group at Napier University. The study aims to look at the effects of zinc and nanoparticles on various aspects of macrophage function such as TNFα, TGFβ and ROS production as well as examining cytoskeletal and apoptotic effects. Preliminary investigations have already shown that, when incubated with zinc chloride salts, low

doses of nanoparticle carbon black induce the release of much higher concentrations of TNFα from macrophages than the particles or the metal alone (See figure 5.1).

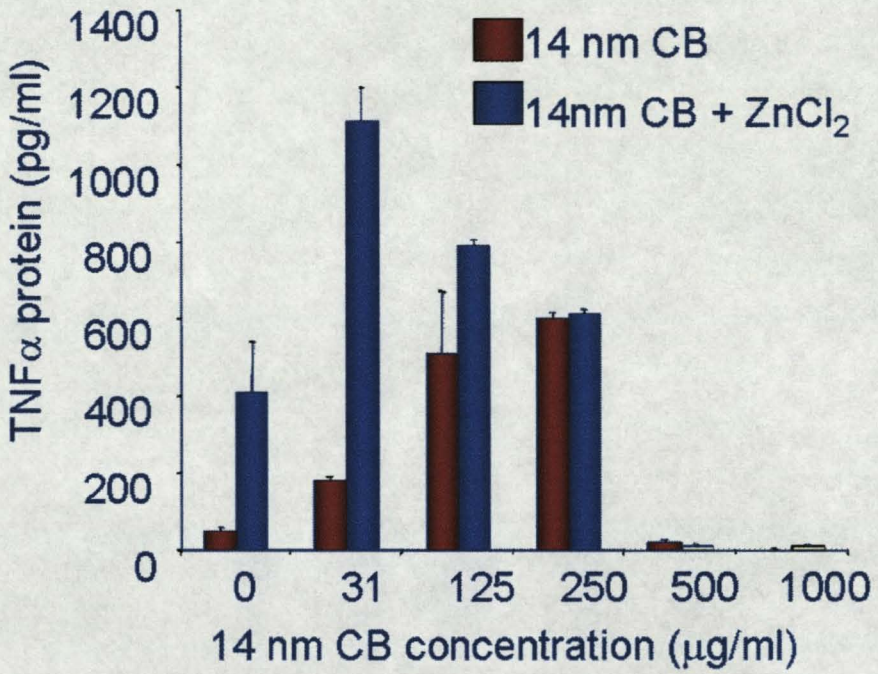

Figure 5.1 – TNFα release from J774.A1 cells treated with varying concentrations of nanoparticle carbon black in the presence or absence of zinc chloride (Courtesy of Alex Griffiths)

This chapter aims to investigate the effects of a range of zinc concentrations on macrophage phagocytosis to determine if any interaction takes place between the zinc and carbon black nanoparticles that would be detrimental to the ability of macrophages to perform phagocytosis.

5.2 MATERIALS AND METHODS

5.2.1 Chemicals and Reagents

L-Glutamine (200mM); penicillin-streptomycin (1000μg/ml) and FBS were obtained from Invitrogen, UK. RPMI 1640 (without L-glutamine) and Zymosan A were both obtained from Sigma Chemicals Company, Dorset, UK; Vybrant phagocytosis assay kit (V-6694) containing fluoroscein-labelled *Escherichia coli* (K-12 strain), HBSS and trypan blue was obtained from Molecular Probes.

5.2.2 Culture of J774.A1 Cell Line

Cell culture was conducted in accordance with the protocol described for J774.2 cells in section 2.2.3.

5.2.3 Flow Cytometry

Flow cytometric analysis was conducted with single colour flow cytometry using a FACSCalibur flow cytometer equipped with an argon-ion laser emitting light at 488nm (BD Biosciences, San Jose, California). An electronic gate was placed around the macrophage population in the flow cytometry scatter plot and at least 10,000 events were acquired for analysis. Light scatter signals were collected in linear mode and fluorescence signals were collected in logarithmic mode.

5.2.4 Treatment of J774.A1 Cells with Nanoparticle Carbon Black – Flow Cytometric Analysis

A confluent culture flask of J774.A1 cells was washed and scraped and a cell count was performed using trypan blue exclusion. A portion of the cells (approx 1 million) were removed and run through the flow cytometer prior to treatment to examine the light scatter properties of untreated J774 cells and to determine the degree of aggregation for the cell population.

J774.A1 cells (2 million) were transferred into a centrifuge tube and centrifuged for 2 minutes at 900 g. Following centrifugation, the supernatant was decanted and 2mls of an nanoparticle carbon black suspension (31.25 μg/ml) in RPMI 1640 was added. The tube was shaken gently and 0.5ml of the cell/particle suspension was added into 4 wells of a 24 well microplate. Untreated J774.A1 cells were also added to 4 wells of the microplate. The plate was incubated for 4 hours in a heated humidified incubator (37°C / 5% CO_2). The particle suspension was removed from the wells and then 0.5ml HBSS was added to each well. The plates were shaken gently and the HBSS was removed.
Using the end of a sterile Pasteur pipette, the cells were scraped off the surface of the microplate and resuspended in 0.5ml of HBSS. The suspensions of the treated and untreated cells were pooled in two separate tubes and the light scatter properties of the cells were analysed using the flow cytometer.

5.2.5 Preliminary Experiment to Determine Effectiveness of Vybrant™ Phagocytosis Assay Kit When Using J774.A1 Macrophages Treated With Metals

J774.A1 cells were seeded at a cell count of 200,000 cells per well in RPMI with 10% FBS in a 24 well microplate. The plate was incubated in a heated humidified incubator for 18 hours at 37°C / 5% CO_2. Control wells were prepared by seeding 6 wells with cells and treating with HBSS only. Cells were also treated with nanoparticle carbon black (31.25μg/ml), $FeCl_3$ (10mM) or $ZnCl_2$ (10mM) suspended in HBSS.

The fluorescein isothiocyanate (FITC)-labelled *E.coli* bioparticle suspension was prepared according to the manufacturers instructions (dessicated particles were suspended in 0.5ml of 10x HBSS with 4.5ml distilled water and sonicated for 5 minutes). The supernatants were aspirated from the wells of the 24 well plate. The bioparticle suspension (250μl) was added to all of the wells except three, to which 250μl of HBSS was added. The cells were then incubated for 2 hours at 37°C / 5% CO_2. Following incubation, the supernatants were aspirated from all of the wells and replaced with 200μl trypan blue solution. The plate was incubated at room temperature for 1 minute and the excess trypan blue was aspirated from the wells. Cells were removed from the wells by scraping with a sterile Pasteur pipette then resuspended in 0.5ml HBSS. Replicate treatments were pooled into single flow cytometry tubes and analysed using single colour flow cytometry.

5.2.6 The Effect of Nanoparticle Carbon Black and Varying Concentrations of Zinc on the Phagocytic Ability of J774.A1 Macrophages

J774.A1 cells were seeded in a 24 well plate according to the method in section 5.2.5. Cells were treated with $ZnCl_2$ at concentrations of 100μM, 1μM and 100nM. The zinc treatments were conducted in the presence and absence of nanoparticle carbon black (31.25μg/ml). The cells and treatments were incubated for 4 hours and the phagocytosis assay was conducted according to the protocol described above. The results of this experiment are displayed in figures 5.4.1 to 5.4.6 and in table 5.4.7.

In the following experiment, cells were treated with $ZnCl_2$ at concentrations of 50μM, 20μM, 10μM. This experiment was repeated twice and the results are displayed in figures 5.5.1 to 5.5.7 and in table 5.5.8. The data from the two experiments are also collated in figure 5.5.9.

5.3 RESULTS

5.3.1 Flow Cytometric Analysis of J774.A1 Cells Treated with Nanoparticle Carbon Black

Figure 5.2.1 shows the scatter plot pattern obtained from the three groups of J774.A1 cells. The first scatter plot (1) represents cells that have been analysed using a flow cytometer immediately after removal from a culture flask. The second plot (2) displays untreated J774.A1 cells following a 4 hour culture incubation period. The third plot (3) demonstrates cells that have been treated with 31.25μg of nanoparticle carbon black for 4 hours. The left hand axis of each plot represents side scatter light signals and the bottom axis represents forward scatter signals. Analysis of these scatter plots reveals that a distinct population is present in each case. A small amount of cellular debris is present in the bottom left hand corner of each scatter plot. The debris was excluded from the light scatter analysis by gating around the cell populations. From these patterns it appears that the J774.A1 have not aggregated either during scraping or following 4 hours incubation in the presence and absence of nanoparticle carbon black. This was confirmed by examination of the cell suspensions by conventional light microscopy.

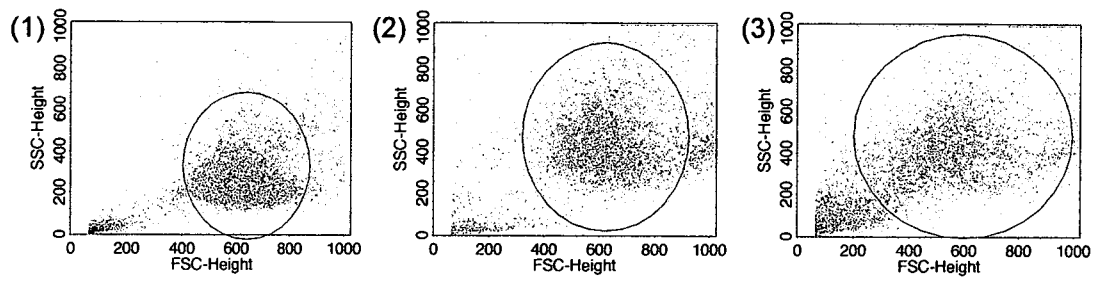

Figure 5.2.1 Flow cytometry scatter plots of J774.A1 cells. The plots represent (1) Cells analysed prior to incubation for 4 hours, (2) Cells incubated for 4 hours with serum-free medium and (3) Cells treated with nanoparticle carbon black (31.25μg) for 4 hours. Circle represents gated population.

Figure 5.2.2 shows the fluorescence profiles for each of the three treatments. The left hand axis is the number of cells per channel and the bottom axis is the fluorescence depicted on a logarithmic scale. In comparison to the untreated cells, the pattern from the treated cells is very similar. The nanoparticle carbon black did not appear to cause any change in the background autofluoresence of the cells. This pattern is shown again in figure 5.2.3 where the treated population of cells (red) is overlayed upon the untreated cells. As can been seen from the graph, the changes in the fluorescence profile are minimal. This is echoed by the data shown in table 5.2.4 which show the mean gated fluorescence obtained from each population, which, as shown in previous figures, remains similar for each treatment.

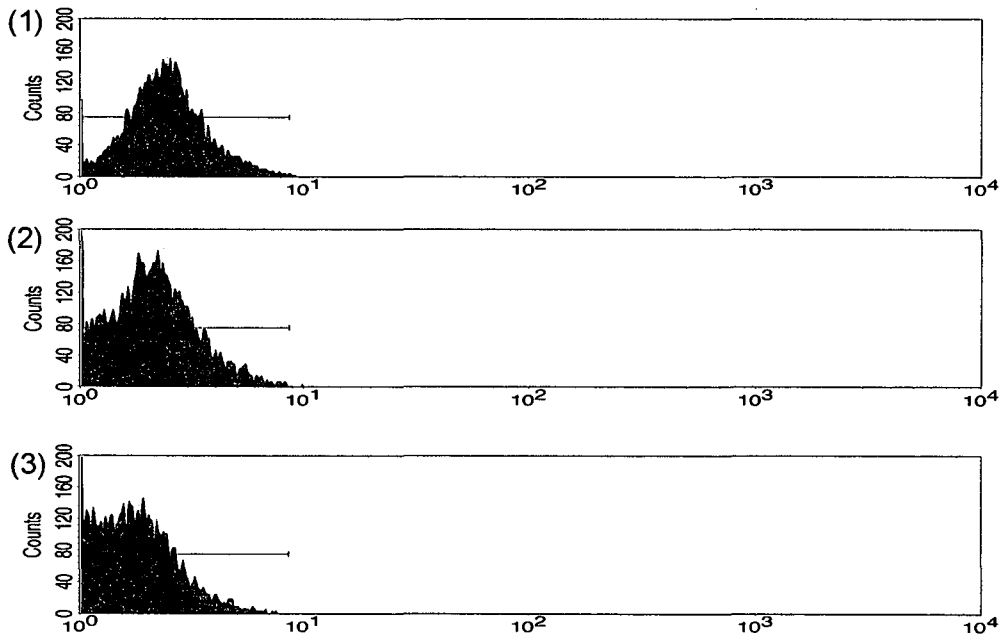

Figure 5.2.2 Histogram plots of flow cytometry analysis of J774.A1 cells. The plots represent (1) Cells analysed prior to incubation for 4 hours, (2) Cells incubated for 4 hours with serum-free medium and (3) Cells treated with nanoparticle carbon black (31.25μg) for 4 hours.

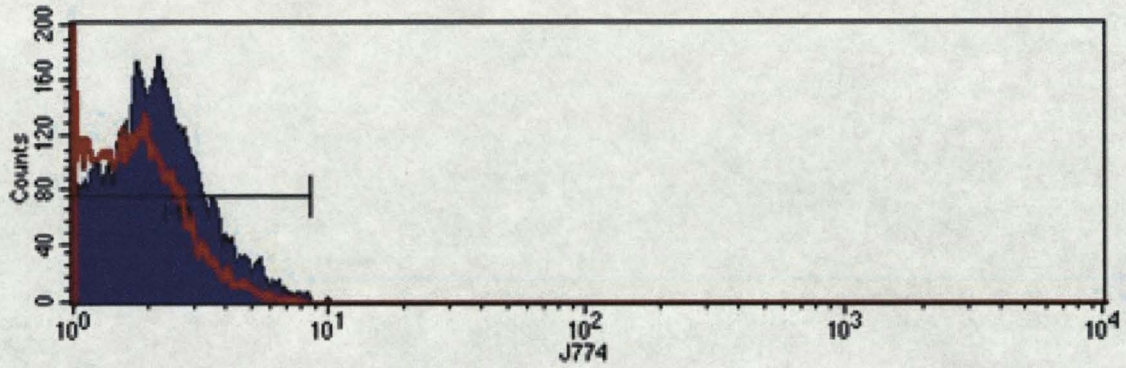

Figure 5.2.3 A histogram plot of treated and untreated J774.A1 cells analysed by flow cytometry. Untreated J774.A1 cells (incubated for 4 hours) are represented by the purple area of the graph. J774.A1 cells treated with 31.25μg of nanoparticle carbon black are represented by the red outline area.

	Cell Treatments	Mean Gated Fluorescence (arbitrary units)
(1)	None (Pre-Incubation Analysis)	2.60
(2)	Serum-Free Medium	2.21
(3)	Nanoparticle Carbon Black (31.25μg)	1.74

Table 5.2.4 Mean fluorescence data for gated population of treated and untreated J774.A1 cells. Results are the mean of one experiment prepared in duplicate.

5.3.2 Flow Cytometric Analysis of the Phagocytic Ability of J774.A1 Cells Exposed to Nanoparticle Carbon Black in the Presence and Absence of Zinc and Iron Salts

Figure 5.3.1 shows the scatter plots for the four cell treatments that were conducted in this experiment. The scatter plots (1) and (2) represent the negative control (untreated cells) and the positive control (cells exposed to bioparticles for 2 hours) respectively. Scatter plots (3) and (4) represent cells treated with 10mM $ZnCl_2$ or 10mM $FeCl_3$ for 4 hours and subsequently treated with bioparticles for 2 hours. As with the previous

experiment, a distinct cell population was visible which was further analysed by excluding the debris present in the bottom left corner.

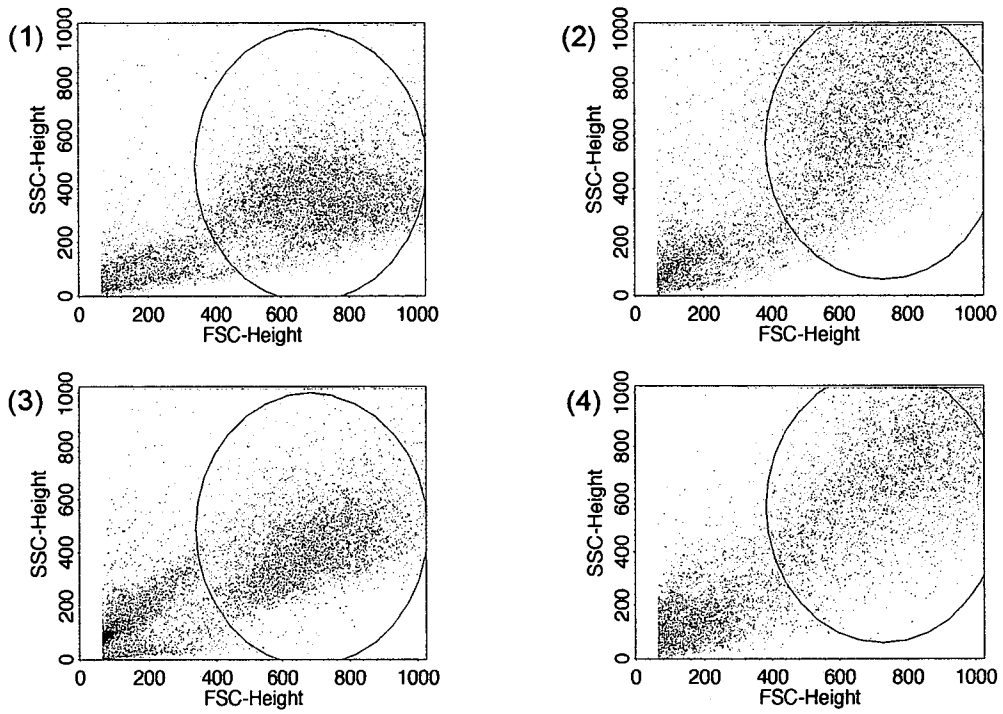

Figure 5.3.1 Flow cytometry scatter plots of J774.A1 cells. The plots represent (1) Untreated cells (negative control), (2) Cells treated with bioparticles (positive control), (3) Cells treated with $ZnCl_2$ (10mM) and bioparticles (4) Cells treated with $FeCl_3$ (10mM) and bioparticles. Circle represents gated population.

Figure 5.3.2 shows the fluorescence profiles for the positive (cells treated with bioparticles for 2 hours) and negative (untreated cells) controls in this experiment. The negative control (purple) has a low fluorescence as indicated by it position at the lower end of the scale. This is consistent with the results obtained in the previous experiment. The positive control (red) shows a much higher fluorescent intensity as demonstrated by its position at the higher end of the fluorescence scale. This is expected due to the exposure of the phagocytic cells to FITC-labelled *E.coli* bioparticles.

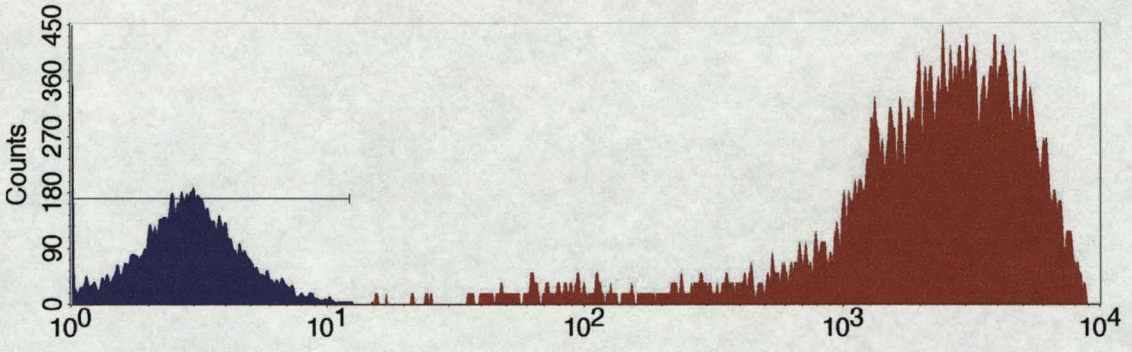

Figure 5.3.2 A histogram plot of treated and untreated J774.A1 cells analysed by flow cytometry. Untreated J774.A1 cells are represented by the purple area of the graph. J774.A1 cells treated with bioparticles are represented by the red area of the graph.

Figure 5.3.3 represents the fluorescence profile of J774.A1 cells treated with 10mM $ZnCl_2$ for 4 hours and has been overlayed with the fluorescence profiles of the positive (red) and negative (green) controls. The graph indicates that the zinc salts have an adverse effect on the phagocytic ability of the macrophages. This is represented by a decrease in fluorescence on the graph when compared to the positive control. However, the fluorescence intensity of these cells is higher than that of the negative control indicating that some phagocytosis of the bioparticles has taken place.

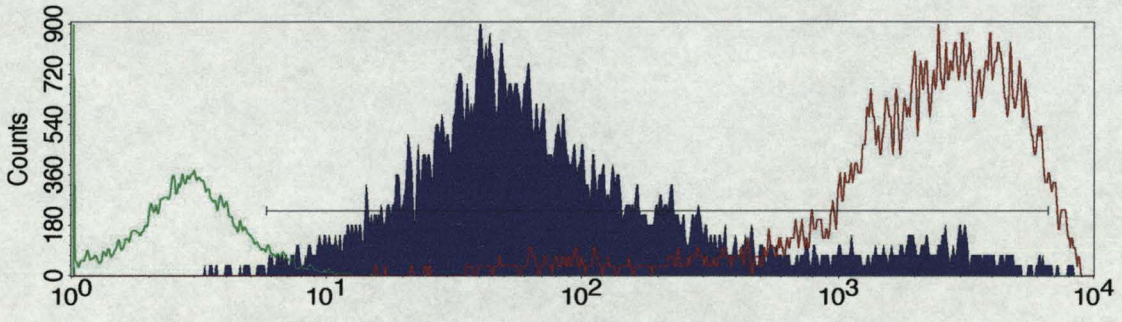

Figure 5.3.3 A histogram plot of treated and untreated J774.A1 cells analysed by flow cytometry. J774.A1 cells treated with $ZnCl_2$ (10mM) and bioparticles are represented by the purple area of the graph. Untreated J774.A1 cells (negative control) are represented by the green outlined area on the graph. J774.A1 cells treated with bioparticles only (positive control) are represented by the red outline area on the graph

Figure 5.3.4 shows J774.A1 cells that have been treated with 10mM $FeCl_3$ for 4 hours and has again been overlayed with the positive (red) and negative (green) control graphs for comparison. As with the previous figure, it can be observed that the iron salts cause a reduction in bioparticle phagocytosis, which is seen on the graph as a reduction in fluorescence intensity. However, as with the zinc treatments, it is apparent that some phagocytosis has taken place. Figure 5.3.5, an overlay of the two metal salt treatments, indicates that the iron does not appear to affect the phagocytic ability of the macrophages as much as zinc does. These comparisons are represented numerically in table 5.3.6 which again indicates that zinc salts have more of an effect on the macrophages' phagocytic ability (approximately 90% reduction in phagocytic ability for zinc treatments compared to around 50% reduction following iron treatments).

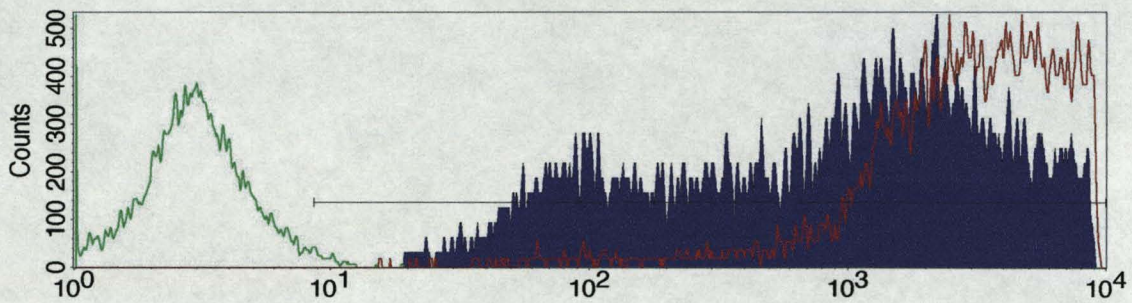

Figure 5.3.4 A histogram plot of treated and untreated J774.A1 cells analysed by flow cytometry. J774.A1 cells treated with $FeCl_3$ (10mM) and bioparticles are represented by the purple area of the graph. Untreated J774.A1 cells (negative control) are represented by the green outlined area on the graph. J774.A1 cells treated with bioparticles only (positive control) are represented by the red outline area on the graph

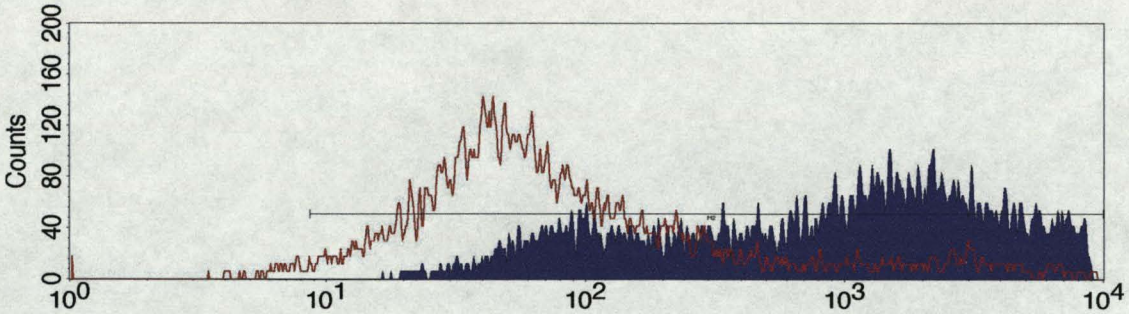

Figure 5.3.5 A histogram plot of treated and untreated J774.A1 cells analysed by flow cytometry. J774.A1 cells treated with $FeCl_3$ (10mM) and bioparticles are represented by the purple area of the graph. J774.A1 cells treated with $ZnCl_2$ (10mM) and bioparticles are represented by the red outline area on the graph

Figure	Cell Treatments	Mean Gated Fluorescence (arbitrary units)
5.3.2	S/F Medium (negative control)	3.16
5.3.3	S/F Medium & Bioparticles (positive control)	3565.18
5.3.4	$ZnCl_2$ (10mM) and Bioparticles	340.92
5.3.5	$FeCl_3$ (10mM) and Bioparticles	1759.43

Table 5.3.6 Mean fluorescence data for gated population of treated and untreated J774.A1 cells. Results are the mean of one experiment prepared in duplicate.

5.3.3 Flow Cytometric Analysis of J774.A1 Macrophage Phagocytosis Following Nanoparticle Carbon Black Treatment in the Presence and Absence of Varying Concentrations of Zinc.

Figure 5.4.1 shows the scatter plots for the nine cell treatments that were conducted with a view to determining the effects of nanoparticle carbon black and $ZnCl_2$ at concentrations of 100μM, 1μM and 100nM on macrophage phagocytosis. The circle shows the cell population that was gated and used to obtain the fluorescence data. The

scatter plots that represent treatments with nanoparticle carbon black i.e. 3,7,8 and 9 show an increase in the amount of debris present in the bottom left corner. It should also be noted that in plot 6 (treatment of 100nM $ZnCl_2$) there was also an increase in debris.

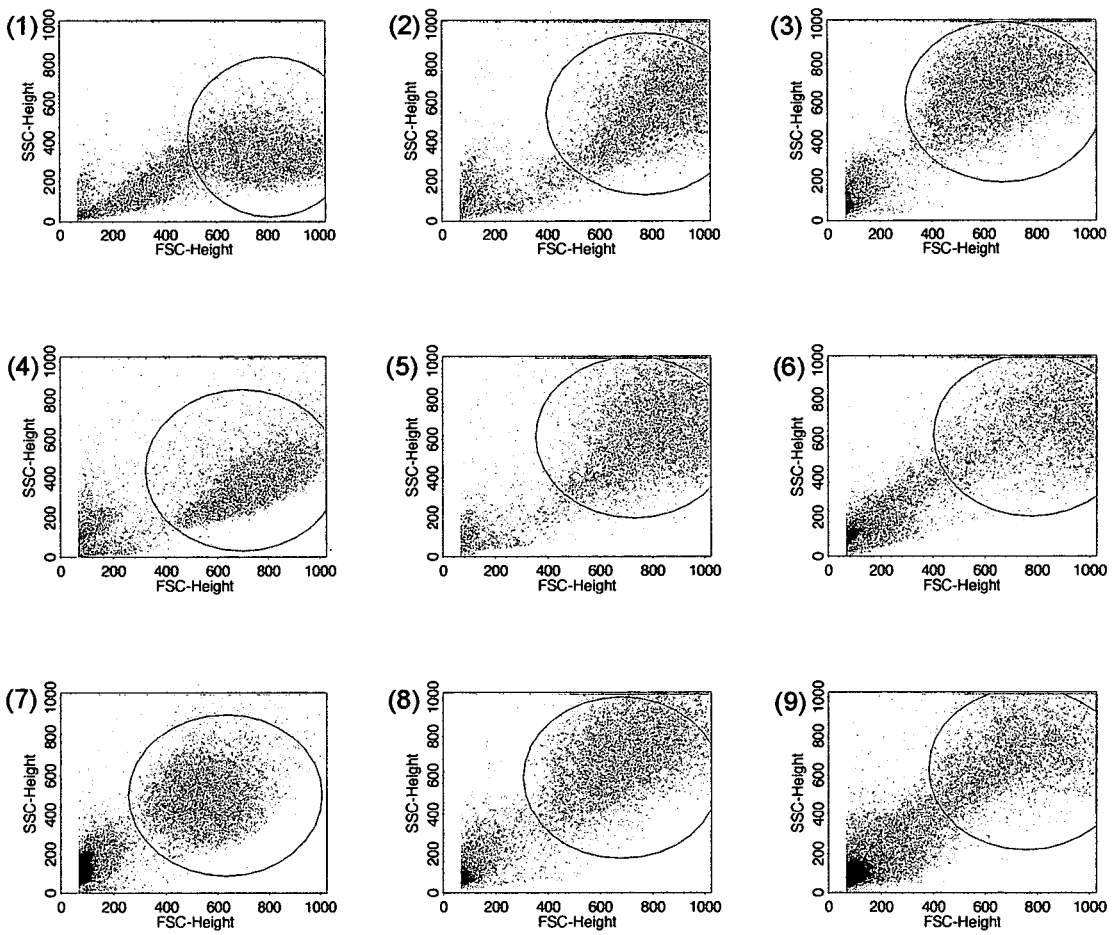

Figure 5.4.1 Flow cytometry scatter plots of J774.A1 cells. The plots represent (1) Untreated cells (negative control), (2) Cells treated with bioparticles (positive control), (3) Cells treated with 31.25µg nanoparticle carbon black (NCB) only (4) Cells treated with $ZnCl_2$ (100µM) and bioparticles, (5) Cells treated with $ZnCl_2$ (1µM) and bioparticles, (6) Cells treated with $ZnCl_2$ (100nM) and bioparticles, (7) Cells treated with $ZnCl_2$ (100µM), NCB and bioparticles, (8) Cells treated with $ZnCl_2$ (1µM), NCB and bioparticles, (9) Cells treated with $ZnCl_2$ (100nM), NCB and bioparticles, Circle represents gated population.

Figure 5.4.2 shows the fluorescence profiles of the untreated cells and the cells that have phagocytosed bioparticles. Bioparticle phagocytosis by the macrophages resulted in a very high level of fluorescence. Figure 5.4.3 is a representation of the cells that have been treated with nanoparticle carbon black (purple) as well as being overlayed with the peak of the positive control (red outline). The treatment with nanoparticle carbon black causes a slight decrease in fluorescence intensity which is indicated by the movement of the peak to the left, i.e. less fluorescent intensity.

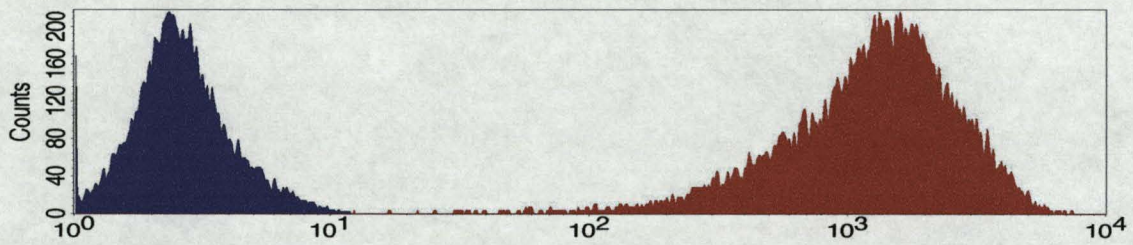

Figure 5.4.2 A histogram plot of treated and untreated J774.A1 cells analysed by flow cytometry. Untreated J774.A1 cells are represented by the purple area of the graph. J774.A1 cells treated with bioparticles are represented by the red area of the graph.

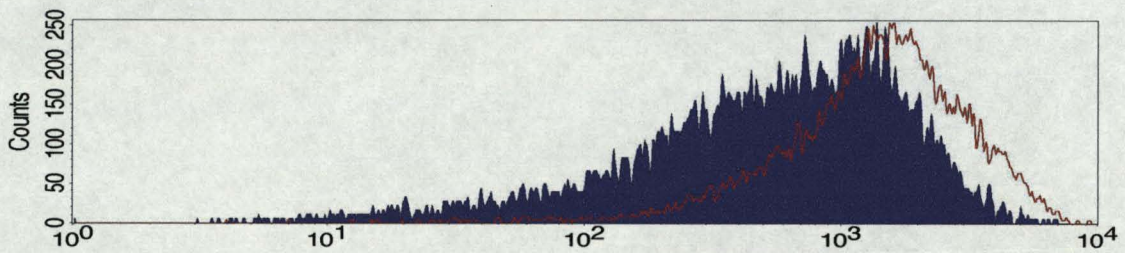

Figure 5.4.3 A histogram plot of treated J774.A1 cells analysed by flow cytometry. J774.A1 cells treated with bioparticles only are represented by the red outline area of the graph. J774.A1 cells treated with 31.25µg nanoparticle carbon black and bioparticles are represented by the purple area of the graph.

The three figures (5.4.4, 5.4.5 and 5.4.6) show the phagocytic responses of the macrophages following treatment with zinc salts in the presence and absence of nanoparticle carbon black. Figure 5.4.4 illustrates the highest dose of zinc salts (10mM) which caused the fluorescent peak from the cells to decrease and move to the left indicating decreased fluorescence compared to the positive control (figure 5.4.2). When the cells are co-incubated in the presence of both zinc and nanoparticle carbon black, the peak moves even further to the left indicating a marked decrease in fluorescence. Figures 5.4.5 and 5.4.6 show very similar patterns in that with zinc treatments alone, the fluorescence peak only changes slightly from the positive control. As with the high zinc concentrations, the addition of nanoparticle carbon black causes a small shift of the peak to the left indicating decreased fluorescence.

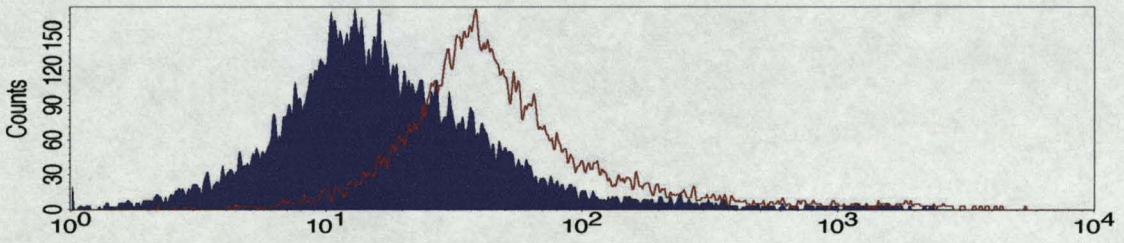

Figure 5.4.4 A histogram plot of J774.A1 cells analysed by flow cytometry. J774.A1 cells treated with 100µM $ZnCl_2$ and bioparticles are represented by the red outline area of the graph. J774.A1 cells co-treated with 100µM $ZnCl_2$ / 31.25µg nanoparticle carbon black and then bioparticles are represented by the purple area of the graph.

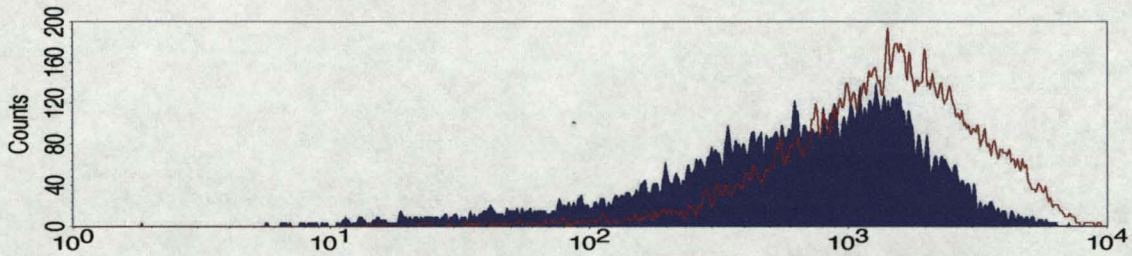

Figure 5.4.5 A histogram plot of J774.A1 cells analysed by flow cytometry. J774.A1 cells treated with 1μM $ZnCl_2$ and bioparticles are represented by the red outline area of the graph. J774.A1 cells co-treated with 1μM $ZnCl_2$ / 31.25μg nanoparticle carbon black and then bioparticles are represented by the purple area of the graph.

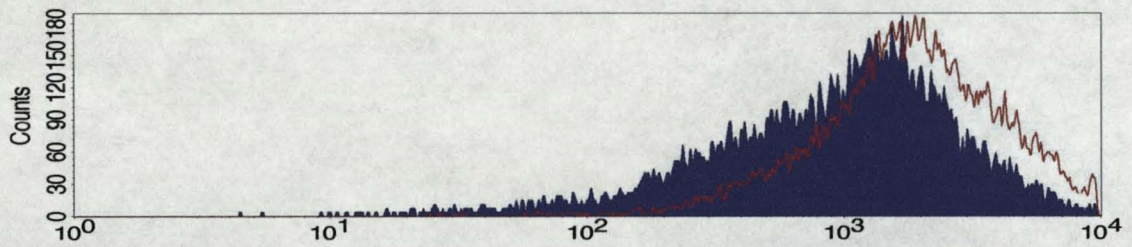

Figure 5.4.6 A histogram plot of J774.A1 cells analysed by flow cytometry. J774.A1 cells treated with 100nM $ZnCl_2$ and bioparticles are represented by the red outline area of the graph. J774.A1 cells co-treated with 100nM $ZnCl_2$ / 31.25μg nanoparticle carbon black and then bioparticles are represented by the purple area of the graph.

Table 5.4.7 shows the mean fluorescence data for each of the cell population represented by the peaks in the previous five figures. The addition of nanoparticle carbon black to the cells causes a decrease in fluorescence units of approximately 50% compared to the positive control. The addition of $ZnCl_2$ at a concentration of 100μM results in a fluorescence decrease of approximately 95% compared to the positive control and this is reduced by a further 50% when the zinc treatment is conducted in the presence of nanoparticle carbon black. The 1μM and 100nM zinc treatments appear to increase the fluorescence to levels above the positive control. Co-treatment with nanoparticle carbon black and zinc at these concentrations reduced the phagocytic potential of the

macrophages by 45% and 20% for the 1μM and 100nM concentrations of zinc respectively.

	Cell Treatments	Mean Gated Fluorescence (arbitrary units)
(1)	S/F Medium (negative control)	3.03
(2)	S/F Medium & Bioparticles (positive control)	1732.31
(3)	Nanoparticle Carbon Black (NCB) and Bioparticles	871.94
(4)	$ZnCl_2$ (100μM) and Bioparticles	98.95
(5)	$ZnCl_2$ (1μM) and Bioparticles	1933.24
(6)	$ZnCl_2$ (100nM) and Bioparticles	2255.51
(7)	$ZnCl_2$ (100μM), NCB and Bioparticles	40.40
(8)	$ZnCl_2$ (1μM), NCB and Bioparticles	951.54
(9)	$ZnCl_2$ (100nM), NCB and Bioparticles	1425.20

Table 5.4.7 Mean fluorescence data for gated population of treated and untreated J774.A1 cells. Results are the mean of one experiment prepared in duplicate.

5.3.4 Flow Cytometric Analysis of J774.A1 Macrophage Phagocytosis Following Nanoparticle Carbon Black Treatment in the Presence and Absence of Low Concentrations of Zinc

This experiment was repeated twice and therefore, the results section contains the scatter plots from each experiment grouped into individual experiments. However, fluorescence graphs representing the individual treatment repetitions have been grouped together to allow for easier comparison between experiments.

Figures 5.5.1 and 5.5.2 show the scatter plots obtained from cells that have been treated with low concentrations of zinc in the presence and absence of nanoparticle carbon black. As with previous experiments the scatter plots from the positive and negative controls are also shown. As can be seen from the plots, the cells are a distinct population that can be accurately excluded from the debris in the bottom left hand corner. It is worth noting, however, that the second repetition of the experiment (figure 5.5.2) shows a decrease amount of debris present compared with figure 5.5.1.

Figure 5.5.3 shows the two fluorescence graphs from the positive and negative control for both repetitions of the experiment. As can be seen from the graphs, the profiles for each control are similar to previous experiments in that the negative control peak indicates low fluorescence and the positive control peak displays high fluorescence indicating that phagocytosis of the bioparticles has taken place. The second experiment shows a slight decrease in the negative control fluorescence but is still located in a similar area to previous negative control peaks.

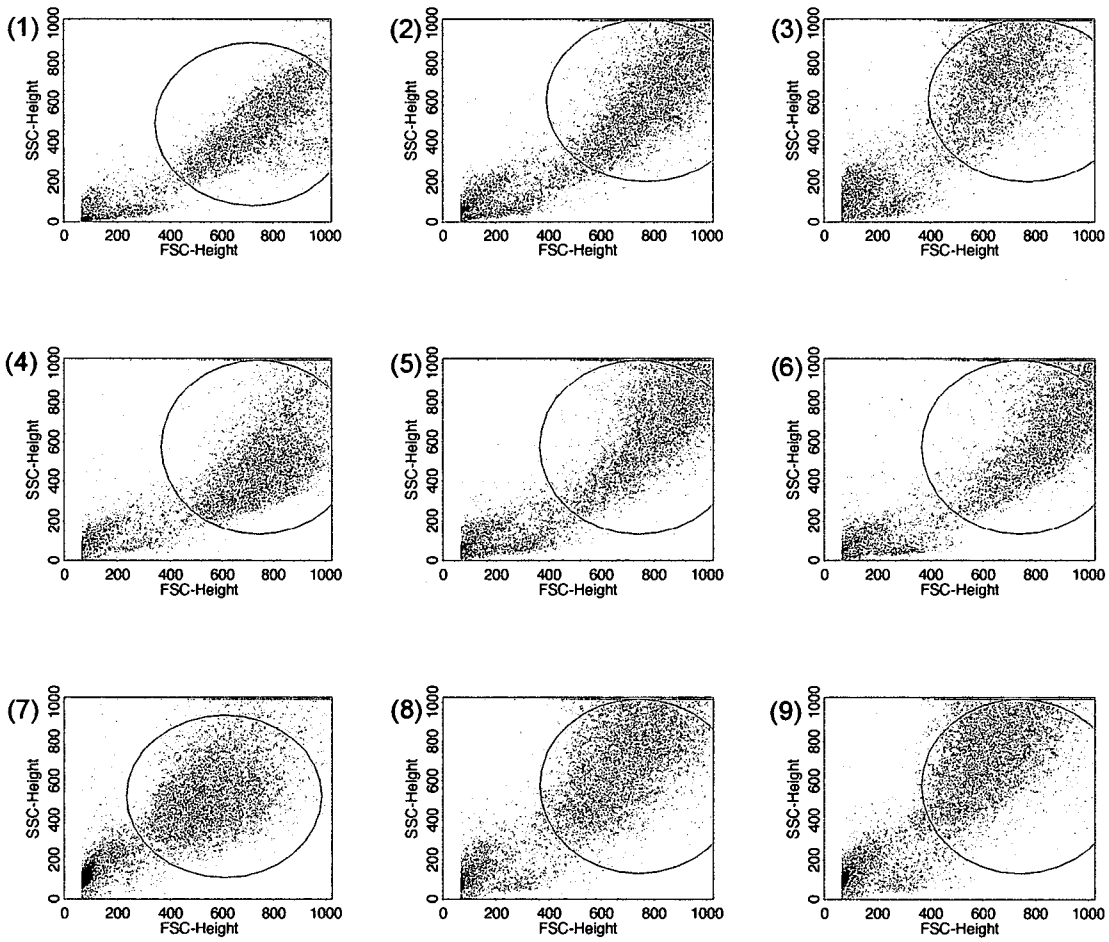

Figure 5.5.1 Flow cytometry scatter plots of J774.A1 cells. The plots represent (1) Untreated cells (negative control), (2) Cells treated with bioparticles (positive control), (3) Cells treated with 31.25μg nanoparticle carbon black (NCB) only (4) Cells treated with $ZnCl_2$ (50μM) and bioparticles, (5) Cells treated with $ZnCl_2$ (20μM) and bioparticles, (6) Cells treated with $ZnCl_2$ (10μM) and bioparticles, (7) Cells treated with $ZnCl_2$ (50μM), NCB and bioparticles, (8) Cells treated with $ZnCl_2$ (20μM), NCB and bioparticles, (9) Cells treated with $ZnCl_2$ (10μM), NCB and bioparticles. Circle represents gated population.

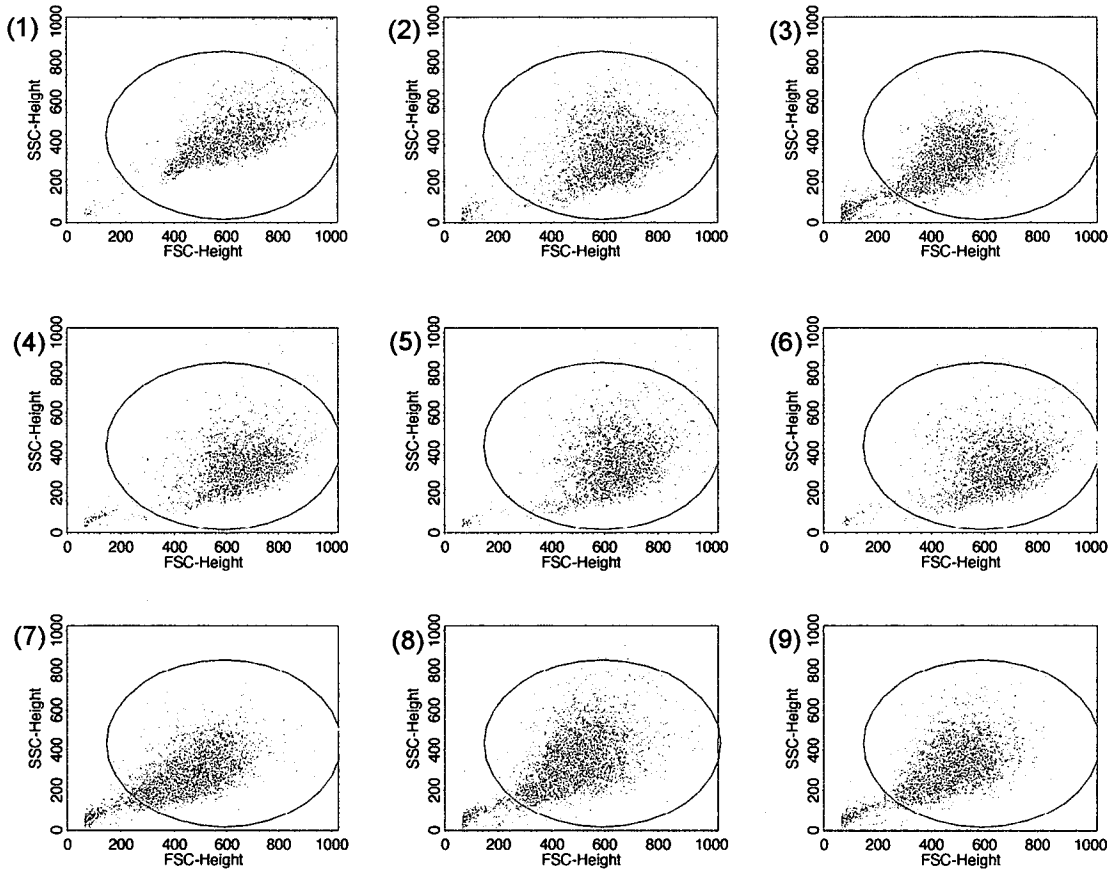

Figure 5.5.2 Repeated Flow cytometry scatter plots of J774.A1 cells. The plots represent (1) Untreated cells (negative control), (2) Cells treated with bioparticles (positive control), (3) Cells treated with 31.25μg nanoparticle carbon black (NCB) only (4) Cells treated with $ZnCl_2$ (50μM) and bioparticles, (5) Cells treated with $ZnCl_2$ (20μM) and bioparticles, (6) Cells treated with $ZnCl_2$ (10μM) and bioparticles, (7) Cells treated with $ZnCl_2$ (50μM), NCB and bioparticles, (8) Cells treated with $ZnCl_2$ (20μM), NCB and bioparticles, (9) Cells treated with $ZnCl_2$ (10μM), NCB and bioparticles. Circle represents gated population.

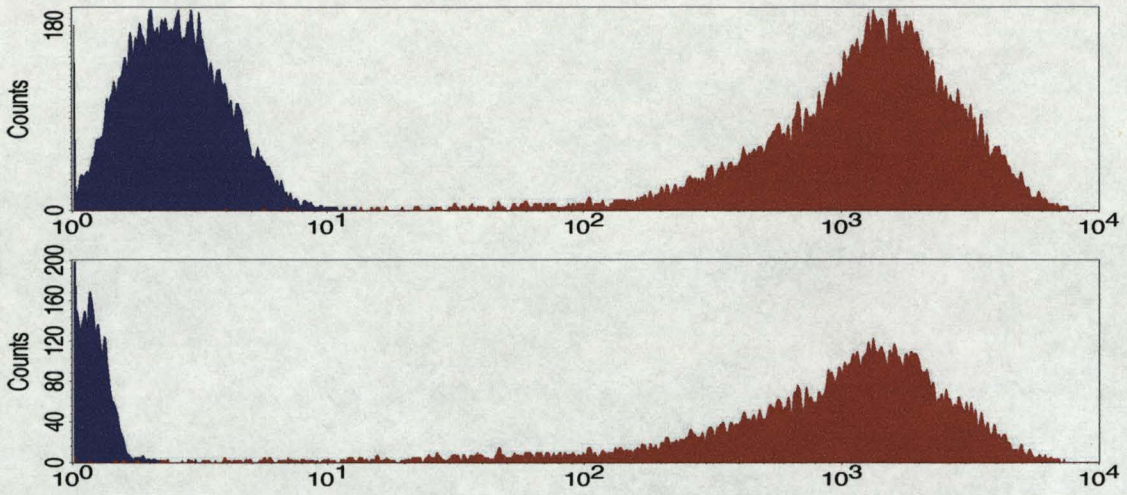

Figure 5.5.3 Two histogram plots of repeat treatments of J774.A1 cells analysed by flow cytometry. In both graphs, untreated J774.A1 cells are represented by the purple area of the graph. J774.A1 cells treated with bioparticles are represented by the red area of the graph.

Figure 5.5.4 shows the two repetitions of the nanoparticle carbon black treatment of the cells compared to the positive control cells. The graph indicates, in both cases, that a slight decrease in fluorescence has occurred which is suggestive of a slight impairment to the phagocytic ability of the macrophages. Figure 5.5.5 shows the graphs obtained when the cells have been treated with 50μM $ZnCl_2$ in the presence and absence of nanoparticle carbon black. The two graphs both reflect a distinct decrease in fluorescence following zinc treatment (red outline) and an even greater decrease when the cells are incubated in the presence of the carbon black. This indicates that macrophage phagocytosis has been inhibited. It should also be noted that the shape of the graphs are different when the experiments are compared to each other. The first repetition shows a much greater drop in fluorescence than the second one and is further decreased in the presence of nanoparticle carbon black. The graph of the zinc-only treatment in experiment one also

appears to show two individual peaks although examination of the scatter plot does not indicate the presence of two individual groups of cells.

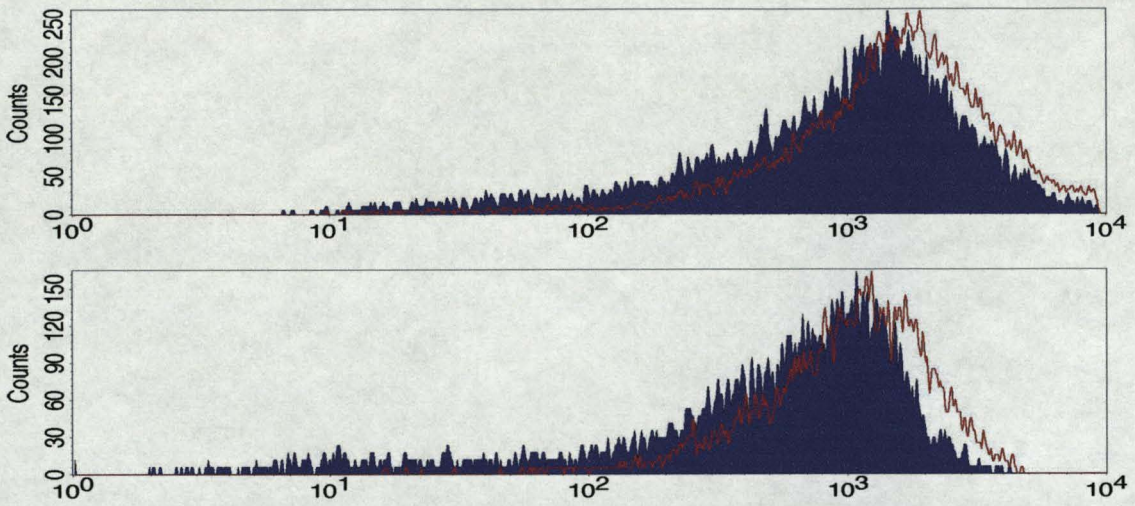

Figure 5.5.4 Two histogram plots of repeat treatments J774.A1 cells analysed by flow cytometry. In both graphs, J774.A1 cells treated with bioparticles only are represented by the red outline area of the graph. J774.A1 cells treated with 31.25µg nanoparticle carbon black and bioparticles are represented by the purple area of the graph.

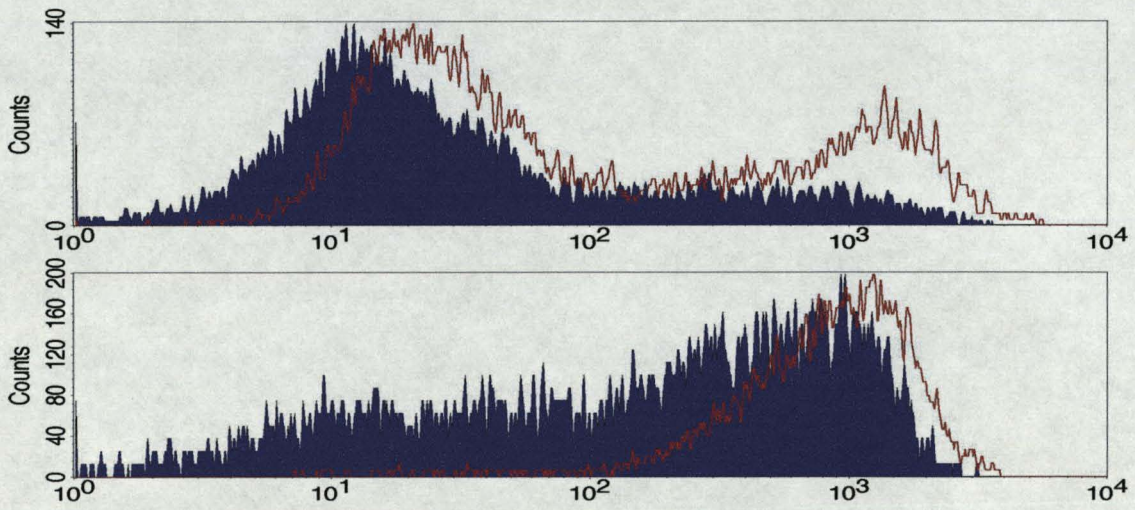

Figure 5.5.5 Two histogram plots of repeated treatments of J774.A1 cells analysed by flow cytometry. In both graphs, J774.A1 cells treated with 50µM $ZnCl_2$ and bioparticles are represented by the red outline area. J774.A1 cells co-treated with 50µM $ZnCl_2$ / 31.25µg nanoparticle carbon black and then bioparticles are represented by the purple area.

Figure 5.5.6 shows the two graphs obtained from treating the J774.A1 cells with 20μM $ZnCl_2$ in the presence and absence of nanoparticle carbon black. The graphs indicate that as a result of the zinc treatment alone (red curve) there is a very slight decrease in fluorescence compared to the positive control, and when co-treatment of zinc and carbon black is carried out there is a further increase in the number of cells showing a lower intensity of fluorescence. This is indicated on the graph as a small peak near the middle of the graph. Figure 5.5.7 shows the effect of 10μM $ZnCl_2$ treatment on the cells. With the zinc only treatment there does not appear to be any change in the level of fluorescence compared to the positive control cells but the fluoresence is decreased in the presence of both zinc and nanoparticle carbon black. This is indicated on the graph as slight shifts in the purple graph at the lower end of the fluorescence scale.

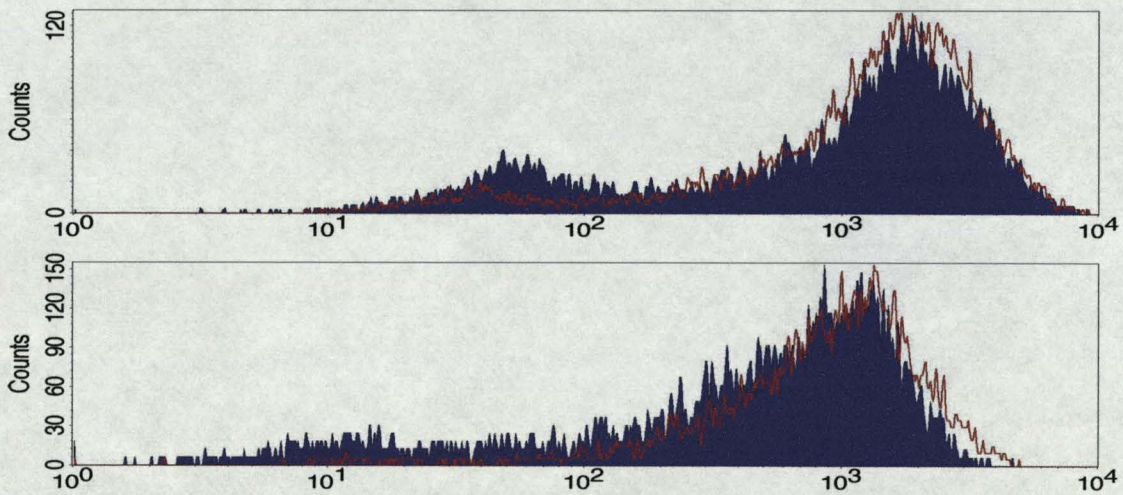

Figure 5.5.6 Two histogram plots of repeated treatments of J774.A1 cells analysed by flow cytometry. In both graphs, J774.A1 cells treated with 20μM $ZnCl_2$ and bioparticles are represented by the red outline area. J774.A1 cells co-treated with 20μM $ZnCl_2$ / 31.25μg nanoparticle carbon black and then bioparticles are represented by the purple area.

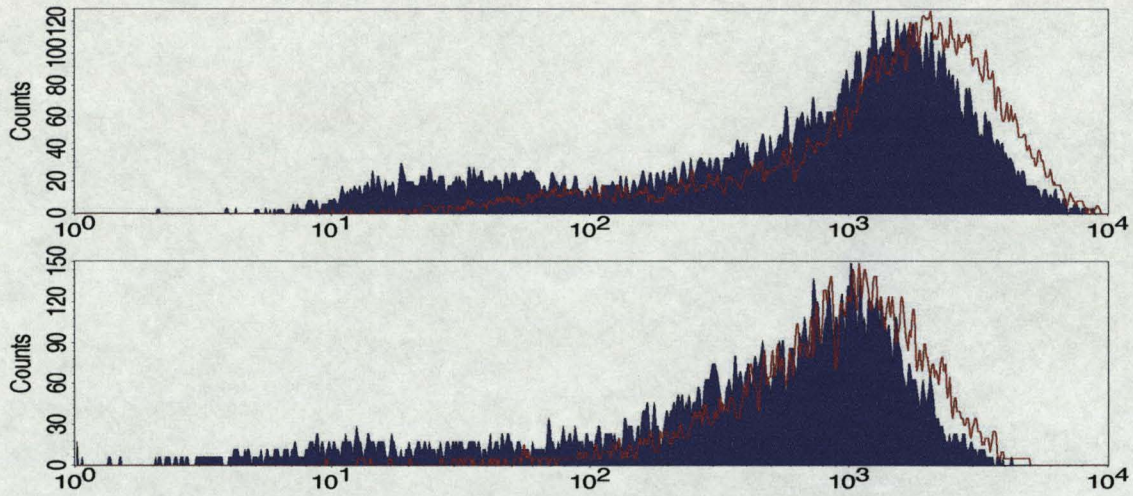

Figure 5.5.7 Two histogram plots of repeated treatments of J774.A1 cells analysed by flow cytometry. In both graphs, J774.A1 cells treated with 10μM $ZnCl_2$ and bioparticles are represented by the red outline area. J774.A1 cells co-treated with 10μM $ZnCl_2$ / 31.25μg nanoparticle carbon black and then bioparticles are represented by the purple area.

Table 5.5.8 shows the mean numerical fluorescence data for each cell population in both experiments. This data is also presented in figure 5.5.9 as a histogram. The figures representing the positive control cells show a difference in that the positive control of experiment 2 was approximately 30% lower than that of experiment 1. Carbon black treatments resulted in decreases of between 30-35% in phagocytic ability. The data indicate that there was only a small decrease in fluorescence following the zinc-only treatment at concentrations of 20 and 10μM. The 50μM shows a dramatic decrease (approximately 65%) in experiment 1 but only 20% in experiment 2. Following carbon black co-treatments with all zinc doses, the phagocytic ability of the macrophages was decreased. The zinc (20 and 10μM) and carbon black treatments decreased to similar levels (approximately 60-75%) but the 50μM zinc / carbon black treatment showed decreases between 65% and 95%.

	Cell Treatments	Mean Gated Fluorescence (arbitrary units)	
		Experiment 1	Experiment 2
(1)	S/F Medium (negative control)	2.74	1.11
(2)	S/F Medium & Bioparticles (positive control)	1954.37	1200.39
(3)	Nanoparticle Carbon Black (NCB) and Bioparticles	1421.79	770.40
(4)	$ZnCl_2$ (50μM) and Bioparticles	610.07	977.74
(5)	$ZnCl_2$ (20μM) and Bioparticles	1728.18	1084.56
(6)	$ZnCl_2$ (10μM) and Bioparticles	1906.47	1086.90
(7)	$ZnCl_2$ (50μM), NCB and Bioparticles	160.44	413.31
(8)	$ZnCl_2$ (20μM), NCB and Bioparticles	1514.31	739.44
(9)	$ZnCl_2$ (10μM), NCB and Bioparticles	1295.86	739.56

Table 5.5.8 Mean fluorescence data for the phagocytic potential of a gated population of treated and untreated J774.A1 cells. Cells were treated with varying concentrations of $ZnCl_2$ in the presence and absence of nanoparticle carbon black (31.25μg). Results are the mean of two separate experiments.

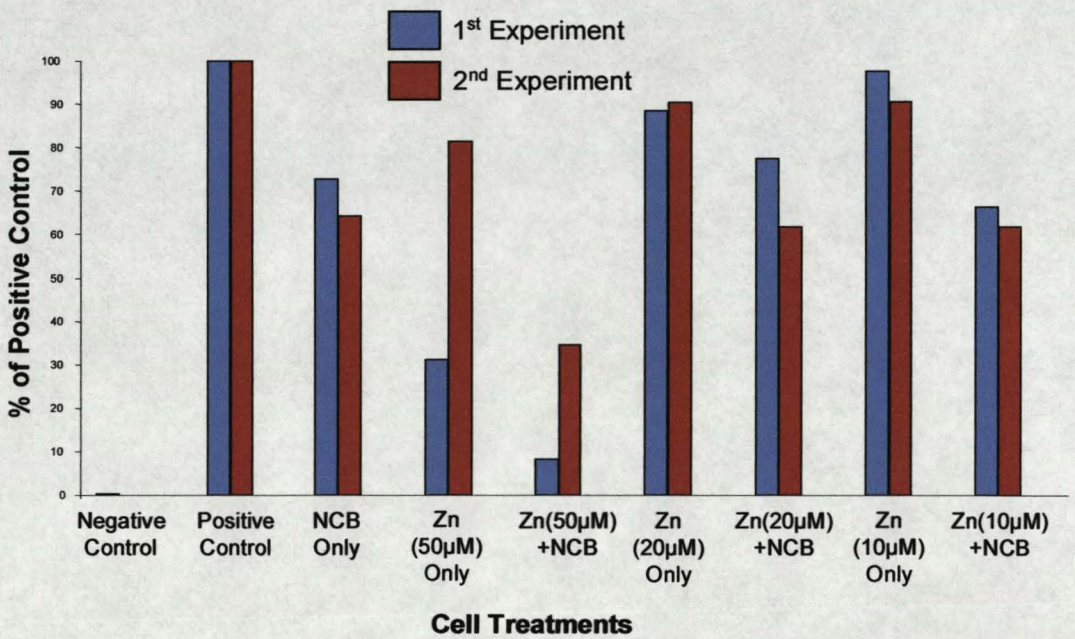

Figure 5.5.9 Graph showing the phagocytic potential of J774.A1 cells treated with varying concentrations of $ZnCl_2$ in the presence and absence of nanoparticle carbon black (31.25μg) Each cell treatment is represented as a % of the fluorescence from the positive control cells. Results shown are from two repeated experiments. The purple bars represent the data from the first experiment and the red bars represent the data from the second experiment

5.4 DISCUSSION

This chapter aimed to investigate if any interactions took place between zinc chloride salts and nanoparticle carbon black that could prove to be deleterious to macrophage phagocytic ability. The results obtained from this study indicate that any interactions between the particles and the metal do not appear to have any adverse effects on macrophage phagocytosis over and above the effects observed when incubating macrophages with zinc or particles individually.

The initial experiments in this study examined the possibility of measuring macrophage phagocytosis using a flow cytometer, using high doses of zinc and iron salts to induce measurable inhibition of phagocytic ability. The addition of zinc salts to the macrophages reduced macrophage phagocytosis by approximately 90% whereas the addition of iron salts reduced macrophage phagocytosis by approximately 50%. Macrophages possess several intracellular iron regulatory proteins such as IRP1, IRP2 as well as possessing receptors for the iron-binding plasma glycoprotein, transferrin (Mulero & Brock, 1999). In fact, Drapier *et al.*, (1993) notes that J774 cells express high levels of transferrin receptors indicating that the J774 cells are capable of binding large amounts of iron. This suggests that J774 cells are physiologically capable of managing iron uptake and, as such, may continue to show adequate phagocytic function even after being exposed to a high dose of iron.

Subsequent experiments in this chapter focussed on the effect of zinc chloride salts on macrophage phagocytosis. The results indicated that, at concentrations higher than

20μM, the zinc chloride salts caused a large decrease in the phagocytic ability of the macrophages. This is not unexpected, as zinc has been shown to be a highly toxic metal in several studies. Chvapil *et al.*, (1977a & 1977b) reported that macrophages showed decreased phagocytic potential and oxygen uptake when exposed to zinc salts. Zinc oxide inhalation studies have shown increases in BAL TNFα and IL-8 concentrations together with impairment of the phagocytic function of alveolar macrophages (Kuschner *et al.*, 1997 and Gordon *et al.*, 1992). Skornik & Brain (1983) also demonstrated significantly reduced macrophage phagocytic function in hamsters following the inhalation of zinc sulphate aerosols. In contrast, Lastra *et al.*, (2001) demonstrated that supplementation of mice with low concentrations of zinc (0.1mM) actually improved macrophage phagocytic function.

The interaction of zinc chloride salts with nanoparticle carbon black particles was also examined at a range of doses. The inhibition of macrophage function by nanoparticle carbon black alone was difficult to assess due to the high variability of the results, which varied from 20% inhibition up to 50% inhibition. Co-incubation of the nanoparticles with varying concentrations of zinc salts resulted in further inhibition of the macrophage phagocytic ability. This inhibition was proportional to the percentage inhibition observed when exposing the macrophages to zinc salts and to nanoparticles individually. These results suggest that any interaction that was taking place between the zinc and the particles was not inducing any further reductions in macrophage phagocytosis but was acting in an additive manner i.e. the addition of zinc chloride to the nanoparticle carbon black treatment caused a decrease that was greater than the carbon black alone.

Studies such as those by Adamson *et al.*, (2000) have stated that zinc is the toxic metal in environmental air pollution. This study did not take into account interactions between the particles and the metals in the air pollution samples. Preliminary investigations by our group have already indicated increased TNFα production by J774 cells in response to incubation with zinc chloride and equivalent doses of nanoparticle carbon black used in this study indicating that an interaction was taking place. However, based on the results of this study, this interaction is unlikely to be manifested as a potentiative decrease in macrophage phagocytic function at the exposure concentrations and timepoints utilised in this study. The decreases in phagocytic ability observed in this study appeared to be additive effects from the zinc and the carbon black particles. Subsequent investigations should focus on using a range of nanoparticle doses as opposed to the single dose utilised in this study together with a wider range of exposure timepoints. Examination of the macrophage cytoskeleton should also be conducted to assess possible changes in the microfilaments which could subsequently affect macrophage phagocytic potential.

CHAPTER 6

GENERAL DISCUSSION

A review of the current literature reveals that there have been numerous studies that have investigated the effects of components of particulate air pollution on the lungs and the mechanisms by which these effects are created. The nanoparticle component has been implicated as a key factor in PM_{10} induced toxicity (Seaton *et al.*, 1995), but the variable nature of PM_{10} means that the interaction of several other components can also have major roles (Stone *et al.*, 2003). The responses of the organisms that are exposed to the particles and physiological mechanisms that have evolved to cope with the constant exposure to particulate air pollution are key areas that must be fully understood in order to determine how particle induced disease is initiated. The studies conducted in this thesis were directed towards learning more about the clearance mechanisms present in the lung and how these mechanisms respond when challenged by PM_{10} and some of its components.

The biological effects of PM_{10} have been examined in a large number of studies. The links between increased levels of environmental particulate pollution and increased respiratory disease have been investigated using modern epidemiological techniques since the 1970's (Dockery & Pope III, 1994). Mathematical and epidemiological studies have demonstrated increased mortality from respiratory and cardiovascular events following instances of increased pollution levels (Donaldson *et al.*, 2000, Braga *et al.*, 2000 and Schwartz, 2001). Several authors have attributed these increases in mortality to the nanoparticle component of PM_{10} (Seaton *et al.*, 1995, Donaldson & MacNee., 1998, Oberdorster *et al.*, 1995). In addition, the toxicological impact of nanoparticles has now come under increased scrutiny due to the emergence of a relatively new technological

discipline; nanotechnology (Donaldson *et al.*, 2004). Substances such as carbon nanotubes are now being investigated for use in a wide range of applications such as potential drug delivery agents, and the toxicological impact of these substances has yet to be fully assessed. By understanding the mechanisms by which the body responds to nanoparticles, we can hope to further understand the potential impact that exposure to nanosubstances would generate.

From the results presented in this thesis, it is apparent that the responses of different types of pneumocytes could influence the biopersistence of nanoparticles in the alveolar region of the lung. In chapter 2, we showed that the alveolar type II cell generates increased chemoattractants in response to nanoparticle exposure compared to equivalent concentrations of fine particle exposure. These findings were in partial concurrence with the original hypothesis for this study i.e. that particles would induce chemoattractant secretion. However, it should be noted that the fine particles used in this study did not appear to share the same properties for chemoattractant generation compared to the fine particles. An important limiting factor in this set of experiments was the dose of particles, and although 125µg/ml was established as a sub-toxic dose for all particles used, it is unknown if higher dose of lower toxicity particles would induce increased generation of chemotactic molecules. However, this area of investigation may be incongruous to chemoattractant generation by resulting in a higher toxicity for the type II cells and ultimately resulting in cell death.

Another aspect of this study to consider is the use of an alveolar macrophage cell line to measure chemoattractant release by the type II cells. Although the alveolar macrophage is the primary mediator of particle clearance in the alveolar region of the lung, the neutrophil may also play an important role and, as such, future studies could focus on the release of neutrophil chemoattractants from type II cells. The isolation and culture of primary type II cells for utilisation in *ex vivo* particle treatments may also yield data that could provide a more accurate picture of events precluding particle uptake by phagocytes.

In chapter 3, it was demonstrated that nanoparticles possess the potential to induce the generation of macrophage chemotactic factors in blood serum. This study acted as a model to ascertain the effects of nanoparticles on complement proteins which are known to be present in the alveolar lining fluid. It was noted that the migration of macrophages towards particle-treated serum could be extremely variable and, as such, the repeated measurements that were made during the course of this study were subject to a degree of variation. This resulted in larger SEM values from this assay compared to other assays. Factors which may have affected these values include variances in the batches of serum used or species-specific effects i.e. murine macrophages migrating towards bovine serum. However, significant increases in macrophage migration were measured in spite of these factors and as such, provided a base upon which to draw conclusions.

A factor in this study which should also be noted is the high dose of particles that was required to activate chemotactic factors within the serum. Although it is unlikely that such a physiological dose of nanoparticles would be deposited in the alveolar regions of

the lung in one instance, it is possible that failed clearance and subsequent retention of particles in the alveolar spaces could result in an accumulated dose of particles. It may be possible that investigations utilising primary rat alveolar macrophages together with blood serum may yield more repeatable results at lower particle doses. Another area of investigation which would be useful to pursue would be an assessment of the potential for PM_{10} samples to activate the complement cascade. Due to limitations in the quantity of PM_{10} samples available for this study, an equivalent dose to that of the carbon black nanoparticles could not be achieved and, as such, this would be a worthy area of comparison to study.

Although further studies are warranted to determine if this phenomenon would also occur in the complement proteins present in epithelial lining fluid, this is a step forward in understanding methods of leukocyte recruitment in the lung. The molecular mechanisms of nanoparticle-induced complement activation should be explored in detail to provide a clearer picture of particle mediated leukocyte recruitment.

Both of the chapters mentioned above describe methods by which the cells of the lung can aid in the rapid removal of inhaled particles from the alveolar region of the lung. Conversely, other data presented in this thesis describes mechanisms by which nanoparticle exposure can decrease this clearance potential. In chapter 4, the potential for PM_{10} to cause adverse effects in macrophage clearance mechanisms is examined. The data indicates that when PM_{10} particles are visibly present inside a cell, the phagocytic

potential of the cell is impaired. We have also shown that the chemotactic potential of cells from particle exposed animals is decreased.

As previously mentioned, the neutrophilic inflammation observed in chapter 4 is consistent with other studies where particle instillation has taken place. The reduction in macrophage number may be due to migration out of the alveolar regions of the lung via the MCE or could be attributed to macrophage apoptosis. However, one of limitations of this study is that one single timepoint was used for all treatments (18 hours). This timepoint was used as it was thought that this would allow inflammatory cells to migrate to the alveolar space following particle treatment. A drawback of this, however, is that 18 hours after instillation, it is feasible that some cells may have already moved out of the alveolar space and would not appear in the lavage fluid. As such, future studies could concentrate on a range of timepoints to provide a more complete picture of cellular activities following particle instillation. However, this would result in increased usage of animals and so the benefits of the results must be considered in relation to the number of animals sacrificed.

The conclusions that are taken from the study in chapter 4 are contrary to that of the previous chapters 2 and 3, but are supported by data obtained from the experiments in chapter 5. In chapter 5, the potential for nanoparticles and zinc chloride to adversely affect the phagocytic potential of a macrophage cell line is examined. The results indicate that the nanoparticles and the zinc chloride salts act in an additive manner to reduce the phagocytic potential of the cells. This study used a range of concentrations of

zinc chloride salt together with a continuous low dose (31.25μg) of nanoparticle carbon black to examine the interaction between zinc and nanoparticles. Although this study used two surrogate materials to represent component of PM_{10}, we believe that this provides an appropriate model to examine the effects of two common PM_{10} components and their effects on phagocytic cells.

The flow cytometric analysis of the phagocytic ability of the macrophages is believed to provide an accurate measurement of the potential for macrophages to phagocytose fluorescent bioparticles following particle and zinc exposure. However, the measurements were subject to fluctuations in the repeatability of the data which may have been due to the presence of nanoparticle carbon black within the cellular solution. It should also be noted that whilst the addition of trypan blue to the cell suspension is designed to quench unphagocytosed bioparticle fluorescence, it is unknown as to how this would affect only partially phagocytosed bioparticles. The macrophage-bioparticle incubation time of 2 hours was based upon the manufacturers recommendations but a time-series measurement of phagocytic potential may be appropriate. Similarly, alteration of nanoparticle and zinc treatment times may also present alternative results.

Both chapter 4 and chapter 5 therefore give examples of how particle exposure can reduce the efficacy of clearance mechanisms as opposed to inducing increased clearance. Should inhibition of these functions occur in the lung of PM_{10} exposed animals, this may result in particle-laden macrophages remaining inside the alveolar space for an extended period of time instead of migrating out of the alveolar space via the MCE or to the lymph

nodes. This could result in the particles causing increased inflammation in the alveolar space over a long period of time resulting in the exacerbation of pre-existing respiratory conditions. Future investigations in this area should focus on the effects of chronic exposure to PM_{10} on alveolar macrophage functions and the effects of PM_{10} exposure on the cytoskeletal and molecular processes involved in macrophage-mediated clearance.

At first glance, the data from chapter 2 and chapter 3 appear to contradict the observations from chapters 4 and 5 in that these chapters suggest that particle clearance is impeded by nanoparticles whereas chapters 2 and 3 would support the hypothesis that particle clearance is promoted by nanoparticles by manner of increased leukocyte recruitment. Based upon the results in this thesis, it is hypothesised that the interaction of nanoparticles with different types of cells causes clearance mechanisms to be initiated within the alveolar space. The success of the activated clearance mechanisms is dependant upon the relative toxicity of the particles towards the alveolar macrophage, the key cell in the clearance process. Figure 6.1 is a schematic diagram outlining the hypothetical pathway that particle deposition and clearance could follow based upon the results described in this thesis. The diagram shows particle entry into the lung and interaction with cell and proteins present in the alveolar space. At this point, leukocytes are recruited to sites of particle deposition via chemoattractant generation from type II cells and complement proteins. At this point, the divergent nature of the pathway could determine the fate of the particles, and indeed, the macrophages that have phagocytosed them. Following phagocytosis of nanoparticles, we have observed that macrophages display decreased potential for further phagocytosis and decreased chemotactic potential.

It is hypothesised, therefore, that macrophages displaying these characteristics would not be able to migrate towards the MCE as would be expected in 'normal' circumstances, but would be retained within the alveolar space i.e. particle retention. However, on the other side of the pathway, the process of leukocyte recruitment, particle phagocytosis and clearance is displayed. This is due to the observation that nanoparticles induce increased generation of chemoattractants.

These outcomes may help to explain the increased toxicity observed when examining the fate of nanoparticles in the lung. Following entry, the nanoparticles appear to stimulate epithelial cells and complement to generate chemotactic factors that recruit macrophages to sites of particle deposition. The macrophages that are recruited may not be able to effectively phagocytose the particles and, as such, the particles and macrophages persist in the lung tissue and the particle-induced inflammation is exacerbated leading to disease.

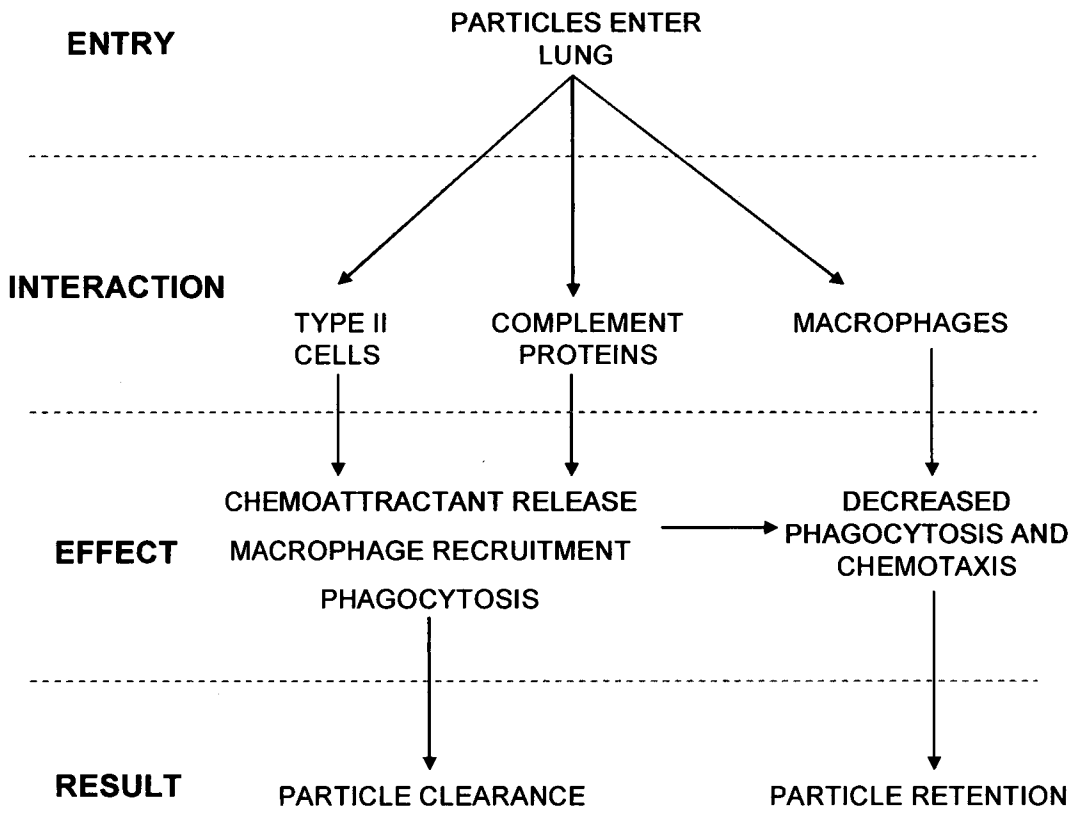

Figure 6.1 – The hypothesised consequences of nanoparticle entry into the alveolar region of the lung.

In summary, it has been shown that the components of particulate air pollution can have a wide range of effects on the clearance mechanisms that have evolved in the mammalian lung. The effective recruitment of phagocytic cells may indeed occur following inhalation of particles, but the impairment of normal macrophage functions such as chemotaxis and phagocytosis may have important ramifications in the continued challenge of air pollution that the lungs face on a daily basis. Further research into the exact nature of these effects is warranted, if only to provide a greater understanding when attempting to regulate human exposure to different types of airborne pollutants.

Furthermore, the models employed in this project will provide useful tools for the study of new and emerging nanoparticles including buckyballs, nanotubes and quantum dots.

REFERENCES

Adams, D. O. and Hamilton, T. A. (1984). The cell biology of macrophage activation. *Annu. Rev. Immunol* **2**: 283-318.

Adamson, I. Y. R. and Bowden, D. H. (1974). The type 2 cell as progenitor of alveolar epithelial regeneration. A cytodynamic study in mice after exposure to oxygen. *Lab Invest.* **30**(1): 35-42.

Adamson, I. Y. R. and Bowden, D. H. (1978). Adaptive responses of the pulmonary macrophagic system to carbon. II. Morphologic studies. *Lab Invest.* **38**(4): 430-438.

Adamson, I. Y. R. and Bowden, D. H. (1981). Dose response of the pulmonary macrophagic system to various particulates and its relationship to transepithelial passage of free particles. *Exp. Lung Res.* **2**(3): 165-175.

Adamson, I. Y. R., Prieditis, H., Hedgecock, C. and Vincent, R. (2000). Zinc is the toxic factor in the lung response to an atmospheric particulate sample. *Toxicol. Appl. Pharmacol.* **166**(2): 111-119.

Aderem, A. and Underhill, D. M. (1999). Mechanism of phagocytosis in macrophages. *Ann. Rev. Immunol.* **17**: 593-623.

Allen, J. I., Perri, R. T., McClain, C. J. and Kay, N. E. (1983). Alterations in human natural killer cell activity and monocyte cytotoxicity induced by zinc deficiency. *J. Lab Clin. Med.* **102**(4): 577-589.

Anderson, P. J., Wilson, J. D. and Hiller, F. C. (1990). Respiratory tract deposition of ultrafine particles in subjects with obstructive or restrictive lung disease. *Chest.* **97**(5): 1115-1120.

Arlaud, G. J. and Colomb, M. G. (1998). Complement: classical pathway. *Nature Encyclopedia of Life Sciences*. London: Nature Publishing Group.

Ashcroft, G. S. (1999). Bidirectional regulation of macrophage function by TGF-beta. *Microbes. Infect.* **1**(15): 1275-1282.

Bailey, M. R., Hodgson, A. and Smith, H. (1985). Respiratory tract retention of relatively insoluble particles in rodents. *J. Aerosol Sci.* **16**(4): 279-293.

Barrett, E. G., Johnston, C., Oberdorster, G. and Finkelstein, J. N. (1999). Silica-induced chemokine expression in alveolar type II cells is mediated by TNF-alpha-induced oxidant stress. *Am. J. Physiol.* **276**(6 Pt 1): L979-L988.

Barrington, R., Zhang, M., Fischer, M. and Carroll, M. C. (2001). The role of complement in inflammation and adaptive immunity. *Immunol. Rev.* **180**: 5-15.

Bayram, H., Devalia, J. L., Sapsford, R. J., Ohtoshi, T., Miyabara, Y., Sagai, M. and Davies, R. J. (1998). The effect of diesel exhaust particles on cell function and release of inflammatory mediators from human bronchial epithelial cells in vitro. *Am. J. Respir. Cell Mol. Biol.* **18**(3): 441-448.

Becher, R., Hetland, R. B., Refsnes, M., Dahl, J. E., Dahlman, H. J. and Schwarze, P. E. (2001). Rat lung inflammatory responses after in vivo and in vitro exposure to various stone particles. *Inhal. Toxicol.* **13**(9): 789-805.

Becker, S., Soukup, J. M., Gilmour, M. I. and Devlin, R. B. (1996). Stimulation of human and rat alveolar macrophages by urban air particulates: effects on oxidant radical generation and cytokine production. *Toxicol. Appl. Pharmacol.* **141**(2): 637-648.

Beisel, W. R. (1982). Single nutrients and immunity. *Am. J. Clin. Nutr.* **35**(2 suppl): 417-468.

BeruBe, K. A., Jones, T. P., Williamson, B. J., Winters, C., Morgan, A. J. and Richards, R. J. (1999). Physiochemical characterisation of diesel exhaust particles: factors for assessing biological activity. *Atmos. Environ.* **33**, 1599-1614.

Bishop, A. E. (2004) Pulmonary epithelial stem cells. *Cell Prolif.* **37**(1): 89-96.

Bitterman, P. B., Saltzman, L. E., Adelberg, S., Ferrans, V. J. and Crystal, R. G. (1984). Alveolar macrophage replication. One mechanism for the expansion of the mononuclear phagocyte population in the chronically inflammed lung. *J. Clin. Invest.* **74**: 460-469.

Blusse Van Oud Ablas, A. and Van Furth, R. (1979). Origin, Kinetics and characteristics of pulmonary macrophages in the normal steady state. *J. Exp. Med.* **149:** 1504-1518.

Bogdan, C., Rollinghoff, M. and Diefenbach, A. (2000). Reactive oxygen and reactive nitrogen intermediates in innate and specific immunity. *Curr. Opin. Immunol.* **12**(1): 64-76.

Bogdan, C. (2001). Macrophages. *Nature Encyclopedia of Life Sciences.* London: Nature Publishing Group.

Boland, S., Bonvallot, V., Fournier, T., Baeza-Squiban, A., Aubier, M. and Marano, F. (2000). Mechanisms of GM-CSF increase by diesel exhaust particles in human airway epithelial cells. *Am. J. Physiol. Lung Cell Mol. Physiol.* **278**(1): L25-L32.

Braga, A. L., Zanobetti, A. and Schwartz, J. (2000). Do respiratory epidemics confound the association between air pollution and daily deaths? *Eur. Respir. J.* **16**(4): 723-728.

Brain, J. D., Gehr, P. and Kavet, R. I. (1984). Airway macrophages. The importance of the fixation method. *Am. Rev. Respir. Dis.* **129**(5): 823-826.

Brieland, J. K., Flory, C. M., Jones, M. L., Miller, G. R., Remick, D. G., Warren, J. S. and Fantone, J. C. (1995). Regulation of monocyte chemoattractant protein-1 gene expression and secretion in rat pulmonary alveolar macrophages by lipopolysaccharide, tumor necrosis factor-alpha, and interleukin-1 beta. *Am. J. Respir. Cell Mol. Biol.* **12**(1): 104-109.

Brown, L. A. (1994). Glutathione protects signal transduction in type II cells under oxidant stress. *Am. J. Physiol.* **266**(2 Pt 1): L172-L177.

Brown, G. M., Brown, D. M., Donaldson, K., Drost, E. and MacNee, W. (1995). Neutrophil sequestration in rat lungs. *Thorax* **50**(6): 661-667.

Brown, D. M., Stone, V., Findlay, P., MacNee, W. and Donaldson, K. (2000). Increased inflammation and intracellular calcium caused by ultrafine carbon black is independent of transition metals or other soluble components. *Occup. Environ. Med.* **57**(10): 685-691.

Brown, J. S., Zeman, K. L. and Bennett, W. D. (2002). Ultrafine particle deposition and clearance in the healthy and obstructed lung. *Am. J. Respir. Crit. Care Med.* **166**(9): 1240-1247.

Carter, J. D., Ghio, A. J., Samet, J. M. and Devlin, R. B. (1997). Cytokine production by human airway epithelial cells after exposure to an air pollution particle is metal dependent. *Toxicol. Appl. Pharmacol.* **146:** 180-188.

Castranova, V., Ma, J. Y., Yang, H. M., Antonini, J. M., Butterworth, L., Barger, M. W., Roberts, J. and Ma, J. K. (2001). Effect of exposure to diesel exhaust particles on the susceptibility of the lung to infection. *Environ. Health Perspect.* **109**(Suppl 4): 609-612.

Chantry, D., Turner, M., Abney, E. and Feldmann, M. (1989). Modulation of cytokine production by transforming growth factor-beta. *J. Immunol.* **142**(12): 4295-4300.

Chen, J. L. and Fayerweather, W. E. (1988). Epidemiologic study of workers exposed to titanium dioxide. *J. Occup. Med.* **30**(12): 937-942.

Cheng, G., Ueda, T., Eda, F., Arima, M., Yoshida, N. and Fukuda, T. (2001). A549 cells can express interleukin-16 and stimulate eosinophil chemotaxis. *Am. J. Respir. Cell Mol. Biol.* **25**(2): 212-218.

Churg, A. and Brauer, M. (2000). Ambient atmospheric particles in the airways of human lungs. *Ultrastruct. Pathol.* **24**(6): 353-361.

Chvapil, M., Stankova, L., Zukoski, C. and Zukoski III, C. (1977) Inhibition of some functions of polymorphonuclear leukocytes by in vitro zinc. *J. Lab. Clin. Med.* **89**(1): 135-146.

Chvapil, M., Stankova, L., Bernhard, D. S., Weldy, P. L., Carlson, E. C. and Campbell, J. B. (1977). Effect of zinc on peritoneal macrophages in vitro. *Infect. Immun.* **16**(1): 367-373.

Clark, H., Palaniyar, N., Strong, P., Edmondson, J., Hawgood, S. and Reid, K. B. (2002). Surfactant protein D reduces alveolar macrophage apoptosis in vivo. *J. Immunol.* **169**(6): 2892-2899.

Clouter, A., Brown, D., Hohr, D., Borm, P. and Donaldson, K. (2001). Inflammatory effects of respirable quartz collected in workplaces versus standard DQ12 quartz: particle surface correlates. *Toxicol. Sci.* **63**(1): 90-98.

Cole, F. S., Matthews, W. J. Jr., Rossing, T. H., Gash, D. J., Lichtenberg, N. A. and Pennington, J. E. (1983). Complement biosynthesis by human bronchoalveolar macrophages. *Clin. Immunol. Immunopathol.* **27**(2): 153-159.

Crapo, J. D., Barry, B. E., Gehr, P., Bachofen, M. and Weibel, E. (1982). Cell number and cell characterisation of the normal human lung. *Am. Rev. Respir. Dis.* **125**: 332-337.

Cross, C. E. (1974). The granular type II pneumocyte and lung antioxidant defence. *Ann. Intern. Med.* **80**: 409-411.

Dai, J., Xie, C., Vincent, R. and Churg, A. (2003). Air pollution particles produce airway wall remodeling in rat tracheal explants. *Am. J. Respir. Cell Mol. Biol.* **29**(3 Pt 1): 352-358.

Daigle, C. C., Chalupa, D. C., Gibb, F. R., Morrow, P. E., Oberdorster, G., Utell, M. J. and Frampton, M. W. (2003). Ultrafine particle deposition in humans during rest and exercise. *Inhal. Toxicol.* **15**(6): 539-552.

Degussa Technical Bulletin Pigments No. 15. (1986). *Carbon blacks for coatings and printing inks – a survey*. Germany: Degussa AG.

Degussa Technical Bulletin Pigments No. 25. (1990). *Technical safety data – carbon blacks and coloured pigments*. Germany: Degussa AG.

Degussa Technical Bulletin Pigments No. 64. (1992). *The biological effects of SiO_2, Al_2O_3 and TiO_2*. Germany: Degussa AG.

Degussa Technical Document – *What is carbon black?* Germany: Degussa AG.

Desai, R. and Richards, R. J. (1978). The adsorption of biological macromolecules by mineral dusts. *Environ. Res.* **16**(1-3): 449-464.

Dick, C. A., Dennekamp, M., Howarth, S., Cherrie, J. W., Seaton, A., Donaldson, K. and Stone, V. (2001). Stimulation of IL-8 release from epithelial cells by gas cooker PM_{10}: a pilot study. *Occup. Environ. Med.* **58**(3): 208-210.

Dick, C. A., Brown, D. M., Donaldson, K. and Stone, V. (2003). The role of free radicals in the toxic and inflammatory effects of four different ultrafine particle types. *Inhal. Toxicol.* **15**(1): 39-52.

Dobbs, L. G. (1990). Isolation and culture of alveolar type II cells. *Am. J. Physiol.* **258**(4 Pt 1): L134-L147.

Dockery, D. W. (2001). Epidemiologic evidence of cardiovascular effects of particulate air pollution. *Environ. Health Perspect.* **109** (Suppl 4): 483-486.

Dockery, D. W. and Pope, C. A., III (1994). Acute respiratory effects of particulate air pollution. *Annu. Rev. Public Health.* **15**: 107-132.

Donaldson, K., Slight, J. and Bolton, R. E. (1988). The effect of products from bronchoalveolar-derived neutrophils on oxidant production and phagocytic activity of alveolar macrophages. *Clin. Exp. Immunol.* **74**(3): 477-482.

Donaldson, K., Slight, J. and Brown, D. M. (1989). Effects of products from inflammatory pulmonary neutrophils on alveolar macrophage chemotaxis, spreading, and thymidine incorporation. *Inflammation* **13**(4): 443-453.

Donaldson, K., Brown, G. M., Brown, D. M., Slight, J., Robertson, M. D. and Davis, J. M. (1990). Impaired chemotactic responses of bronchoalveolar leukocytes in experimental pneumoconiosis. *J. Pathol.* **160**(1): 63-69.

Donaldson, K., Beswick, P. H. and Gilmour, P. S. (1996). Free radical activity associated with the surface of particles: a unifying factor in determining biological activity? *Toxicol. Lett.* **88**(1-3): 293-298.

Donaldson, K., Brown, D. M., Mitchell, C., Dineva, M., Beswick, P. H., Gilmour, P. and MacNee, W. (1997). Free radical activity of PM10: iron-mediated generation of hydroxyl radicals. *Environ. Health Perspect.* **105**(Suppl 5): 1285-1289.

Donaldson, K., Stone, V., Clouter, A., Renwick, L. and MacNee, W. (2001a). Ultrafine particles. *Occup. Environ. Med.* **58**(3): 211-215.

Donaldson, K. and MacNee, W. (2001b). Potential mechanisms of adverse pulmonary and cardiovascular effects of particulate air pollution (PM_{10}). *Int. J. Hyg. Environ. Health.* **203**(5-6): 411-415.

Donaldson, K., and MacNee, W. (1998). The mechanism of injury caused by PM_{10}. *Issues In Environ. Sci. Technol.* **10:** 21-32.

Donaldson, K. and Tran C L (2002). Inflammation caused by particles and fibers. *Inhal. Toxicol.* **14**: 5-27.

Donaldson, K., Stone, V., Gilmour, P., Brown, D. M. and MacNee, W. (2000a). Ultrafine particles: mechanisms of lung injury. *Phil. Trans. R. Soc. Lond. A.* **358**: 2741-2749.

Donaldson, K., Gilmour, M. I. and MacNee, W. (2000). Asthma and PM_{10}. *Respir. Res.* **1**(1): 12-15.

Donaldson, K., Stone, V., Borm, P. J., Jimenez, L. A., Gilmour, P. S., Schins, R. P., Knaapen, A. M., Rahman, I., Faux, S. P., Brown, D. M. and MacNee, W. (2003). Oxidative stress and calcium signaling in the adverse effects of environmental particles (PM_{10}). *Free Radic. Biol. Med.* **34**(11): 1369-1382.

Donaldson, K., Stone, V., Tran, C L., Kreyling, W. and Borm, P. J. (2004). Nanotoxicology. *Occup. Environ. Med.* **61**(9): 727-728.

Dong, W., Lewtas, J. and Luster, M. I. (1996). Role of endotoxin in tumor necrosis factor alpha expression from alveolar macrophages treated with urban air particles. *Exp. Lung Res.* **22**(5): 577-592.

Dorger, M. and Krombach, F. (2000). Interaction of alveolar macrophages with inhaled mineral particulates. *J. Aerosol Med.* **13**(4): 369-380.

Dormans, J. A. M. A. and Van Bree, L. (1995). Function and response of type 2 cells to inhaled toxicants. *Inhal. Toxicol.* 7: 319-342.

Drapier, J. C., Hirling, H., Wietzerbin, J., Kaldy, P. and Kuhn, L. C. (1993). Biosynthesis of nitric oxide activates iron regulatory factor in macrophages. *Embo. J.* **12**(9): 3643-3649.

Driscoll, K. E., Lindenschmidt, R. C., Maurer, J. K., Higgins, J. M. and Ridder, G. (1990). Pulmonary response to silica or titanium dioxide: inflammatory cells, alveolar macrophage-derived cytokines, and histopathology. *Am. J. Respir. Cell Mol. Biol.* **2**(4): 381-390.

Driscoll, K. E., Carter, J. M., Howard, B. W., Hassenbein, D. G., Pepelko, W., Baggs, R. B. and Oberdorster, G. (1996a). Pulmonary inflammatory, chemokine, and mutagenic responses in rats after subchronic inhalation of carbon black. *Toxicol. Appl. Pharmacol.* **136**(2): 372-380.

Driscoll, K. E., Howard, B. W., Carter, J. M., Asquith, T., Johnston, C., Detilleux, P., Kunkel, S. L. and Isfort, R. J. (1996). Alpha-quartz-induced chemokine expression by rat lung epithelial cells: effects of in vivo and in vitro particle exposure. *Am. J. Pathol.* **149**(5): 1627-1637.

Driscoll, K. E. (1996). Role of inflammation in the development of rat lung tumours in response to chronic particle exposure. *Inhal. Toxicol.* **8**(Suppl 1): 139-153.

Driscoll, K. E., Deyo, L. C., Carter, J. M., Howard, B. W., Hassenbein, D. G. and Bertram, T. A. (1997a). Effects of particle exposure and particle-elicited inflammatory cells on mutation in rat alveolar epithelial cells. *Carcinogenesis.* **18**(2): 423-430.

Driscoll, K. E., Carter, J. M., Hassenbein, D. G. and Howard, B. (1997). Cytokines and particle-induced inflammatory cell recruitment. *Environ. Health Perspect.* **105**(Suppl 5): 1159-1164.

Driscoll, K. E. (2000). TNF alpha and MIP-2: role in particle-induced inflammation and regulation by oxidative stress. *Toxicol. Lett.* **112-113**: 177-184.

Drost, E. M. and MacNee, W. (2002). Potential role of IL-8, platelet-activating factor and TNF-alpha in the sequestration of neutrophils in the lung: effects on neutrophil deformability, adhesion receptor expression, and chemotaxis. *Eur. J. Immunol.* **32**(2): 393-403.

Duffin, R., Gilmour, P. S., Schins, R. P., Clouter, A., Guy, K., Brown, D. M., MacNee, W., Borm, P. J., Donaldson, K. and Stone, V. (2001). Aluminium lactate treatment of DQ12 quartz inhibits its ability to cause inflammation, chemokine expression, and nuclear factor-kappaB activation. *Toxicol. Appl. Pharmacol.* **176**(1): 10-17.

Elo, R., Maatta, K., Uksila, E. and Arstila, A. V. (1972). Pulmonary deposits of titanium dioxide in man. *Arch. Pathol.* **94:** 417-424.

Englert, N. (2004). Fine particles and human health - a review of epidemiological studies. *Toxicol.Lett.* **149**(1-3): 235-242.

Ercan, M. T. and Bor, N. M. (1991). Phagocytosis by macrophages in zinc-deficient rats. *Int. J. Rad. Appl. Instrum. B.* **18**(7): 765-768.

Fantone, J. C. and Ward, P. A. (1983). Chemotactic mechanisms in the lung: Vol 19 Lung biology in health and disease *Immunopharmacology of the lung*. Marcel Dekker, New York: 243-272.

Faurschou, M. and Borregaard, N. (2003). Neutrophil granules and secretory vesicles in inflammation. *Microbes. Infect.* **5**(14): 1317-1327.

Fehrenbach, H. (2001). Alveolar epithelial type II cell: defender of the alveolus revisited. *Respir. Res.* **2**(1), 33-46.

Fels, A. O. and Cohn, Z. A. (1986). The alveolar macrophage. *J. Appl. Physiol.* **60**(2): 353-369.

Ferin, J., Oberdorster, G. and Penney, D. P. (1992). Pulmonary retention of ultrafine and fine particles in rats. *Am. J. Respir. Cell Mol. Biol.* **6**(5): 535-542.

Ferin, J. and Feldstein, M. L. (1978). Pulmonary clearance and hilar lymph node content in rats after particle exposure. *Environ. Res.* **16**(1-3): 342-352.

Finkelstein, J. N., Johnston, C., Barrett, T. and Oberdorster, G. (1997). Particulate-cell interactions and pulmonary cytokine expression. *Environ. Health Perspect.* **105**(Suppl 5): 1179-1182.

Folinsbee, L. J. (1993). Human health effects of air pollution. *Environ. Health Perspect.* **100**: 45-56.

Frampton, M. W. (2001). Systemic and cardiovascular effects of airway injury and inflammation: ultrafine particle exposure in humans. *Environ. Health Perspect.* **109** (Suppl 4): 529-532.

Freeman, B. A., and Crapo, J. D. (1982). Biology of disease: free radicals and tissue injury. *Lab. Invest.* **47**(5): 412-426.

Geiser, M., Schupbach, R., Waber, U. and Gehr, P. (1998). Bioassay for hamster macrophage chemotaxis: application to study particle-lung interactions. *Cell Mol. Life Sci.* **54**(2): 179-185.

Georgsen, J., Rasmussen, S. and Pederson, J. O. (1990). Granulocyte chemotaxis. Influence of radiographic contrast media on the chemoattractive properties of serum. *Acta. Radiol.* **31**(5): 531-536.

Gilmour, P. S., Brown, D. M., Lindsay, T. G., Beswick, P. H., MacNee, W. and Donaldson, K. (1996). Adverse health effects of PM_{10} particles: involvement of iron in generation of hydroxyl radical. *Occup. Environ. Med.* **53**(12): 817-822.

Gilmour, P. S., Rahman, I., Hayashi, S., Hogg, J. C., Donaldson, K. and MacNee, W. (2001). Adenoviral E1A primes alveolar epithelial cells to PM_{10}-induced transcription of interleukin-8. *Am. J. Physiol. Lung Cell Mol. Physiol.* **281**(3): L598-L606.

Gilmour, P. S., Ziesenis, A., Morrison, E. R., Vickers, M. A., Drost, E. M., Ford, I., Karg, E., Mossa, C., Schroeppel, A., Ferron, G. A., Heyder, J., Greaves, M., MacNee, W. and Donaldson, K. (2004). Pulmonary and systemic effects of short-term inhalation exposure to ultrafine carbon black particles. *Toxicol. Appl. Pharmacol.* **195**(1): 35-44.

Goerdt, S., Politz, O., Schledzewski, K., Birk, R., Gratchev, A., Guillot, P., Hakiy, N., Klemke, C. D., Dippel, E., Kodelja, V. and Orfanos, C. E. (1999). Alternative versus classical activation of macrophages. *Pathobiology.* **67**(5-6): 222-226.

Gordon, T., Chen, L. C., Fine, J. M., Schlesinger, R. B., Su, W. Y., Kimmel, T. A and Amdur, M. O. (1992). Pulmonary effects of inhaled zinc oxide in human subjects, guinea pigs, rats, and rabbits. *Am. Ind. Hyg. Assoc. J.* **53**(8): 503-509.

Gordon, S. (2003). Alternative activation of macrophages. *Nat. Rev. Immunol.* **3**(1): 23-35.

Gormand, F., Cheria-Sammari, S., Aloui, R., Guibert, B., Malicier, D., Perrin-Fayolle, M., Lagarde, M. and Pacheco, Y. (1995). Granulocyte-macrophage colony stimulating factors (GM-CSF) and interleukin 8 (IL-8) production by human bronchial epithelial cells (HBEC) in asthmatics and controls. Lack of in vitro effect of salbutamol compared to sodium nedocromil. *Pulm. Pharmacol.* **8**(2-3): 107-113.

Governa, M., Fenoglio, I., Amati, M., Valentino, M., Bolognini, L., Coloccini, S., Volpe, A. R., Carmignani, M. and Fubini, B. (2002). Cleavage of the Fifth Component of Human Complement and Release of a Split Product with C5a-like Activity by Crystalline Silica through Free Radical Generation and Kallikrein Activation. *Toxicol. Appl. Pharmacol.* **179**(3): 129-136.

Greenwell, L. L., Moreno, T., Jones, T. P. and Richards, R. J. (2002). Particle-induced oxidative damage is ameliorated by pulmonary antioxidants. *Free Radic. Biol. Med.* **32**(9): 898-905.

Halliwell, B. (2001). Role of free radicals in the neurodegenerative diseases: therapeutic implications for antioxidant treatment. *Drugs Aging.* **18**(9): 685-716.

Harrison, R. M. and Yin, J. (2000). Particulate matter in the atmosphere: which particle properties are important for its effects on health? *Sci. Total Environ.* **249**(1-3): 85-101.

Hasselbacher, P. (1979). Binding of immunoglobulin and activation of complement by asbestos fibers. *J. Allergy Clin. Immunol.* **64**(4): 294-298.

Heasman, S. J., Giles, K. M., Rossi, A. G., Allen, J. E., Haslett, C. and Dransfield, I. (2004). Interferon gamma suppresses glucocorticoid augmentation of macrophage clearance of apoptotic cells. *Eur. J. Immunol.* **34**(6): 1752-1761.

Hermanowski-Vosatka, A., Mundt, S. S., Ayala, J. M., Goyal, S., Hanlon, W. A., Czerwinski, R. M., Wright, S. D. and Whitman, C. P. (1999). Enzymatically inactive macrophage migration inhibitory factor inhibits monocyte chemotaxis and random migration. *Biochemistry.* **38**(39): 12841-12849.

Hetland, R. B., Cassee, F. R., Refsnes, M., Schwarze, P. E., Lag, M., Boere, A. J. and Dybing, E. (2004). Release of inflammatory cytokines, cell toxicity and apoptosis in epithelial lung cells after exposure to ambient air particles of different size fractions. *Toxicol. In Vitro.* **18**(2): 203-212.

Heyder, J., Gebhart, R. G., Schiller, C. F. and Stahkhofen, W. (1986). Deposition of particles in the human respiratory tract in the size range 0.005-15μM. *J. Aerosol Sci.* **17**(5): 811-825.

Hill, J. O., Rothenberg, S. J., Kanapilly, G. M., Hanson, R. L. and Scott, B. R. (1982). Activation of immune complement by fly ash particles from coal combustion. *Environ Res.* **28**(1): 113-122.

Hoet, P. H. and Nemery, B. (2001). Stimulation of phagocytosis by ultrafine particles. *Toxicol. Appl. Pharmacol.* **176**(3): 203.

Hofmann, W. and Asgharian, B. (2003). The effect of lung structure on mucociliary clearance and particle retention in human and rat lungs. *Toxicol. Sci.* **73**(2): 448-456.

Hoffman, R. M., Claypool, W. D., Katyal, S. L., Singh, G., Rogers, R. M. and Dauber, J. H. (1987). Augmentation of rat alveolar macrophage migration by surfactant protein. *Am. Rev. Respir. Dis.* **135**(6): 1358-1362.

Hohr, D., Steinfartz, Y., Schins, R. P., Knaapen, A. M., Martra, G., Fubini, B. and Borm, P. J. (2002). The surface area rather than the surface coating determines the acute inflammatory response after instillation of fine and ultrafine TiO_2 in the rat. *Int. J. Hyg. Environ. Health.* **205**(3): 239-244.

Horn, J. K., Goldstein, I. M. and Flick, M. R. (1984). Complement and endotoxin-induced lung injury in sheep. *J. Surg. Res.* **36**(5): 420-427.

Hunninghake, G. W., Gader, J. E., and Lawley, T. J. (1981). Mechanisms of neutrophil accumulation in the lungs of patients with idiopathic pulmonary fibrosis. *J. Clin. Invest.* **68:** 259-269.

IARC Monograph (1989). IARC Monograph on the Evaluation of the Carcinogenic Risk of Chemicals to Humans. Vol 47: Some organic solvents, resin monomers and related compounds, pigments and occupational exposures in paint manufacture and painting. IARC Press, Lyon, France.

IARC Monograph (1996). IARC Monograph on the Evaluation of the Carcinogenic Risk of Chemicals to Humans. Vol 65: Printing process and printing inks, Carbon Black, and some nitro compounds. IARC Press, Lyon, France.

Janeway, C. A., Travers, P., Walport, M. and Capra, J. D. (1999). *Immunobiology: The immune system in health and disease (4th Edition).* Elsevier Science Ltd / Garland Publishing. USA.

Jimenez, L. A., Thompson, J., Brown, D. A., Rahman, I., Antonicelli, F., Duffin, R., Drost, E. M., Hay, R. T., Donaldson, K. and MacNee, W. (2000). Activation of NF-kappaB by PM_{10} occurs via an iron-mediated mechanism in the absence of IkappaB degradation. *Toxicol. Appl. Pharmacol.* **166**(2): 101-110.

Johnson, E. and Hetland, G. (1988). Mononuclear phagocytes have the potential to synthesize the complete functional complement system. *Scand. J. Immunol.* **27**(5): 489-493.

Jones, B. M., Edwards, J. H., and Wagner, J. C. (1972). Absorption of serum proteins by inorganic dusts. Br. J. Ind. Med. **29**(3): 287-292.

Kanemitsu, H., Nagasawa, S., Sagai, M. and Mori, Y. (1998). Complement activation by diesel exhaust particles (DEP). *Biol. Pharm. Bull.* **21**(2): 129-132.

Keen, C. L. and Gershwin, M. E. (1990). Zinc deficiency and immune function. *Annu. Rev. Nutr.* **10**: 415-431.

Keshav, S., Chung, L. P. and Gordon, S. (1990). Macrophage products in inflammation. *Diagn. Microbiol. Infect. Dis.* **13**(5): 439-447.

Kim, K. J. and Malik, A. B. (2003). Protein transport across the lung epithelial barrier. *Am. J. Physiol. Lung Cell Mol. Physiol.* **284**(2): L247-L259.

Kreyling, W. G., Semmler, M., Erbe, F., Mayer, P., Takenaka, S., Schulz, H., Oberdorster, G. and Ziesenis, A. (2002). Translocation of ultrafine insoluble iridium particles from lung epithelium to extrapulmonary organs is size dependent but very low. *J. Toxicol. Environ. Health A.* **65**(20): 1513-1530.

Koyama, S., Sato, E., Nomura, H., Kubo, K., Miura, M., Yamashita, T., Nagai, S. and Izumi, T. (1998). Bradykinin stimulates type II alveolar cells to release neutrophil and monocyte chemotactic activity and inflammatory cytokines. *Am. J. Pathol.* **153**(6): 1885-1893

Kruth, H. S., Chang, J., Ifrim, I. and Zhang, W. Y. (1999). Characterization of patocytosis: endocytosis into macrophage surface- connected compartments. *Eur. J. Cell Biol.* **78**(2): 91-99.

Kuschner, W. G., D'Alessandro, A., Wong, H. and Blanc, P. D. (1997). Early pulmonary cytokine responses to zinc oxide fume inhalation. *Environ. Res.* **75**(1): 7-11.

LaForce, F. M., Kelly, W. J. and Huber, G. L. (1973). Inactivation of staphylococci by alveolar macrophages with preliminary observations on the importance of alveolar lining material. *Am. Rev. Respir. Dis.* **108**(4): 784-790.

Lang, J. D., McArdle, P. J., O'Reilly, P. J. and Matalon, S. (2002). Oxidant-antioxidant balance in acute lung injury. *Chest.* **122**(6 Suppl): 314S-320S.

Laskin, D. L., and Laskin, J. D. (1996). Macrophages, inflammatory mediators, and lung injury. *Methods.* **10**(1): 61-70.

Lastra, M. D., Pastelin, R., Camacho, A., Monroy, B. and Aguilar, A. E. (2001). Zinc intervention on macrophages and lymphocytes response. *J. Trace Elem. Med. Biol.* **15**(1): 5-10.

Lightbody, J., Hutchison, G., Donaldson, K and Stone, V. (2003). The influence of particle composition and size on in vitro and in vivo biological models. DEFRA report EPG1/3/147.

Lee, K. P., Trochimowicz, H. J., and Reinhardt, C. F. (1985). Pulmonary response of rats exposed to titanium dioxide (TiO_2) by inhalation for two years. *Toxicol. Appl. Pharmacol.* **79**(2): 179-192.

Lehnert, B. E., Valdez, Y. E. and Stewart, C. C. (1986). Translocation of particles to the tracheobronchial lymph nodes after lung deposition: kinetics and particle-cell relationships. *Exp. Lung Res.* **10**: 245-266.

Lemiere, C., Cartier, A., Malo, J. L. and Lehrer, S. B. (2000). Persistent specific bronchial reactivity to occupational agents in workers with normal nonspecific bronchial reactivity. *Am. J. Respir. Crit. Care Med.* **162**(3 Pt 1): 976-980.

Letterio, J. J. and Roberts, A. B. (1998). Regulation of immune responses by TGF-beta. *Annu. Rev. Immunol.* **16**: 137-161.

Li, X. Y., Gilmour, P. S., Donaldson, K. and MacNee, W. (1996). Free radical activity and pro-inflammatory effects of particulate air pollution (PM_{10}) in vivo and in vitro. *Thorax* **51**(12): 1216-1222

Li, X. Y., Brown, D., Smith, S., MacNee, W. and Donaldson, K. (1999). Short-term inflammatory responses following intratracheal instillation of fine and ultrafine carbon black in rats. *Inhal. Toxicol.* **11**(8): 709-731.

Lippmann, M., Yeates, D. B. and Albert, R. E. (1980). Deposition, retention, and clearance of inhaled particles. *Br. J. Ind. Med.* **37**(4): 337-362.

Lippmann, M. and Schlesinger, R. B. (1984). Interspecies comparisons of particle deposition and mucociliary clearance in tracheobronchial airways. *J. Toxicol. Environ. Health.* **13**(2-3): 441-469.

Little, F. F., Cruikshank, W. W. and Center, D. M. (2001). IL-9 stimulates release of chemotactic factors from human bronchial epithelial cells. *Am. J. Respir. Cell Mol. Biol.* **25**(3): 347-352.

Lohmann-Matthes, M. L., Steinmuller, C. and Franke-Ullmann, G. (1994). Pulmonary macrophages. *Eur. Respir. J.* 7(9): 1678-1689.

Lukacs, N. W. and Ward, P. A. (1999). Inflammatory mediators, cytokines, and adhesion molecules in pulmonary inflammation and injury. *Adv. Immunol.* **62**: 257-304.

Lundborg, M., Johansson, A., Lastbom, L. and Camner, P. (1999). Ingested aggregates of ultrafine carbon particles and interferon-gamma impair rat alveolar macrophage function. *Environ. Res.* **81**(4): 309-315.

Lundborg, M., Johard, U., Lastbom, L., Gerde, P., and Camner, P. (2001). Human alveolar macrophage phagocytic function is impaired by aggregates of ultrafine carbon particles. *Environ. Res.* **86**(3): 244-253.

MacNee, W. and Donaldson, K. (2000). Exacerbations of COPD: environmental mechanisms. *Chest* **117**(5 Suppl 2): 390S-397S.

Malpel, S. and Cardroso, W. V. (2001). Lung development. *Nature Encyclopedia of Life Sciences.* London: Nature Publishing Group.

Matalon, S., Holm, B. A., Baker, R. R., Whitfield, M. K. and Freeman, B. A. (1990). Characterization of antioxidant activities of pulmonary surfactant mixtures. *Biochim. Biophys. Acta.* **1035**(2): 121-127.

Mauderly, J.L. (1996). Lung overload: the dilemma and opportunities for resolution. *Inhal. Toxicol.* **8**(Suppl 1): 1-28.

Metchnikoff, E. (1905). *Immunity to infectious diseases.* Cambridge/London/NY: Cambridge University Press.

Mercer, R. R., Russell, M. L., Roggli, V. L. and Crapo, J. D. (1994). Cell number and distribution in human and rat airways. *Am. J. Respir. Cell Mol. Biol.* **10**(6): 613-624.

McCormack, F. X. (2001). Functional mapping of surfactant protein A. *Pediatr. Pathol. Mol. Med.* **20**(4): 293-318.

Milanowski, J., Sorenson, W. G., Lewis, D. M. and Dutkiewicz, J. (1995). Chemotaxis of alveolar macrophages and neutrophils in response to microbial products derived from organic dust. *J. Investig. Allergol. Clin. Immunol.* **5**(4): 221-227.

Miller, F. J. (2000). Dosimetry of particles in laboratory animals and humans in relationship to issues surrounding lung overload and human health risk assessment: a critical review. *Inhal. Toxicol.* **12**(1-2): 19-57.

Mills, P. R., Davies, R. J. and Devalia, J. L. (1999). Airway epithelial cells, cytokines, and pollutants. *Am. J. Respir. Crit. Care Med.* **160**(5 Pt 2): S38-S43.

Möller, W., Hofer, T., Ziesenis, A., Karg, E. and Heyder, J. (2002). Ultrafine particles cause cytoskeletal dysfunctions in macrophages. *Toxicol. Appl. Pharmacol.* **182**(3): 197-207.

Monn, C. and Becker, S. (1999). Cytotoxicity and induction of proinflammatory cytokines from human monocytes exposed to fine ($PM_{2.5}$) and coarse particles ($PM_{10-2.5}$) in outdoor and indoor air. *Toxicol. Appl. Pharmacol.* **155**(3): 245-252.

Monn, C., Fendt, R. and Koller, T. (2002). Ambient PM_{10} extracts inhibit phagocytosis of defined inert model particulates by alveolar macrophages. *Inhal. Toxicol.* **14**(4): 369-385.

Morrow, P. E. (1988). Possible mechanisms to explain dust overloading of the lungs. *Fundam. Appl. Toxicol.* **10**(3): 369-384.

Mulero, V. and Brock, J. H. (1999). Regulation of iron metabolism in murine J774 macrophages: role of nitric oxide-dependent and -independent pathways following activation with gamma interferon and lipopolysaccharide. *Blood.* **94**(7): 2383-2389.

Murphy, S. A., BeruBe, K. A., Pooley, F. D. and Richards, R. J. (1998). The response of lung epithelium to well characterised fine particles. *Life Sci.* **62**(19): 1789-1799.

Namangala, B., De Baetselier, P., Noel, W., Brys, L. and Beschin, A. (2001). Alternative versus classical macrophage activation during experimental African trypanosomosis. *J. Leukoc. Biol.* **69**(3): 387-396.

Nemery, B. (1990). Metal toxicity and the respiratory tract. *Eur. Respir. J.* **3**(2): 202-219.

Nemmar, A., Vanbilloen, H., Hoylaerts, M. F., Hoet, P. H., Verbruggen, A. and Nemery, B. (2001). Passage of intratracheally instilled ultrafine particles from the lung into the systemic circulation in hamster. *Am. J. Respir. Crit. Care Med.* **164**(9): 1665-1668.

Nemmar, A., Hoet, P. H., Vanquickenborne, B., Dinsdale, D., Thomeer, M., Hoylaerts, M. F., Vanbilloen, H., Mortelmans, L. and Nemery, B. (2002). Passage of inhaled particles into the blood circulation in humans. *Circulation* **105**(4): 411-414.

Neumann, B., Zantl, N., Veihelmann, A., Emmanuilidis, K., Pfeffer, K., Heidecke, C. D. and Holzmann, B. (1999). Mechanisms of acute inflammatory lung injury induced by abdominal sepsis. *Int. Immunol.* **11**(2): 217-227.

Newman, V., Gonzalez, R. F., Matthay, M. A. and Dobbs, L. G. (2000). A novel alveolar type I cell-specific biochemical marker of human acute lung injury. *Am. J. Respir. Crit. Care Med.* **161**(3 Pt 1): 990-995.

Ning, Y., Imrich, A., Goldsmith, C. A., Qin, G. and Kobzik, L. (2000). Alveolar macrophage cytokine production in response to air particles in vitro: role of endotoxin. *J. Toxicol. Environ. Health. A.* **59**(3): 165-180.

Ning, Y., Tao, F., Qin, G., Imrich, A., Goldsmith, C. A., Yang, Z. and Kobzik, L. (2003). Particle-epithelial interaction: effect of priming and bystander neutrophils on interleukin-8 release. *Am. J. Respir. Cell Mol. Biol.* **30**(5): 744-750.

O'Brien, A. D., Standiford, T. J., Christensen, P. J., Wilcoxen, S. E. and Paine, R., III (1998). Chemotaxis of alveolar macrophages in response to signals derived from alveolar epithelial cells. *J. Lab. Clin. Med.* **131**(5): 417-424.

Oberdorster, G., Ferin, J. and Lehnert, B. E. (1994). Correlation between particle size, in vivo particle persistence, and lung injury. *Environ. Health Perspect.* **102** (Suppl 5): 173-179.

Oberdorster, G. (1995). Lung particle overload: implications for occupational exposures to particles. *Regul. Toxicol. Pharmacol.* **21**(1): 123-135.

Oberdorster, G., Sharp, Z., Atudorei, V., Elder, A., Gelein, R., Kreyling, W. and Cox, C. (2004). Translocation of inhaled ultrafine particles to the brain. *Inhal. Toxicol.* **16**(6-7): 437-445.

Obot, C. J., Morandi, M. T., Beebe, T. P., Hamilton, R. F. and Holian, A. (2002). Surface components of airborne particulate matter induce macrophage apoptosis through scavenger receptors. *Toxicol. Appl. Pharmacol.* **184**(2): 98-106.

Olenchock, S. A., Mull, J. C., Major, P. C., Peach III, M. J., Gladish, M. E. and Taylor, G. (1978). In vitro activation of the alternative pathway of complement by settled grain dust. *J. Allergy. Clin. Immunol.* **62**(5): 295-300.

Otto, W. R. (2002). Lung epithelial stem cells. *J. Pathol.* **197**(4): 527-535.

Paine, R., III, Rolfe, M. W., Standiford, T. J., Burdick, M. D., Rollins, B. J. and Strieter, R. M. (1993). MCP-1 expression by rat type II alveolar epithelial cells in primary culture. *J. Immunol.* **150**(10): 4561-4570.

Pendino, K. J., Shuler, R. L., Laskin, J. D. and Laskin, D. L. (1994). Enhanced production of interleukin-1, tumor necrosis factor-alpha, and fibronectin by rat lung phagocytes following inhalation of a pulmonary irritant. *Am. J Respir. Cell. Mol. Biol.* **11**(3): 279-286.

Penttinen, P., Timonen, K. L., Tiittanen, P., Mirme, A., Ruuskanen, J. and Pekkanen, J. (2001). Ultrafine particles in urban air and respiratory health among adult asthmatics. *Eur. Respir. J.* **17**(3): 428-435.

Perkins, R. C., Scheule, R. K., Hamilton, R., Gomes, G., Freidman, G. and Holian, A. (1993). Human alveolar macrophage cytokine release in response to in vitro and in vivo asbestos exposure. *Exp. Lung Res.* **19**(1): 55-65.

Peters, A., Wichmann, H. E., Tuch, T., Heinrich, J. and Heyder, J. (1997). Respiratory effects are associated with the number of ultrafine particles. *Am. J. Respir. Crit. Care Med.* **155**(4): 1376-1383.

Pope, C. A., III, Burnett, R. T., Thun, M. J., Calle, E. E., Krewski, D., Ito, K. and Thurston, G. D. (2002). Lung cancer, cardiopulmonary mortality, and long-term exposure to fine particulate air pollution. *JAMA* **287**(9): 1132-1141.

Prieditis, H. and Adamson, I. Y. (2002). Comparative pulmonary toxicity of various soluble metals found in urban particulate dusts. Exp. *Lung Res.* **28**(7): 563-576.

Pritchard, R. J., Ghio, A. J., Lehmann, J. R., Winsett, D. W., Tepper, J. S., Park, P., Gilmour, I. N., Dreher, K. L. and Costa, D. L. (1996). Oxidant generation and lung injury after particulate air pollutant exposure increase with the concentration of associated metals. *Inhal. Toxicol.* **8**: 457-477.

Putman, E., van Golde, L. M. and Haagsman, H. P. (1997). Toxic oxidant species and their impact on the pulmonary surfactant system. *Lung* **175**(2): 75-103.

Rahman, I. and MacNee, W. (1999). Oxidant/antioxidant imbalance in smokers and chronic obstructive pulmonary disease. *Thorax.* **51**(4): 348-350.

Regoli, D., Rizzi, A., Perron, S. I. and Gobeil Jr., F. (2001). Classification of kinin receptors. *Biol. Chem.* **201**(1): 31-35.

Rehn, B., Seiler, F., Rehn, S., Bruch, J. and Maier, M. (2003). Investigations on the inflammatory and genotoxic lung effects of two types of titanium dioxide: untreated and surface treated. *Toxicol. Appl. Pharmacol.* **189**(2): 84-95.

Renwick, L. C., Donaldson, K. and Clouter, A. (2001). Impairment of alveolar macrophage phagocytosis by ultrafine particles. *Toxicol. Appl. Pharmacol.* **172**(2): 119-127.

Renwick, L. C., Brown, D., Clouter, A. and Donaldson, K. (2004). Increased inflammation and altered macrophage chemotactic responses caused by two ultrafine particle types. *Occup. Environ. Med.* **61**(5): 442-447.

Rice, T. M., Clarke, R. W., Godleski, J. J., Al Mutairi, E., Jiang, N. F., Hauser, R. and Paulauskis, J. D. (2001). Differential ability of transition metals to induce pulmonary inflammation. *Toxicol. Appl. Pharmacol.* **177**(1): 46-53.

Rink, L. and Gabriel, P. (2000). Zinc and the immune system. *Proc. Nutr. Soc.* **59**(4): 541-552.

Rosseau, S., Selhorst, J., Wiechmann, K., Leissner, K., Maus, U., Mayer, K., Grimminger, F., Seeger, W. and Lohmeyer, J. (2000). Monocyte migration through the alveolar epithelial barrier: adhesion molecule mechanisms and impact of chemokines. *J. Immunol.* **164**(1): 427-435.

Roveri, A., Bruni, R., Baritussio, A., Coassin, M., Benevento, M., Maiorino, M. and Ursini, F. (1989). Antioxidant defences of rabbit alveolar lining fluid. *Respiration.* **55**(Suppl 1): 68-73.

Rylander, R. and Haglind, P. (1984). Airborne endotoxins and humidifier disease. *Clin. Allergy.* **14**(1): 109-112.

Sahu, A. and Lambris, J. D. (2000). Complement inhibitors: a resurgent concept in anti-inflammatory therapeutics. *Immunopharmacology.* **49**(1-2): 133-148.

Saint-Remy, J. M. and Cole, P. (1980). Interactions of chrysotile asbestos fibres with the complement system. *Immunology.* **41**(2): 431-437.

Salvi, S., Blomberg, A., Rudell, B., Kelly, F., Sandstrom, T., Holgate, S. T. and Frew, A. (1999). Acute inflammatory responses in the airways and peripheral blood after short-term exposure to diesel exhaust in healthy human volunteers. *Am. J. Respir. Crit. Care Med.* **159**(3): 702-709.

Schins, R. P., Lightbody, J. H., Borm, P. J., Shi, T., Donaldson, K. and Stone, V. (2004). Inflammatory effects of coarse and fine particulate matter in relation to chemical and biological constituents. *Toxicol. Appl. Pharmacol.* **195**(1): 1-11.

Schneider, E. and Dy, M. (1985). Activation of macrophages. *Comp. Immunol. Microbiol. Infect. Dis.* **8**(2): 135-146.

Schwartz, J. (2001). Is there harvesting in the association of airborne particles with daily deaths and hospital admissions? *Epidemiology* **12**(1): 55-61.

Seaton, A., MacNee, W., Donaldson, K. and Godden, D. (1995). Particulate air pollution and acute health effects. *Lancet.* **345**(8943): 176-178.

Shellito, J., Esparza, C. and Armstrong, C. (1987). Maintenance of the normal rat alveolar macrophage cell population. The roles of monocyte influx and alveolar macrophage proliferation in situ. *Am. Rev. Respir. Dis.* **135**(1): 78-82.

Shin, H. S., Snyderman, R., Friedman, E., Mellors, A. and Mayer, M. M. (1968). Chemotactic and anaphylatoxic fragment cleaved from the fifth component of guinea pig complement. *Science.* **162**(851): 361-363.

Sibille, Y. and Reynolds, H. Y. (1990). Macrophages and polymorphonuclear neutrophils in lung defense and injury. *Am. Rev. Respir. Dis.* **141**(2): 471-501.

Simon, R. H. and Paine III, R., (1995). Participation of pulmonary alveolar epithelial cells in lung inflammation. *J. Lab. Clin. Med.* **126**(2): 108-118.

Skornik, W. A. and Brain, J. D. (1983). Relative toxicity of inhaled metal sulfate salts for pulmonary macrophages. *Am. Rev. Respir. Dis.* **128**(2): 297-303.

Sladowski, D., Kinsner, A., Langezaal, I., Kay, S. and Coecke, S. (2001). Activation of the complement system as an indicator of pyrogenic reaction to lipopolysaccharide (LPS). *Toxicol. In Vitro.* **15**(4-5): 339-342.

Smith, K. R. and Aust, A. E. (1997). Mobilization of iron from urban particulates leads to generation of reactive oxygen species in vitro and induction of ferritin synthesis in human lung epithelial cells. *Chem. Res. Toxicol.* **10**(7): 828-834.

Snyderman, R., Shin, H. S., Phillips, J. K., Gewurz, H. and Mergenhagen, S. E. (1969). A neutrophil chemotatic factor derived from C'5 upon interaction of guinea pig serum with endotoxin. *J. Immunol.* **103**(3): 413-422.

Snyderman, R., Shin, H. S. and Hausman, M. H. (1971). A chemotactic factor for mononuclear leukocytes. *Proc. Soc. Exp. Biol. Med.* **138**(2): 387-390.

Soukup, J. M. and Becker, S. (2001). Human alveolar macrophage responses to air pollution particulates are associated with insoluble components of coarse material, including particulate endotoxin. *Toxicol. Appl. Pharmacol.* **171**(1): 20-26.

Stahlhofen, W., Gebhart, J. and Heyder, J. (1983). New regional deposition data of the human respiratory tract. *J. Aerosol Sci.* **14**: 186-188.

Stahlhofen, W., Rudolf, G. and James, A. C. (1989). Intercomparison of experimental regional aerosol deposition data. *J. Aerosol Med.* **2**: 285-308.

Standiford, T. J., Kunkel, S. L., Phan, S. H., Rollins, B. J. and Strieter, R. M. (1991). Alveolar macrophage-derived cytokines induce monocyte chemoattractant protein-1 expression from human pulmonary type II-like epithelial cells. *J. Biol. Chem.* **266**(15): 9912-9918.

Stone, V., Shaw, J., Brown, D. M., MacNee, W., Faux, S. P. and Donaldson, K. (1998). The role of oxidative stress in the prolonged inhibitory effect of ultrafine carbon black on epithelial cell function. *Toxicol. In Vitro* **12**: 649-659.

Stone, V., Tuinman, M., Vamvakopoulos, J. E., Shaw, J., Brown, D., Petterson, S., Faux, S. P., Borm, P., MacNee, W., Michaelangeli, F. and Donaldson, K. (2000a). Increased calcium influx in a monocytic cell line on exposure to ultrafine carbon black. *Eur. Respir. J.* **15**(2): 297-303.

Stone, V. (2000b). Environmental air pollution. *Am. J. Respir. Crit. Care Med.* **162**(2 Pt 2): S44-S47.

Stone, V., Wilson, M. R., Lightbody, J. H. and Donaldson, K. (2003). Investigating the potential for interaction between the components of PM_{10}. *Environmental Health & Preventative Medicine.* 7(6): 246-253.

Stringer, B. and Kobzik, L. (1998). Environmental particulate-mediated cytokine production in lung epithelial cells (A549): role of pre-existing inflammation and oxidant stress. *J. Toxicol. Environ. Health A.* **55**(1): 31-44.

Strunk, R. C., Eidlen, D. M. and Mason, R. J. (1988). Pulmonary alveolar type II epithelial cells synthesize and secrete proteins of the classical and alternative complement pathways. *J. Clin. Invest.* **81**(5): 1419-1426.

Sunyer, J. O. and Lambris, J. D. (1999). Complement. *Nature Encyclopedia of Life Sciences.* London: Nature Publishing Group.

Tao, F., Gonzalez-Flecha, B. and Kobzik, L. (2003). Reactive oxygen species in pulmonary inflammation by ambient particulates. *Free Radic. Biol. Med.* **35**(4): 327-340.

Tarling, J. D. and Coggle, J. E. (1982). Evidence for the pulmonary origin of alveolar macrophages. *Cell Tissue Kinet.* **15**(6): 577-584.

Tarling, J. D., Lin, H. S. and Hsu, S. (1987). Self-renewal of pulmonary alveolar macrophages: evidence from radiation chimera studies. *J. Leukoc. Biol.* **42**(5): 443-446.

Teran, L. M., Campos, M. G., Begishvilli, B. T., Schroder, J. M., Djukanovic, R., Shute, J. K., Church, M. K., Holgate, S. T. and Davies, D. E. (1997). Identification of neutrophil chemotactic factors in bronchoalveolar lavage fluid of asthmatic patients. *Clin. Exp. Allergy.* **27**(4): 396-405.

Thompson, A. B., Robbins, R. A., Romberger, D. J., Sisson, J. H., Spurzem, J. R., Teschler, H. and Rennard, S. I. (1995). Immunological functions of the pulmonary epithelium. *Eur. Respir. J.* **8**(1): 127-149.

Tone, K., Suzuki, T. and Todoroki, T. (1991). Influence of zinc deficiency on phagocytosis in mice. *Kitasato Arch. Exp. Med.* **64**(4): 263-269.

Tortora, G. J. and Grabowski, S. R. (1996). *Principles of anatomy and physiology (8^{th} Edition)*. John Wiley & Sons. USA.

Tran, C. L., Buchanan, D., Cullen, R. T., Searl, A., Jones, A. D. and Donaldson, K. (2000). Inhalation of poorly soluble particles II: Influence of particle surface area on inflammation and clearance. *Inhal. Toxicol.* **12**(12): 1113-1126.

Tsutahara, S., Shijubo, N., Hirasawa, M., Honda, Y., Satoh, M., Kuroki, Y. and Akino, T. (1993). Lung adenocarcinoma with type II pneumocyte characteristics. *Eur. Respir. J.* **6**(1): 135-137.

Turi, J. L., Yang, F., Garrick, M. D., Piantadosi, C. A. and Ghio, A. J. (2004). The iron cycle and oxidative stress in the lung. *Free Radic. Biol. Med.* **36**(7): 850-857.

Turner, M., Chantry, D. and Feldmann, M. (1990). Transforming growth factor beta induces the production of interleukin 6 by human peripheral blood mononuclear cells. *Cytokine.* **2**(3): 211-216.

Uhal, B. D. (1997). Cell cycle kinetics in the alveolar epithelium. *Am. J. Physiol.* **272**(6 Pt 1): L1031-L1045.

Utell, M. J., and Frampton, M. W. (2000). Acute health effects of ambient air pollution: the ultrafine particle hypothesis. *J. Aerosol Med.* **13**(4): 355-359.

Verkman, A. S., Matthay, M. A. and Song, Y. (2000). Aquaporin water channels and lung physiology. *Am. J. Lung Cell Mol. Physiol.* **278**(5): L867-L879.

Vogt, W., Damerau, B., von, Z., I, Nolte, R. and Brunahl, D. (1989). Non-enzymic activation of the fifth component of human complement, by oxygen radicals. Some properties of the activation product, C5b-like C5. *Mol. Immunol.* **26**(12): 1133-1142.

Wahl, S. M. (1992). Transforming growth factor beta (TGF-beta) in inflammation: a cause and a cure. *J. Clin. Immunol.* **12**(2): 61-74.

Wanner, A. (1977). Clinical aspects of muco-ciliary transport. *Am Rev. Respir. Dis.* **116**: 73-125

Ward, P. A. (2004). The dark side of C5a in sepsis. *Nature Reviews Immunology* **4**: 1-11.

Warheit, D. B. and Hartsky, M. A. (1990). Species comparisons of proximal alveolar deposition patterns of inhaled particulates. *Exp. Lung Res.* **16**(2): 83-99.

Warheit, D. B., Chang, L. Y., Hill, L. H., Hook, G. E., Crapo, J. D. and Brody, A. R. (1984). Pulmonary macrophage accumulation and asbestos-induced lesions at sites of fiber deposition. *Am.Rev. Respir. Dis.* **129**(2): 301-310.

Warheit, D. B., George, G., Hill, L. H., Snyderman, R. and Brody, A. R. (1985). Inhaled asbestos activates a complement-dependent chemoattractant for macrophages. *Lab. Invest.* **52**(2): 505-514.

Warheit, D. B., Hill, L. H., George, G. and Brody, A. R. (1986). Time course of chemotactic factor generation and the corresponding macrophage response to asbestos inhalation. *Am. Rev. Respir. Dis.* **134**(1): 128-133.

Warheit, D. B., Overby, L. H., George, G. and Brody, A. R. (1988). Pulmonary macrophages are attracted to inhaled particles through complement activation. *Exp. Lung Res.* **14**(1): 51-66.

Warheit, D. B. and Hartsky, M. A. (1990). Species comparisons of proximal alveolar deposition patterns of inhaled particulates. *Exp. Lung Res.* **16**(2): 83-99.

Warheit, D. B., Hansen, J. F., Yuen, I. S., Kelly, D. P., Snajdr, S. I. and Hartsky, M. A. (1997). Inhalation of high concentrations of low toxicity dusts in rats results in impaired pulmonary clearance mechanisms and persistent inflammation. *Toxicol. Appl. Pharmacol.* **145**(1): 10-22.

Watford, W. T., Ghio, A. J. and Wright, J. R. (2000). Complement-mediated host defense in the lung. *Am. J. Physiol. Lung Cell Mol. Physiol.* **279**(5): L790-L798.

Weissbach, S., Neuendank, A., Pettersson, M., Schaberg, T. and Pison, U. (1994). Surfactant protein A modulates release of reactive oxygen species from alveolar macrophages. *Am. J. Physiol.* **267**(6 Pt 1): L660-L666.

Widdicombe, J. G. and Pack, R. J. (1982). The clara cell. *Eur. J. Respir. Dis.* **63**(3): 202-220.

Wilkinson, P. C. (1998). Assays of leukocyte locomotion and chemotaxis. *J. Immunol. Methods.* **216**(1-2): 139-153.

Wilson, M. R., Gaumer, H. R. and Salvaggio, J. E. (1977). Activation of the alternative complement pathway and generation of chemotactic factors by asbestos. *J. Allergy Clin. Immunol.* **60**(4): 218-222.

Wilson, M. R., Lightbody, J. H., Donaldson, K., Sales, J. and Stone, V. (2002). Interactions between ultrafine particles and transition metals in vivo and in vitro. *Toxicol. Appl. Pharmacol.* **184**(3): 172-179.

Yano, E., Takeuch, A., Yukiyamo, Y. and Brown, R. C. (1984). Chemotactic factor generation by asbestos. Fibre type differences and the effects of leaching. *Br. J. Exp. Pathol.* **65**(2): 223-229.

Zipfel, P. F. (1999). Complement: alternative pathway. *Nature Encyclopedia of Life Sciences.* London: Nature Publishing Group